ELSEVIER

Journal of African Earth Sciences 36 (2003) 99–134

Journal of African Earth Sciences

www.elsevier.com/locate/jafrearsci

Geological Society of Africa Presidential Review, No. 5

Syndepositional dissolution of calcium carbonate in neritic carbonate environments: geological recognition, processes, potential significance

Diethard Sanders *

Institute of Geology and Palaeontology, University of Innsbruck, Innrain 52, A-6020 Innsbruck, Austria

Received 10 October 2002; accepted 4 April 2003

Abstract

Within carbonate sediments below tropical–subtropical oceanic surface waters, syndepositional "chemical" dissolution of $CaCO_3$ driven by organic matter oxidation can modify substantially the textural, compositional and early diagenetic characteristics of the resulting rock.

Main actuogeological evidence for "chemical" dissolution includes pore-water chemistry of carbonate sediments, and corrosion of bioclasts. Geological evidence includes taphonomic bias towards bioclasts of primary low-magnesium calcite, ghosts of aragonitic or high-magnesium calcitic bioclasts or fossils, lateral variations in early lithification, corroded early cements, pores overprinted by dissolution, and aragonite relicts in microspar. To date, evidence for syndepositional dissolution has been identified, with gaps in documentation, in Silurian to Cretaceous limestones. During organic matter oxidation in the sediment, aerobic respiration, sulfate reduction and oxidation of reaction by-products (e.g. H_2S) may result in local undersaturation for $CaCO_3$. Depending on the degree of openness of the diagenetic system, microbial sulfate reduction and, in open systems, reactions involving reaction by-products may in one case lead to precipitation, in another to dissolution of calcium carbonate. Both organic matter oxidation and fluctuations in pore water carbonate saturation are amplified by bioturbation. In burrowed carbonate sediments, carbonate dissolution is coupled to sulfate reduction and oxidation of hydrogen sulfide [Geochim. Cosmochim. Acta 63 (1999) 2529]. Part of the dissolved $CaCO_3$ is recycled to the sea, but the amount of dissolution recycling is difficult to estimate. Below the bioturbated layer, perhaps much of the dissolved calcium carbonate reprecipitates. In Phanerozoic neritic carbonate environments, syndepositional dissolution proceeded at least largely independent from aragonite seas or calcite seas, and appears mainly controlled by site-related factors. Over Phanerozoic time, both bioerosion and factors favourable for "chemical" dissolution within the sediment increased.

Keywords: Calcium carbonate; Dissolution; Phanerozoic; Carbonate environments

Contents

* Corresponding author. Tel.: +43-512-507-5584; fax: +43-512-507-2914.
E-mail address: diethard.g.sanders@uibk.ac.at (D. Sanders).

0899-5362/03/$ - see front matter © 2003 Elsevier Ltd. All rights reserved.
doi:10.1016/S0899-5362(03)00027-7

1. Introduction

"Although the overlying waters are more supersaturated than the pore waters, carbonate dissolution, not precipitation, dominates in these sediments... The carbonate sediments of the Bahamas are remarkable for their purity." For years to come this statement, made by Morse et al. (1985, p. 147), had little impact on field- and thin-section oriented carbonate sedimentologists. Previously, dissolution of calcium carbonate in marine waters was indicated by Emery (1946), Revelle and Emery (1957) and Seibold (1962) for tropical coastal solution basins. In addition, data from sediment pore waters of the Florida Bay indicated active dissolution (Seibold, 1962, p. 73; Taft and Harbaugh, 1964; Berner, 1966). Pytkowicz (1971) ascribed the lack of cementation in Bermuda carbonate beaches to both organic coatings and to carbonate dissolution mediated by oxidation of organic matter. Walter and Burton (1990) documented carbonate dissolution within the Holocene sediments of South Florida, resulting in net loss of calcium carbonate (see also Rude and Aller, 1991; Walter et al., 1993; Patterson and Walter, 1994), with an influence of site-specific conditions (Walter and Burton, 1990, p. 625; Burns and Swart, 1992; Ku et al., 1999). Perhaps, a reason why dissolution in neritic carbonates was appreciated comparatively late was the recognition that rapid marine cementation locally takes place (e.g. Dravis, 1979; Grammer et al., 1993). Many features of early dissolution, in marine-derived pore fluids, for instance, of reef cement (see Tobin and Walker, 1996) and skeletal mound matrix (see below) commonly are visible only in thin section. Moreover, in shallow subtidal areas, early microscale dissolution and reprecipitation most probably are widespread within Mg-calcitic and aragonitic bioclasts, but may be difficult or impossible to recognize in thin sections of the final rock (see e.g. Walter, 1985; Henrich and Wefer, 1986; Patterson and Walter, 1994; Reid and Macintyre, 1998; Perry, 2000; Hover et al., 2001).

For deep-water limestones, syn- to early post-depositional dissolution of calcium carbonate is well-known (e.g. Garrison and Fischer, 1969; Seilacher, 1971; Jenkyns, 1974; Schlager, 1974; Tucker, 1974; Eder, 1982; Möller and Kvingan, 1988; Brachert and Dullo, 2000). The biostratinomic and petrographic features of dissolution in marine-derived pore fluids may look identical to those interpreted for meteoric diagenesis (Schlager, 1974; Tucker, 1974; Melim et al., 1995, 2002). In periplatform carbonates deposited under a few hundreds to about 1000 m water depth, dissolution of aragonite and high-Mg calcite followed by reprecipitation of low-Mg calcite and/or dolomite (e.g. Schlager and James, 1978; Mullins et al., 1985) is driven by oxidation of organic

matter (e.g. Dix and Mullins, 1988; Malone et al., 2001). Syngenetic dissolution of aragonitic shells, or shell parts, may lead to strong taphonomic bias (e.g. Schlager, 1974; Cherns and Wright, 2000). Early diagenetic carbonate dissolution in deep-water settings differs from that in shallow water mainly with respect to the organic carbon flux to the bottom, the relative amount of aerobic and anaerobic processes of organic matter oxidation, the depth of oxygen penetration into the sediment, and the role of metals in redox reactions (see e.g. Froelich et al., 1979; Berner, 1981; Bender and Heggie, 1984; Boudreau, 1987; Henrichs and Reeburgh, 1987; Archer et al., 1989; Henrichs, 1992, p. 121). Moreover, extensive dissolution of aragonite in marine-derived pore waters, in a burial environment without meteoric influence, has been documented for slope limestones of the Bahama Banks (Melim et al., 1995, 2002).

Shallow-water carbonate platforms are manifests of carbonate production, but at the same time, "biological" dissolution by macroboring, grazing, destructive micritization and microbial infestation results in substantial loss of calcium carbonate (e.g. Neumann, 1966; Fütterer, 1974; Tudhope and Scoffin, 1984; Tudhope and Risk, 1985; Henrich and Wefer, 1986; Chazottes et al., 1995; Freiwald, 1995; Perry, 1999, 2000; Vogel et al., 2000; Pari et al., 2002). Although the dissolution kinetics of major carbonate minerals is still poorly unravelled (Morse and Arvidson, 2002), field measurements indicate that a significant amount of calcium carbonate is dissolved by microbially-mediated chemical processes in the soft to firm sediment (Morse et al., 1985; Walter and Burton, 1990; Ku et al., 1999). For neritic siliciclastics, destructive diagenesis involving widespread carbonate dissolution is long known (e.g. Driscoll, 1970; Smith, 1971; Alexandersson, 1978; Fitzgerald et al., 1979; Cummins et al., 1986; Reaves, 1986; Davies et al., 1989; Murray and Alve, 1999). For deep neritic to upper bathyal limestones, dissolution of aragonite and/or Mg-calcite, commonly in association with crustacean burrows or along hardgrounds, has been documented (e.g. Rasmussen, 1971; Kennedy and Garrison, 1975; Bottjer, 1981; Koch and Sohl, 1983; Palmer et al., 1988). For shallow neritic carbonate successions, by contrast, early carbonate dissolution that probably proceeded in marine-derived pore fluids is yet scarcely documented, but may have been significant. Syndepositional dissolution of calcium carbonate has implications for palaeoecology and taphonomy, for carbonate budgets, and for the interpretation of fossil assemblages (see Fürsich and Pandey, 1999; Ku et al., 1999; Sanders, 1999, 2001; Cherns and Wright, 2000; El Albani et al., 2001). Main questions with respect to syndepositional dissolution in neritic carbonates are (1) What features indicate dissolution? (2) What are the driving processes? and (3) What are possible implications of dissolution? To establish a list of criteria for recognition of dissolution, a survey of thin sections ranging in age, with gaps, from Ordovician to Tertiary was made, supplemented by papers of other authors. A conceptual frame of carbonate dissolution in unlithified sediment is presented. The survey indicates that syndepositional dissolution in marine-derived pore fluids was active over at least large parts of Phanerozoic time, and proceeded at least in part independent of calcite seas and aragonite seas.

2. Data base, approach

As far as the depositional water depth of investigated carbonate rocks could be estimated, in rocks from subtidal environments, no depth limit of evidence for syndepositional dissolution was identified. Herein, the term neritic is used for depositional water depths of generally less than about 100 m. For the present paper, about 2600 thin sections of neritic limestones were inspected (Fig. 1). Only thin sections from logged sections were considered, to increase certainty with respect to depositional history. Where possible, the observations were discussed with the persons that logged the sections. Selected thin sections were investigated under cathodoluminescence. Limestones from bathyal environments were also investigated, but are not documented here.

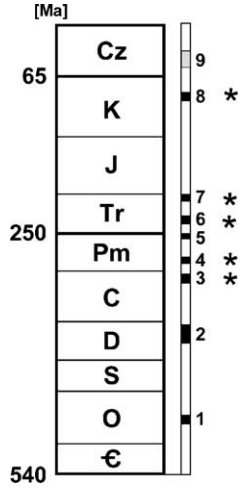

Fig. 1. Black bars beside the Phanerozoic time scale (IUGS scale; Remane, 2000) indicate the approximate chronostratigraphic range of limestones investigated for the present paper. Asterisks: intervals where evidence for syndepositional dissolution was found. (1) Platform lithoclasts, Cowhead Group, Newfoundland, Canada. (2) Reefal to lagoonal limestones (mainly Kellergrat Limestone, Cellon Limestone, Pal Limestone), Carnic Alps, Austria. (3) Neritic limestones, Auernig Group, Carnic Alps, Austria. (4) Neritic limestones, Rattendorf Group, Carnic Alps, Austria. (5) Neritic limestones and fine-grained dolostones, Bellerophon Formation, Carnic Alps, Austria. (6) Lagoonal limestones, Wettersteinkalk Formation, Karwendel, Austria. (7) Neritic limestones, Kössener Formation, Tyrol, Austria. (8) Neritic limestones, Gosau Group, Austria (and a few samples from Greece and Sinai). (9) Eocene to Oligocene limestones from the Eastern Alps and Southern Alps, Austria/Italy: limited data.

In the interpretation of syndepositional dissolution, the guideline was that an observed compositional and/or textural feature can reasonably or at least most parsimoniously be explained by considering dissolution in marine-derived pore fluids, in unlithified to semi-lithified sediment. If this could not be satisfied, the interpretation is ambiguous (this is more often the case than not) and was not considered here. In the following Section 3, compositional and textural indicators are described and discussed. Early dissolution of calcium carbonate is summarized in more detail in Section 4.

3. Indications of dissolution

3.1. Calcite-biased bioclastic fraction

Where aragonite-secreting shallow-water biota is sparse or absent, such as in marine tropical environments subject to impingement of cool waters, to elevated nutrient level or to sea water of very low Mg/Ca ratio, the resulting carbonate sediments are mainly composed of calcitic bioclasts (e.g. many benthic foraminifera, bryozoans, molluscs) (e.g. Lees and Buller, 1972; James, 1997; Steuber, 2002). In many cases, however, the bioclastic fraction of tropical to subtropical shallow-water carbonates is locally strongly dominated by or consists exclusively of bioclasts of primary calcitic mineralogy, irrespective of grain size and sorting. A bias towards calcitic bioclasts is most obvious in limestones with their bioclastic fraction derived from organisms that secreted both aragonite and calcite, such as many molluscs (Table 1). The shell of most molluscs consists of a thin periostracum of organic material, and of a layer each of calcite (ostracum) and aragonite (hypostracum) (Fig. 2(1)). Most commonly, the former aragonite is preserved as sparry calcite. Where significant syndepositional dissolution of aragonite occurred, the sediment consists of bioclasts devoid of the aragonitic shell layer, or of calcitic bioclasts only, and bioclasts of former aragonitic composition (typically preserved as sparry calcite) are rare to absent (Fig. 3).

3.1.1. Interpretation

Calcite bias is best recognized where the bioclastic fraction is (nearly) exclusively composed of calcitic bioclasts of fossils that originally consisted of both aragonite and calcite. Inference of calcite bias, however, must take into account the taphonomy of the respective organisms. In some fossil molluscs, for instance, calcitic shell parts tended to disintegrate into fragments of low hydraulic radius that often became enriched in distinct layers by feeble currents (Amico, 1978; Sanders, 1999). Calcite-bias because of syndepositional aragonite dissolution thus can be assumed where the bioclastic fraction is composed of fragments of sand to gravel size that are unsorted for both shape and size, that are derived from breakdown of shells that originally consisted of both aragonite and calcite, and that had a similar hydrodynamic behaviour.

In bioclastic sediments composed of bioclasts of different taxonomic groups and of different primary mineralogy, such as calcitic benthic foraminifera, aragonitic green algae and high-magnesium calcitic red algae, preferred dissolution of the more soluble bioclasts may lead to taphonomic bias. In incubation experiments, for instance, coralline algal clasts (high-magnesium calcite) dissolved much more rapidly than coral and echinoid grains (Walter and Burton, 1990, p. 632; Patterson and Walter, 1994). In rocks, if dissolution proceeded in soft, bioturbated sediment so as to leave no ghost fabrics, such a style of taphonomic loss may be difficult to recognize, since an estimate of dissolution loss necessitates knowing the original ratio of different bioclasts (cf. Murray and Alve, 1999). Taphonomic loss may be inferred if other indicators of syndepositional dissolution are present (see below). Where ghost fabrics of dissolved aragonitic bioclasts are present, within a rock containing both clasts of calcitic and formerly aragonitic fossils, taphonomic loss of a portion of the aragonitic bioclastic fraction is indicated (Fig. 4).

Besides mineralogy, the vulnerability of bioclasts to dissolution is influenced or even controlled by their micro/ultrastructure, and by the type and content of organic matrix (e.g. Flessa and Brown, 1983; Walter and Morse, 1984; Walter, 1985; Glover and Kidwell, 1993). Loss of organic matrix from shells by microbial decomposition is a very common early diagenetic alteration, also in aerobic environments and in waters under- to supersaturated for calcium carbonate. Organic matrix decomposition makes shells vulnerable to fracture, and also increases the potential for dissolution by exposing shell crystallites to pore water (Glover and Kidwell, 1993; Powell et al., 2002). Shell fragmentation and crystallite exposure both speed loss of organic matrix and carbonate dissolution, adding grain size and reactive surface as controls on dissolution (cf. Flessa and Brown, 1983; Walter and Morse, 1984; Walter, 1985; Glover and Kidwell, 1993). For some neritic shell beds at least, fabrics suggest that shells become preserved because of "self-buffering" of the pore water by dissolution of small shell fragments down to mud size (e.g. Kidwell, 1989). Distinct differences in organic matrix content of different types of shells may override the influence of primary mineralogy. In addition, preservation of formerly aragonitic shell fragments does not necessarily preclude dissolution of other aragonitic fragments that were more vulnerable to dissolution (Glover and Kidwell, 1993). Thus, preservation of bioclasts or shells of formerly aragonitic molluscs does not prove that all aragonitic bioclasts or fossils are preserved (Flessa and Brown, 1983; Glover and Kidwell, 1993, p. 744). These

Table 1
Textural, compositional and taphonomic features of syn- to early post-depositional carbonate dissolution in marine-derived fluids

Criterion	Description	Environment of dissolution	Processes	Figures, references
Calcite-biased bioclastic fraction	(1) Prevalence of calcitic fragments of fossils that consisted of both aragonite and calcite (2) Aragonitic fossils showing other indications of dissolution	Soft sediment	Dissolution of aragonitic bioclasts during organic matter oxidation	Fig. 3, Sanders (1999)
Partly to completely dissolved shells/skeletons	(1) Internal mould embedded in matrix (2) Aragonitic parts of shell or skeleton filled by matrix (= calcitic shell parts in direct contact with matrix) (3) Primary cavities in skeleton/shells widened (not by boring)	Soft to firm sediment	Dissolution of aragonitic or Mg-calcitic shells/skeletons during organic matter oxidation	Figs. 4–11, Sanders (1999, 2001) and Fürsich and Pandey (1999)
Preservation gradients	(1) Vertical/lateral gradient from internal moulds to thinned shells to (locally) well-preserved shells, on a scale of millimeters to decimeters (2) Fossil assemblage of both calcitic and formerly aragonitic shells/skeletons, grades laterally into assemblage of calcitic shells/skeletons only, without change in environment (substrate) and depositional water depth indicated (3) Uncompacted carbonate concretions with fossils, within compacted marls to marly limestones without fossils (or with fossil ghosts)	Soft to firm sediment	Dissolution of aragonitic shells/skeletons along saturation gradients related to organic matter oxidation	Figs. 13 and 14, Cherns and Wright (2000) and El Albani et al. (2001)
Corroded cement	Cement crystals truncated by dissolution surfaces	Firm to semi-lithified sediment, or in intraskeletal pores of fossils embedded in soft sediment	Dissolution in pore waters undersaturated by (1) oxidation of organic matter, and/or (2) in episodically oxidized, anoxic pore waters derived from overlying anoxic oceanic water	Fig. 16, Tobin and Walker (1996) and Tobin and Bergstrom (2002)
Pores formed or overprinted by dissolution	Pores with a highly irregular, embayed and pitted outline, locally with ferromanganese crusts or pyrite along the margin. Dissolution/corrosion of bioclasts	Firm to lithified sediment. Initial pore development probably related to (1) firmground burrowing, (2) decomposition of organisms, (3) dewatering	Dissolution by reoxidation of H_2S, by iron sulfide precipitation, by oxidation of Mn and Fe in biofilms	Figs. 17–19, cf. Ginsburg and Schroeder (1973) and James and Ginsburg (1979)
Dissolution along hardgrounds	Hardgrounds with highly irregular, embayed and pitted surface, coated by crusts of phosphorite, ferromanganese minerals, or of laminated iron sulfide	Formed on firm to lithified sediment, related to vertical fluctuations of anoxic/oxic interface or of oxygen minimum layer in water column	Dissolution by oxidation of hydrogen sulfide, by iron sulfide precipitation, by oxidation of reduced iron and manganese	Read (1982)
Pitted microspar crystals	SEM investigation: (1) microspar crystals with elongated pits similar to aragonite needles, (2) preserved aragonite relicts in microspar crystals	Soft to semi-lithified sediment	Dissolution of aragonite mud (probably upon organic matter oxidation)	Munnecke and Samtleben (1996) and Munnecke et al. (1997)

The features may be present alone or in combination. See text for discussion.

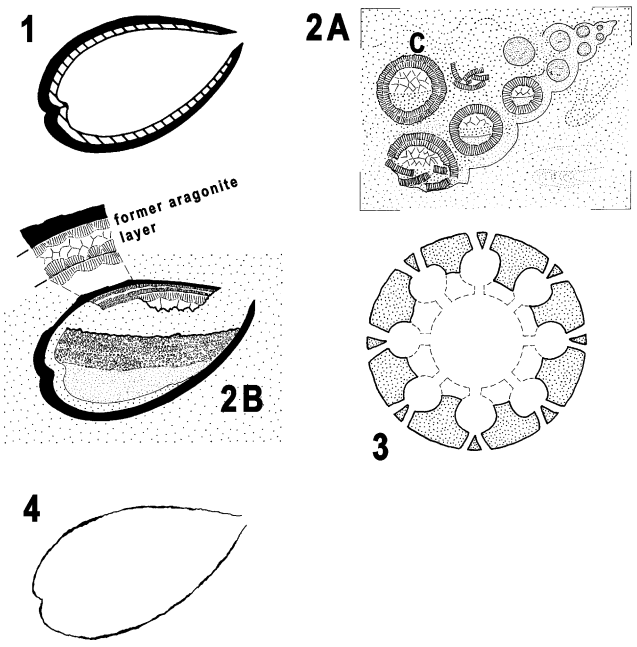

Fig. 2. Criteria to recognize dissolution. (1) Section through completely preserved bivalve shell, showing calcitic shell layer (ostracum, black) and aragonitic shell layer (hypostracum, cross-hatched). (2A) Dissolved, formerly aragonitic gastropod. The original, inner surface of the whorls may be covered by marine cement that, locally, is crushed by compaction. The shell is largely or entirely replaced by sediment that is identical to and in physical continuity with the matrix; only cements and/or the sediment fill of the whorls indicate the former presence of the shell. (2B) Bivalve shell with the aragonite layer replaced by sediment in physical continuity with the matrix (lower part), or with the aragonite layer replaced by fibrous marine cement and, locally, blocky calcite spar (upper part). Early-precipitated cements, including calcite spar, may be corroded in contact with the matrix. (3) Cross-section through calcareous algae (shown: dasycladacean), with primary central channel (dashed) widened by dissolution. (4) Internal moulds of totally dissolved bivalves may show by faint relicts of shell periostracum.

more subtle types of calcite bias will be difficult to recognize or quantify in carbonate rocks. Where complete dissolution of fossils took place within soft sediment, no fabric indicative of their former presence may be formed (e.g. Cherns and Wright, 2000; see Section 3.3 below).

3.2. Partly to completely dissolved shells/skeletons

This category comprises more-or-less entire shells or skeletons that were dissolved, partly to completely, in unlithified sediment (Table 1). In case of fossils that were entirely composed of aragonite, such as scleractinian corals or some molluscs, dissolution in the soft sediment is indicated by a relictic fossil or fossil ghost or internal mould, that is filled by sediment that is closely similar to and in physical continuity with the matrix (Figs. 2(2A) and 5). With respect to both colour and texture, the similarity of the infill with the matrix in many cases is so high that such ghosts appear quite faint

Fig. 3. Very poorly sorted bioclastic packstone composed exclusively of fragments from the calcitic shell layer of rudists. Note that the preservation of the shell fragments ranges from angular, unmicritized to rounded with a micrite rim; note also macroborings in some of the fragments. This packstone is the matrix of a rudist biostrome with an open to packed, parautochthonous rudist fabric. Upper Santonian, Gosau, Austria. Width of view 12 mm.

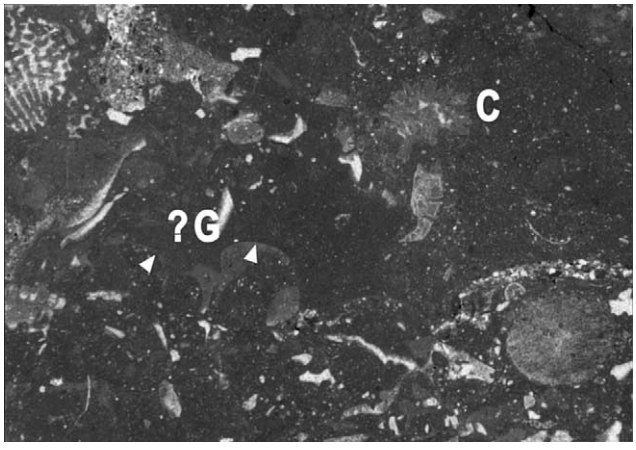

Fig. 4. Bioclastic wackestone to lime mudstone with faint ghost fabrics. Ghost labelled C shows a cross-section of a coral branch fragment; note that the sediment replacing the septae is of identical nature and in physical continuity with the lime mudstone matrix in which the coral fragment has been embedded. Arrowed ghost fabric labelled ?G shows a crescentic outline that is reminiscent of the whorls of a neritoid gastropod, or a fragment thereof. This limestone is the matrix to an interval of coral–sponge–rudist bafflestones to floatstones that probably accumulated from gentle mounds to level-bottoms in a shallow subtidal environment (see Sanders and Pons, 1999, pp. 261–270, for description). Lower Coniacian, Brandenberg, Austria. Width of view 17 mm.

even in thin section (Fig. 4). In some cases, precipitation of a cement fringe before fossil dissolution or infill by internal sediment of different texture and/or colour than the matrix aid in recognition of ghost fossils (Figs. 2(2A,4) and 6). Where wholesale dissolution occurred, the former fossil may be recorded by an internal mould of slightly different texture and/or colour than the matrix or, for molluscs, by a very thin, brown to black

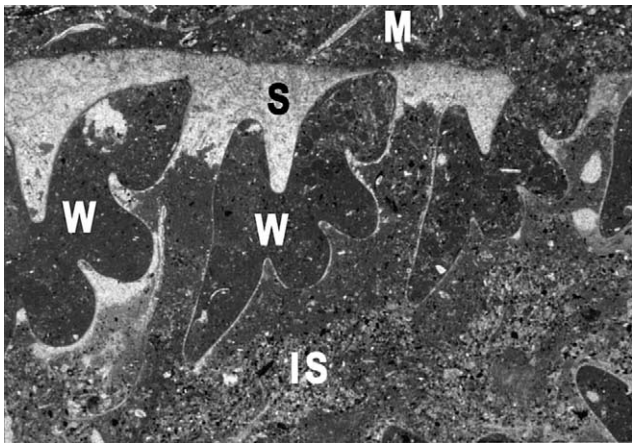

Fig. 5. Longitudinal section through nerineid gastropod, showing typical cross-sections of whorls (W). The former inner, massive part of the shell is nearly completely filled by an internal sediment (IS) of lime mudstone to bioturbated, peloidal-bioclastic wackestone to packstone that sharply abuts shell relicts (S) along an irregular, embayed boundary. The packstone within the space formerly occupied by shell aragonite is of similar composition and in physical continuity with the matrix (M) in which the gastropod is embedded. Upper Turonian, Brandenberg, Austria. Width of view 17 mm.

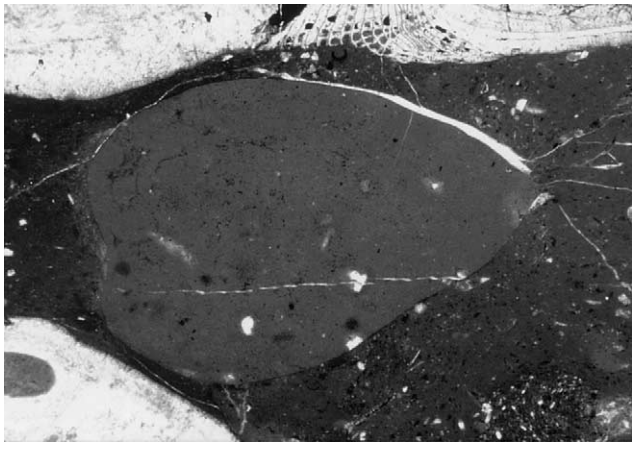

Fig. 6. Steinkern of a bivalve that has been completely dissolved. The rock is a floatstone with nerineid gastropods and large radiolitid fragments, with a matrix of lime mudstone to mixed bioclastic–siliciclastic wackestone riddled by firmground burrows. The light fringe on top of the bivalve is a later crack. Coniacian, Brandenberg, Austria. Width of view 17 mm.

"hair line" that may represent a relict of the periostracum (Fig. 2(4)). Periostracum can be quite resistant to dissolution (e.g. Scoffin, 1992, p. 66; Powell et al., 2002), even over geological time (Brett and Baird, 1986, p. 215; Clark II, 1999).

The central part of aragonitic calcareous algae (dasycladaceans, codiaceans) in many cases displays an interior cavity of highly irregular shape. Along the surface of the interior cavity, the canals in the algal medulla are truncated. Well-preserved fossils of algae indicate that the irregular interior cavity is, either, a widened primary central canal (such as in many Mesozoic dasycladaceans, Fig. 2(3)) or has been newly excavated from a once thoroughly calcified medulla (such as in anthracoporellid dasycladaceans, Figs. 7 and 8). In fossils originally composed of both aragonite and calcite, such as molluscs, most commonly the aragonite was dissolved while the calcite was preserved. The former aragonitic portion may have disappeared completely, and the matrix abuts the calcite shell layer (Fig. 9). In some cases, internal sediment was infilled before dissolution of the aragonitic shell layer (Figs. 2(2B) and 10). In thin section, shells or skeletons of primary calcite rarely show clear-cut indications for dissolution. In some groups, a thin-walled shell/skeleton of calcite favoured dissolution, such as observed for radiolitid

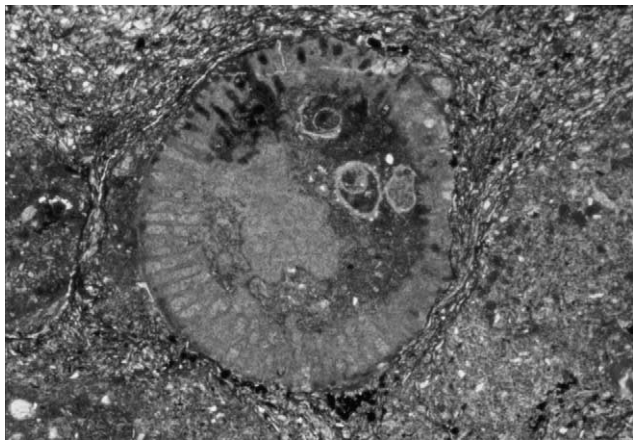

Fig. 7. Cross-section through *Anthracoporella*, with the central part of the medulla largely removed by early dissolution. This is the prevalent style of preservation of these algae in *Anthracoporella* mounds; completely preserved specimens are comparatively rare. Upper Carboniferous, Auernig Group, Carnic Alps, Austria. Width of view 10 mm.

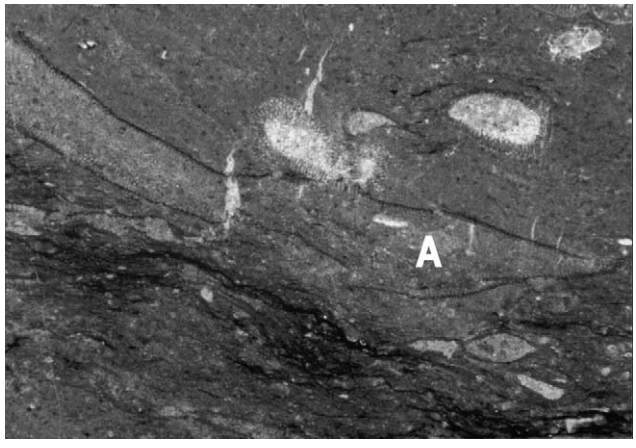

Fig. 8. Floatstone from an *Anthracoporella* mound, with the algae in various stages of taphonomic alteration by dissolution. The *Anthracoporella* (A) in the center of view has been largely dissolved, with only the external part of the medulla preserved. Upper Pseudoschwagerina Formation, Lower Permian, Carnic Alps, Austria. Width of view 10 mm.

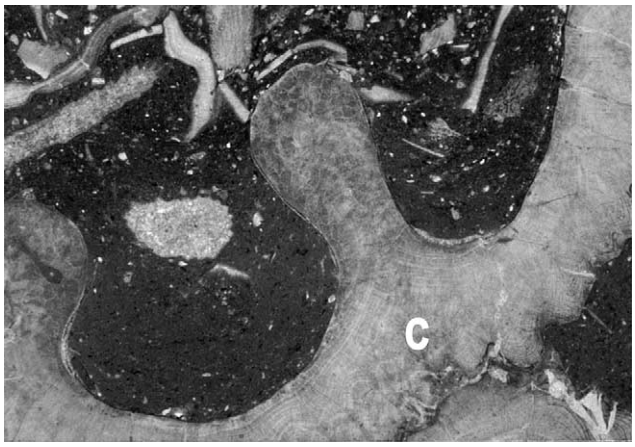

Fig. 9. Transversal section through *Hippurites* from a rudist biostrome. The aragonitic shell layer has been completely dissolved, and the calcitic shell layer (C) directly abuts the matrix of the biostrome. Upper Turonian, Gams, Austria. Width of view 17 mm.

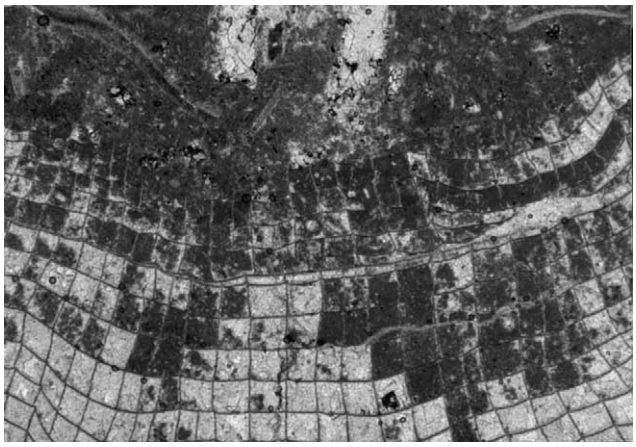

Fig. 11. Detail of transversal section through *Eoradiolites*. The inner, aragonitic shell layer has been completely dissolved and the calcitic shell layer with a boxwork composed of thin-walled cells also was subject to localized dissolution. Note also that the calcitic boxwork shell layer directly abuts the sediment fill of the shell. Upper Cenomanian, Abu Qada Formation, Central Sinai. Width of view 12 mm.

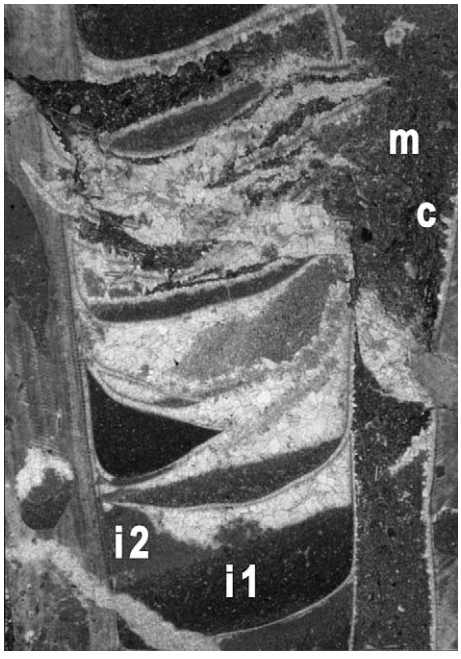

Fig. 10. Longitudinal section through *Vaccinites* from a rudist biostrome with a parautochthonous fabric. The former aragonitic shell layer, now preserved as calcite pseudospar, was preserved locally and provided the substrate for geopetal infill of at least two generations of internal sediment (i1, i2). Locally, however, the aragonitic layer was dissolved, and the substrate was overgrown by a fringe of skalenohedral calcite spar (c). Subsequently, the spar became overlain by a bioclastic siltstone (m) that is in physical continuity with the matrix in which the rudist is embedded. Upper Santonian, Gosau, Austria. Width of view 17 mm.

rudists (Fig. 11). For radiolitids, complete dissolution of both aragonite and calcite may produce patches of internal breccia composed of the sedimentary fills of the intertabular chambers (Sanders, 1999, 2001). In Palaeozoic corals, tabulozoans and stromatoporoids, in the thin sections available to the author, despite the construction of their skeletons of thin walls of calcite or aragonite, clear-cut indications of early dissolution were not observed. A Devonian rugose coral that was partly dissolved while exposed on the sea floor is shown by Brett and Baird (1986, Fig. 8).

3.2.1. Interpretation

Contact between matrix and calcitic shell parts, along the largest part or all of the calcitic fossil relict, is a good indicator for dissolution of the aragonitic shell part within the soft sediment. Similarly, sediment-filled moulds of fossils that are in contact, over all their extent, with the matrix were produced by dissolution. In the case of moulds of fossils that, in part or entirely, consisted of aragonite and that are filled by matrix, physical continuation of the biomould fill into the adjacent matrix should be checked for (cf. Sanders, 1999, 2001). Biomoulds filled by crystal silt do not necessarily indicate subaerial exposure. Crystal silt, resembling vadose silt, is common as a partial replacement of ammonite shells dissolved within the firm sediment on the sea floor (e.g. Schlager, 1974, p. 52). In neritic successions as are discussed here, except for obvious features of karstification (e.g. dykes, speleothems), similar sediment-filled biomoulds may be produced along and closely below emersion surfaces (see e.g. Walkden and De Matos, 2000). Filling of biomoulds with marine sediment further below an inferred emersion surface, however, necessitates that there existed a continuous karstic porosity along which the sediment could infiltrate; the existence of such pathways, equally, should be checked. Moreover, filling of moulds of shells that were dissolved, without subaerial exposure while resting in neritic car-

bonate sediment, by sediment of different composition has been described by Boyd et al. (1999).

Most extant calcareous green algae calcify from the margin towards the interior. Thus, the interior of calcareous green algae may be intrinsically less densely calcified than the marginal parts and, hence, is prone to dissolution. This may be reflected by the common observation that in Palaeozoic to Tertiary calcareous green algae, dissolution proceeded mainly from the central part towards the margin. In shells, or shell parts of primary low-magnesium calcite, dissolution is related to a thin-walled or otherwise delicate construction (such as thin, hollow spines). In such shells, because of their large total surface, microbial infestation and/or diagenetic microenvironments conducive to dissolution may have been effective (Sanders, 1999).

In thin section view, gaps in shells resulting from dissolution or corrosion (see e.g. Flessa and Brown, 1983) may be difficult to distinguish from mechanical breakage. For molluscs, a small amount of more-or-less equally distributed thinning of shells due to dissolution in the unlithified sediment is widespread but, with few exceptions (see Section 3.3 below), is difficult to recognize unequivocally in thin section. Chemical dissolution does not necessarily produce embayed, deeply pitted surfaces, but is often associated with a gradual thinning and pinchout of shells/skeletons, or parts thereof, as is well-documented for mollusc shells (e.g. Driscoll, 1970; Alexandersson, 1978; Flessa and Brown, 1983). To judge whether dissolution had occurred, basic knowledge of the original structure of a skeleton or shell is needed. The septae of rugose corals, for instance, are long in the lower part of the polypar and are shorter near its upper margin. In oblique cross-section of a rugose, thus, a part with short septae is opposed to a part with longer septae. In tabulozoans, the polypar walls are connected by gaps (stolons) that are a primary feature. As mentioned above, presence of fossils of formerly aragonitic composition does not necessarily indicate that the entire aragonitic biocoenosis is fossilized.

3.3. Contrasts in preservation

In some beds of shell coquina, a distinct vertical gradient in shell preservation across the bed was observed (Figs. 12(1), Table 1). In the lower part of these beds, most or all of both articulated and disarticulated shells are extremely thin; internal moulds of articulated bivalves recognizable by a slightly different colour of the sediment fill or as brown "hair lines" are common (Fig. 13(A)). Up-section, in the middle part of the beds, the shells overall are thicker, may show pinch and swell of thickness along their extent, and may be partly pyritized. Pinching and swelling does not follow growth features of bivalves, such as shell thinning with decreasing age of a given shell sector, or ornamentation, but occurs randomly along the shell transect (Fig. 13(B)). In the upper part, the shells commonly are largely preserved (Fig. 13(C)). In bioturbated limestones, on a scale of a few centimeters to about 10 cm, patches with formerly aragonitic mollusc shells largely preserved were observed adjacent to patches rich in internal moulds (Fig. 14(A) and (B)). In a Cretaceous neritic succession, levels with uncompacted carbonate concretions up to more than 1 m in size with fossils are embedded in compacted marlstones to organic-rich limestones with a few fossil ghosts only (El Albani et al., 2001) (Fig. 12(2)). In Silurian neritic limestones, on a lateral scale of kilometers, Cherns and Wright (2000) found that a fauna mainly of silicified molluscs and unsilicified brachiopods laterally grades into pure limestones with brachiopods only, without a significant change in environment (substrate) and depositional water depth indicated (Fig. 12(3)).

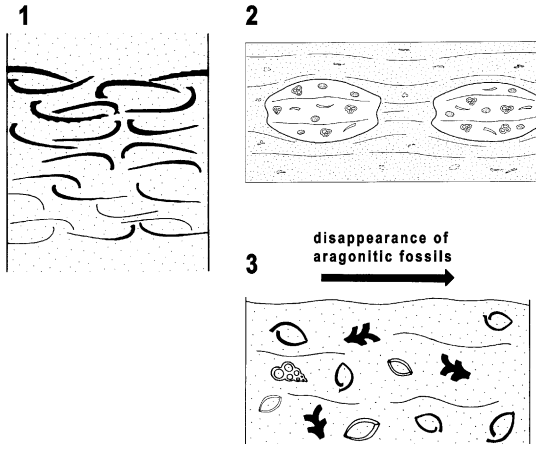

Fig. 12. Criteria to recognize dissolution. (1) Across shell beds that most probably originated during a single event of transport and deposition, a gradual vertical transition from steinkerns or thinned, disarticulated shells at the base to more-or-less completely preserved shells at the top is present. (2) Marine cements lining or filling early pores contain a surface of irregular outline that may be encrusted by metal oxides or pyrite. (3) Cavities of highly irregular outline that may, in part or completely, be fringed by metal oxides or pyrite; fossil shells may show features of dissolution.

3.3.1. Interpretation

The preservation gradient of shells across the coquina beds, the internal moulds of bivalves, the very thin shells, and the shells showing pinching and swelling unrelated to ontogenetic growth or sculpture are all interpreted as a result of dissolution within the sediment. The gradient in shell preservation indicates that dissolution at least largely proceeded at the site of final deposition of the coquina. The dark brown "hair lines" that locally define the outline of bivalve shells may represent a remnant of the periostracal shell layer. In some beds, the partly pyritized shells suggest that

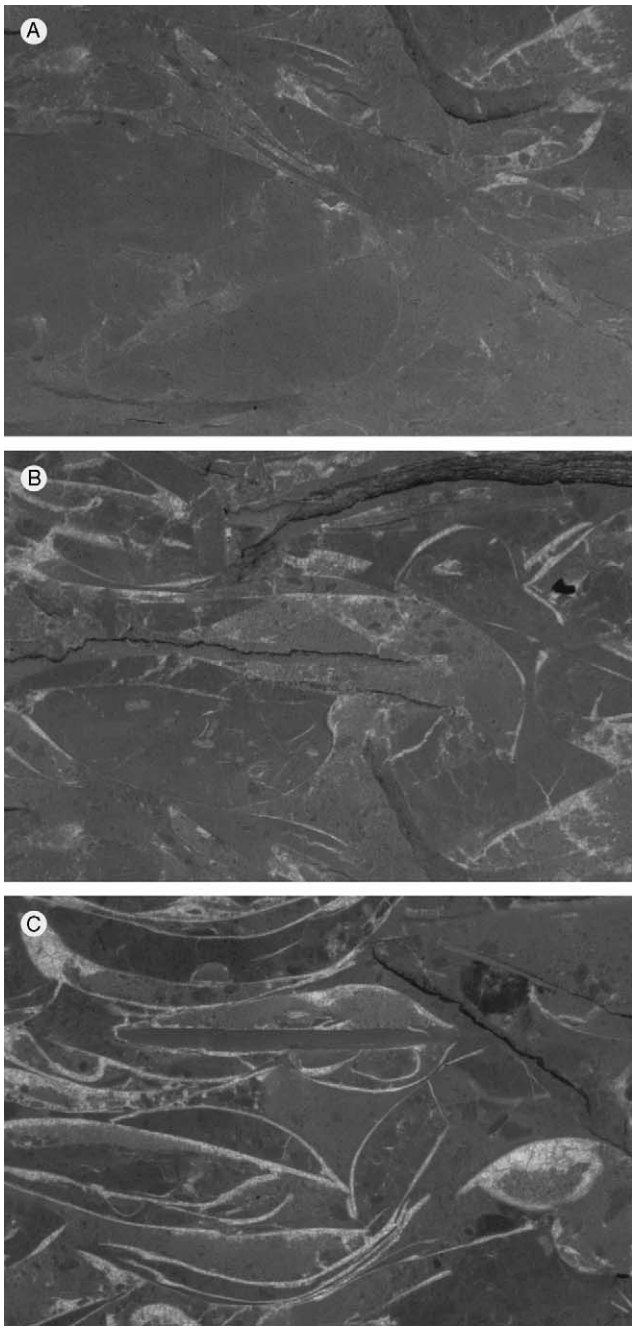

Fig. 13. Three details, from bottom to top, across a bed of bivalve coquina about 7 cm thick. (A) Lower part of bed: bivalve steinkerns visible by slightly different colour relative to matrix, and bivalve shells are visible as faint lines only. (B) Middle part: bivalve shells are recognizable, but show irregular thickness along their extent. (C) Closely below top of bed: Shells are overall fairly well-preserved. Upper Triassic, Kössener Formation, Tyrol, Austria. Width of view for all photos 17 mm.

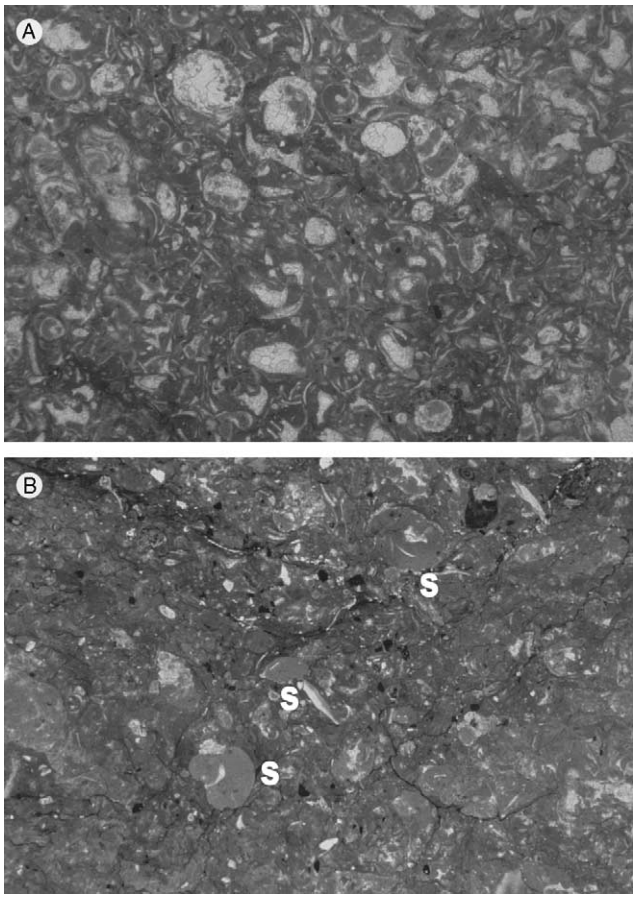

Fig. 14. (A) Bioturbated packstone to fine-grained rudstone composed of abundant small cerithiaceans and nerineids. (B) Same thin section, about 5 cm away from photo A. Here, the limestone is a bioturbated wackestone to floatstone with steinkerns (S) of small gastropods and small bivalves. Coniacian, Brandenberg, Austria. Width of view 17 mm.

dissolution was accompanied or closely followed by sulfate reduction and sulfide precipitation (see Section 4 for discussion). The observation that the thinned shells and the internal moulds, and the vertical gradient in shell preservation are preserved in situ indicates that these coquina beds were not subject to significant macrofaunal burrowing since deposition. A moderate amount of shell dissolution is very common, at least for bivalves, in carbonate depositional environments (e.g. Powell et al., 2002). Revelle and Fairbridge (1957, p. 281) and Fairbridge (1967, p. 34) described experiments by other authors who recorded a sharp decrease in pH during onset of decay and ensuing death within the shell microenvironment. The drop in pH by microbial metabolism within the decaying tissue leads to rapid corrosive attack of the shell from within (Revelle and Fairbridge, 1957, p. 281; Fairbridge, 1967, p. 34; Berner, 1969). Experiments on shell dissolution upon burial showed that thin shells suffer comparatively more dissolution; thus, the initial thickness of the shell may also influence the process (Revelle and Fairbridge, 1957, p. 281f).

"Paper shells" linked by taphonomic transitions to fully preserved bivalve shells were described by Alexandersson (1978, p. 325) from siliciclastic shelf sediments. Surface photographs from bivalve shells thinned

by dissolution while resting in soft siliciclastic sediments were shown by Aller (1982, Fig. 5). On the bivalve surfaces, dissolution did not produce a pitted surface, but typically removed a layer of more-or-less equal thickness over a larger area of the shell. The layer removed by dissolution is delimited by a small "scarp" less than 1 mm in height towards uncorroded, or less corroded, shell (see Aller, 1982, Fig. 5). In bioturbated limestones, the described centimeter- to decimeter-scale variations in shell preservation may have originated either before or concomitant to bioturbation (see also Sanders, 2001).

In the mentioned Cretaceous neritic succession mainly of marlstones and organic-rich limestones, the large calcite concretions with fossils probably formed by carbonate dissolution (micrite, fossils) related to sulfate reduction in unlithified, unbioturbated sediment; the dissolved calcium carbonate migrated by diffusion towards preferred sites of precipitation, where the concretions formed (El Albani et al., 2001). Similarly, in Silurian neritic limestones, the large-scale preservation gradient from a fauna of brachiopods plus silicified molluscs into a brachiopod fauna only, without a change in substrate and depositional water depth indicated, is interpreted by Cherns and Wright (2000) as a product of early dissolution in marine-derived pore fluids. In the example described by Cherns and Wright (2000), dissolution was complete and proceeded in the soft sediment; thus, ghost fabrics of fossils did not form. Preservation gradients related to syn- to early post-depositional carbonate dissolution thus occur on a wide range of scales in space.

3.4. Corroded early cements

Within pores in Ordovician buildups, fibrous marine cements are present that are cross-cut by surfaces that show an irregular outline, and that are coated locally by a sub-millimetre thin layer of iron sulfide, or pseudomorphs thereafter (Fig. 15(1), Table 1) (Tobin and Walker, 1996; Tobin and Bergstrom, 2002, Fig. 5). The surfaces that cross-cut the marine cements were interpreted as corrosion surfaces, resulting from early post-depositional dissolution in marine-derived pore fluids (Tobin and Walker, 1996). The dissolution surfaces covered by iron sulfide or its pseudomorphs probably formed upon H^+ release from oxidation of hydrogen sulfide and from precipitation of iron sulfide; these phenomena were, at least in the examples described, related to a fluctuating anoxic–oxic interface in the sea water column (Tobin and Bergstrom, 2002; see also Read, 1982) (see Section 3.6 below).

In rudist biostromes with a parautochthonous fabric (see Sanders and Pons, 1999; Johnson et al., 2002, for description of rudist fabrics), corrosion of early cements in contact with sediment is common locally. The formerly aragonitic shell parts of the rudists have been, in part or totally, dissolved before cement growth and/or before sediment infill (Fig. 16). Marine cements, typically thin fringes of radial-fibrous cement, may have precipitated before or after aragonite dissolution, to judge from the position of the cements relative to the aragonite layer and/or relative to sediment infill (see Fig. 2(2B)). In many cases, the radial-fibrous cement (often preserved relictically as a "crypto-fibrous calcite cement"; see Lees and Miller, 1995, Fig. 39, for term) is overlain by blocky calcite spar that partly fills the intraskeletal pore space of the shell. The blocky calcite spar and/or the fibrous cement are overlain, along a boundary that cross-cuts cathodoluminescence zones, by internal sediments (typically lime mudstones, wackestone to packstones). The internal sediment may be bioturbated (see also Fig. 5), and is in physical continuity with the matrix in which the shells are embedded; the internal sediment may contain floating clasts, with irregular outline, of the cements it is in contact with (Fig. 16). Very similar early diagenetic pathways were observed by the author in gastropod shell beds (unpubl. data).

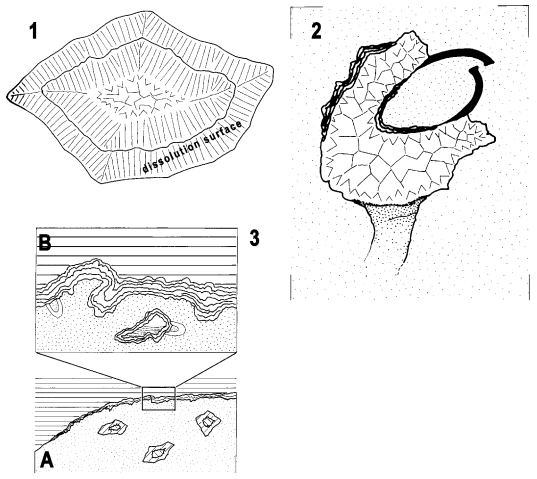

Fig. 15. Criteria to recognize dissolution. (1) Pore filled by marine cement and blocky calcite spar. The marine cement is cross-cut by a dissolution surface (see also Fig. 2(2B)). (2) Pore with a highly irregular outline, locally with a marginal fringe of pyrite or of metal (iron, manganese) oxides. Bioclasts may show evidence of dissolution. (3A) Buildup covered by pyritic hardground. In pores below the hardground, marine cements are cross-cut by dissolution surfaces. (3B) The contact of the pyrite hardground with the underlying limestone is highly irregular, fossils are truncated. Pores just below the hardground may be coated by pyrite, too.

3.4.1. Interpretation

For the rudist biostromes, the described succession of, typically, aragonite dissolution, radial-fibrous cement precipitation, precipitation of blocky calcite spar, and infill of (bioturbated) internal sediment that is in physical continuity with and of similar to identical

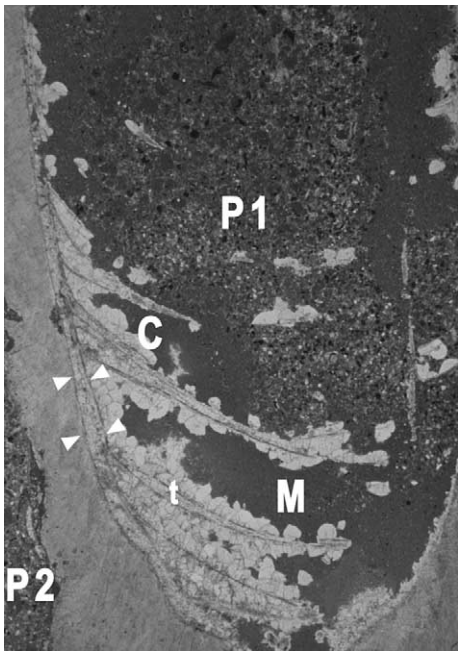

Fig. 16. Oblique section through *Hippurites* from an interval of rudist limestone. The aragonitic shell layer has been partly dissolved, and is partly preserved as blocky calcite spar (relict outline of the aragonite shell layer indicated by white arrow tips; t: formerly aragonitic tabulae of the rudist shell), before growth of cryptofibrous cement and blocky calcite spar (C). Both the blocky calcite spar and, locally, the cryptofibrous cement are truncated along the contact (checked by cathodoluminescence) with an overlying lime mudstone (M) that contains floating cement clasts. The mudstone, in turn, is ''riddled'' by patches of a peloidal-pelletal packstone (P1) that is identical in composition and, locally, in physical continuity with the matrix packstone (P2) in which the rudist is embedded. Upper Turonian, Brandenberg, Austria. Width of view 12 mm.

composition as the matrix hosting the shells, indicates repeated changes from under- to oversaturation for calcium carbonate, while the shells rested in soft to firm sediment. Although the taphonomic successions differ from site to site in detail, overall identical phenomena were observed in rudist shells from Upper Cretaceous successions in Austria, Italy, Spain and Greece. Growth of blocky calcite spar in unlithified sediment may be aided by the large intraskeletal pore space of rudist shells, providing a hard substrate for crystals to nucleate. Blocky calcite spar thus may grow very early, under shallow burial in soft sediment, and from marine-derived pore fluids. Although the compartmentalized intraskeletal pore space of rudists may have been conducive to early calcite spar growth, the observation of similar phenomena and similar taphonomic pathways in gastropod shells suggests that growth of blocky calcite spar in soft to firm, bioturbated sediment may not be uncommon. Similarly, disseminated ''jigsaw piece'' dolomite has been interpreted as a result of dolomite growth in soft, bioturbated sediments (Hendry et al., 2000).

The fluctuations in saturation state for calcium carbonate, as indicated by at least two phases of dissolution, may have been caused by several processes, for instance by changes of burial depth and consequent shift of the anerobic/anaerobic boundary (e.g. Brandes and Devol, 1995, p. 793), and/or burial and subsequent turnover by burrowers (cf. Ku et al., 1999; see Section 4). Aragonite dissolution may have started while the shells were still partly exposed on the sea floor, where aerobic oxidation of organic matter may have effectively produced CO_2 and an associated decrease in saturation state. Prior to subsequent (partial) aragonite dissolution, fringes of radial-fibrous cement precipitated. Upon burial of the shell into the zone of sulfate reduction (including anaerobic methane oxidation), alkalinity rise associated with sulfate reduction may have triggered the precipitation of blocky calcite spar; this may have been effective, or possible, only in intraskeletal pores. Upon removal of part of the sediment, for instance during high-energy events, the shells became re-exposed on the sea floor, or were re-introduced into the burrowed layer. In iron-poor sediments such as carbonates, reoxidation of reduced by-products of organic matter remineralization, such as hydrogen sulfide, can lead to carbonate dissolution (e.g. Boudreau and Canfield, 1993; Ku et al., 1999). A single to several cycles of burial followed by exhumation or an intermittent shallowing of burial depth are characteristic taphonomic pathways of many shell beds (e.g. Kidwell and Bosence, 1991; Kidwell, 1998), and are also recorded for the early diagenesis of septarian shales, nodular limestones and marine carbonate firmgrounds to hardgrounds (e.g. Fürsich, 1971; Kennedy and Garrison, 1975; Baird, 1976; Möller and Kvingan, 1988; Wilson et al., 1992; Kim and Lee, 1996). Irrespective of the precise processes that produced the fluctuations of saturation state, in the shallow subtidal, tropical carbonate palaeoenvironments considered, these fluctuations most probably were coupled to the remineralization of organic matter (see Section 4).

3.5. Pores overprinted by dissolution

In limestones from shallow subtidal to bathyal carbonate environments, a specific type of pore has been observed (the bathyal limestones were inspected as a check to increase certainty with respect to interpretation of pore origin, and to recognize potential effects of subaerial exposure on pore development in the shallow subtidal suite of muddy limestones). In neritic limestones, these pores are fairly common in bafflestones to floatstones deposited from lime mud-rich skeletal mounds (locally with microbialites) to level-bottoms, but were observed in mudstones to fine-grained, bioclastic-peloidal wackestones to floatstones, too. The pores range from a few millimeters to 2–3 cm in width, and are associated with evidence for softground bur-

rowing and firmground burrows. The overall shape of the pores is highly variable, and ranges from vertically elongated to plume-like to elongate parallel to bedding (stromatactoid) (Fig. 15(2), Table 1).

The lower part of many pores is filled geopetally by lime mudstone to wackestone to microspar to pseudospar (Fig. 17). Within the geopetal pore-fills, a gradual vertical transition from lime mudstone into wackestone into pseudospar is common. The wackestone to pseudospar contains a similar bioclast spectrum to the matrix. The lower part of many pores may develop gradually from the host limestone, in that the geopetal pore-fill becomes gradually distinct from the host limestone with respect to colour and/or texture, while the pore margins become increasingly more distinct upsection. In the upper part of the pores, the boundary towards the host limestone is sharp and of irregular, embayed outline. Alternatively, the pores are filled by a single generation or several generations of internal sediment, and the entire pore margin is sharply defined (Figs. 18 and 19). The upper part of the pores, if devoid of internal sediment, is filled by luminescent blocky calcite spar. Within some pores, clasts with pitted, embayed outline and fossil relicts are present that are derived from the host limestone (Fig. 17). The irregular surface of the pores in many cases is stained brown, or is coated by a sub-millimetre thin brown crust, or by a thin fringe of pyrite (Figs. 15(2), 17, 18 and 19). Most commonly, no microscopically identifiable pyrite is present in the host limestone. The pores may show all transitions from sediment-filled firmground burrows (circular

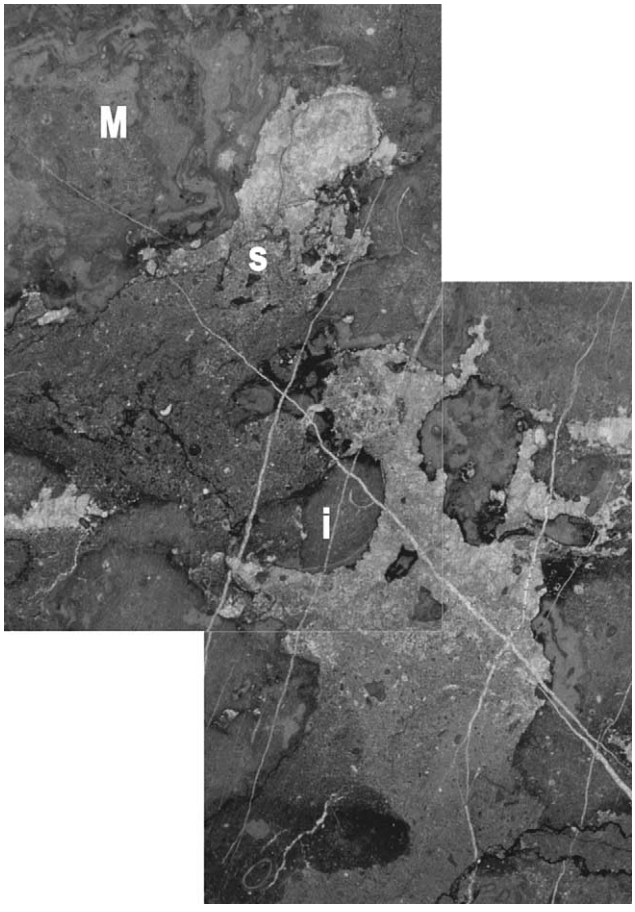

Fig. 17. Thin section from an interval rich in microbialites (M), deposited in deep neritic to upper bathyal depths. In this limestone, cavities up to about 2 cm in width are present that show a highly irregular outline. Along the margins of the cavities, crusts of finely crystalline pyrite are present locally (black in photo). Note also intraclasts (i) with truncated shells, and faint shell relicts (s). Lower Jurassic, Tyrol, Austria. Width of view 17 mm.

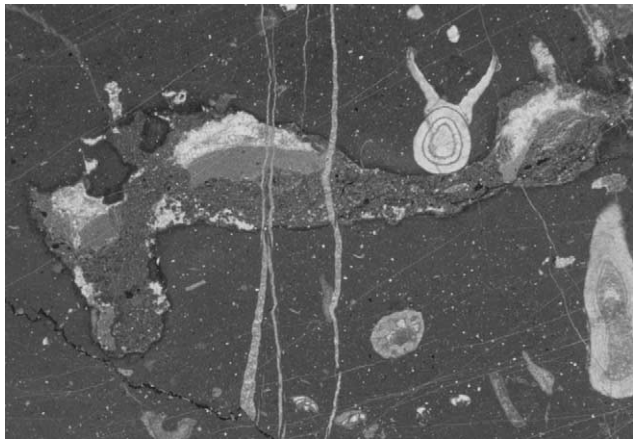

Fig. 18. Auloporid coral bafflestone from an auloporid mound. In these mounds, the matrix of lime mudstone is riddled by cavities up to about 3 cm in size that show a highly irregular, pitted and embayed outline. The cavities are filled geopetally by a single or several generations of internal sediments that locally cross-cut each other along irregular boundaries. Upper Carboniferous, Auernig Group, Carnic Alps, Austria. Width of view 17 mm.

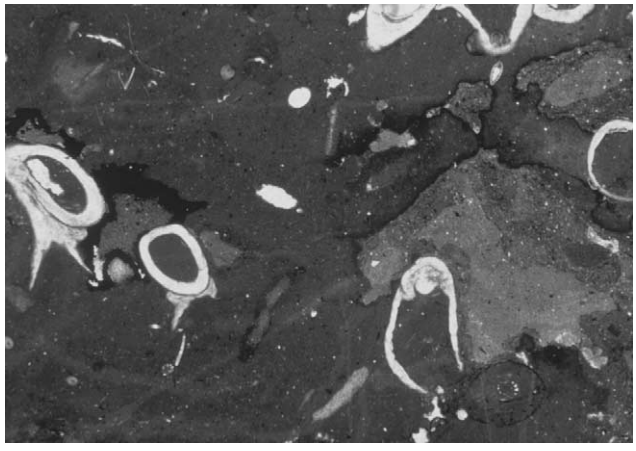

Fig. 19. Auloporid coral bafflestone from an auloporid mound. The lime mudstone matrix is riddled by cavities with a highly irregular outline and that are filled by internal sediments. The black fringe along the margin of the cavities consists of finely crystalline pyrite. The cavities probably originated from firmground burrows, but were overprinted and widened by dissolution. Upper Carboniferous, Auernig Group, Carnic Alps, Austria. Width of view 17 mm.

to tunnel-shaped tracts with smooth margins, filled by sediment that may show backfill lamination) to geopetally sediment-filled, subcircular to elongated pores with pitted margins, to highly irregularly shaped pores with stained margins, and with internal clasts derived from the host limestone (see above). In the examples shown, no hints of subaerial exposure of mounds were identified (Krainer, 1992, 1995). Locally, the pores are associated with short cracks filled by blocky calcite spar. The cracks may open from below or from the lateral margins into a pore, but most commonly debouch from above. Crack margins may fit, but more commonly are irregularly embayed and pitted.

3.5.1. Interpretation

The sharply defined, highly irregular outline of the described pores, and the presence of fossil relicts and small intraclasts of the host limestone with irregular outline, and the presence of corroded-truncated shells all indicate that these pores were overprinted by dissolution, early after deposition of the sediment. The brown stain and brown crusts that line the margins of many pores are closely similar to ''ferromanganese'' crusts described by Reitner (1993) in association with light-independent microbialites in Recent coral reefs. The ferromanganese biofilms grow under oxic to suboxic conditions, are reported to cause dissolution of more than 40% of the carbonate (Reitner, 1993, p. 12), and are associated with dissolution surfaces and dissolution-widened pores up to at least a few millimeters in width (cf. Reitner, 1993, p. 12, 20f, pls. 2, 3). In oxic to suboxic pore waters within sediments, Fe^{2+} can be oxidized to insoluble Fe oxide by Mn oxides, liberating dissolved Mn^{2+} into solution (see e.g. Canfield et al., 1993, p. 3869). Manganese reduction can also proceed independently at low oxygen concentrations (cf. Froelich et al., 1979; Berner, 1981). Oxidation of reduced iron and manganese is associated with release of two moles H^+ per one mole of Fe or Mn (Boudreau, 1991, Eqs. (VI) and (VII)); this may, at least in part, explain the dissolution capacity of ferromanganese biofilms. Alternatively, the pyrite fringes locally present along the margins of some pores suggest that dissolution was related to release of hydrogen ions (H^+) during reaction of hydrogen sulfide with reduced iron. The hydrogen sulfide most probably was produced by bacterial sulfate reduction (see Section 4). In anoxic environments, bacteria metabolizing by disproportionation of elemental sulfur (a product of sulfate reduction; see e.g. Machel et al., 1995, Fig. 2) increase the concentration of both sulfate and hydrogen ions, leading to pH decrease (Böttcher et al., 2001). In presence of iron (as FeOOH), the iron reacts with H_2S to pyrite; this, in turn, leads to production of elemental sulfur that may fuel further disproportionation (cf. Böttcher et al., 2001, Eqs. (1)–(4), p. 1607).

Although the presence of partly dissolved shells and limestone solution intraclasts suggest that the formation of at least some of the pores was associated with substantial pore widening by dissolution, it is considered unlikely that the pores formed entirely by dissolution. Probably, some initial pathway was necessary for focussing of pore fluids within. Because the pores were observed in limestone showing evidence for softground to firmground burrowing, pore development may have commenced from burrows that, either, were open, or that were filled with more permeable, organic-rich sediment. The presence of pyrite along the pore margins indicates that the pores provided a specific microenvironment. Perhaps, episodic bioirrigation of open firmground burrows, and/or an enhanced content of (partly) filled burrow networks in organic matter provided additional iron and sulfur for pyrite formation. In addition, compactional dewatering focussed or debouching into burrow networks may have provided a source for reduced chemical species. That dewatering was involved, at least in some cases, is suggested by both the gradual upward development of some pores from the host limestone, and by the vertically elongated to plume-shape of many pores. The short cracks that locally are associated with the pores formed by localized extension, probably due to compaction and (episodic) dewatering. Similar short cracks related to dewatering and/or rapid deformation were described from deep-water limestones by Enos (1977, Fig. 35) and by Pratt (2001) for septarian concretions. The observation that some of the cracks described in the present paper show irregular, embayed, non-fitting margins suggests local dissolution.

Commonly, early post-depositional carbonate dissolution is not considered as a process of diagenesis in fossil bioconstructions and burrow-mottled muddy limestones. In lithified reef frameworks, however, below a depth of commonly more than a few decimeters, suboxic to anoxic pore waters with near-seawater sulfate concentrations, rich in biogenic methane, and with a pH lower than sea water are present (Sansone et al., 1990; Tribble et al., 1990; Haberstroh and Sansone, 1999). Carbonate saturation of the pore waters is low to, in a few cases, negative, probably because of bacterial oxidation of organic matter (Sansone et al., 1990). Chemical modelling also suggests that aragonite dissolution may be common within reefs (Tribble et al., 1990; Tribble, 1993). In cavities of Recent reefs, crusts of iron–manganese bacteria are associated with distinct corrosion of limestone (Reitner, 1993; see e.g. Boudreau, 1991, for chemistry). Within Holocene algal cup reefs of the Bermudas, Ginsburg and Schroeder (1973, p. 588, Figs. 14, 18 and 22) observed irregular pores up to a few centimeters wide that, on cut slabs, appear arranged into anastomosing channels and vugs. The pore surfaces are coated by black veneers less than a millimetre thick, and cross-cut both the reef framework and lithified internal

sediments, thus indicating formation "by solution of unknown origin" (Ginsburg and Schroeder, 1973, p. 588). No indication was given that the algal cup reefs had been subaerially exposed (Ginsburg and Schroeder, 1973, p. 610). In Holocene reef limestones of Belize, James and Ginsburg (1979, p. 147ff, Figs. 6–27) observed open pores up to a few centimeters in width that show a highly irregular, pitted outline. The pore surfaces are coated by a layer up to 0.5 mm thick of iron oxide or iron–manganese oxides. Identical metal oxide coatings locally are also intercalated into successions of internal sediments in the pores, or between successive generations of aragonite cement (James and Ginsburg, 1979, p. 149). As pointed out by James and Ginsburg (1979, p. 152), no evidence for subaerial exposure was found, and they conclude (p. 180) that "the presence of iron oxide coatings alone in ancient limestones is an undependable criterion for subaerial exposure." Similar red–brown coatings with a highly irregular outline were observed by the present author on the surface of bioclasts, below aragonite cement, and intercalated between successive generations of botryoidal aragonite cements in frame cavities of Pleistocene reefs of the Red Sea (unpubl. data). Tobin and Walker (1996, p. 731) described iron-oxide coated, marine dissolution discontinuities within Ordovician "Kullsberg" reef cement successions. Similar to the limestones that contain the dissolution pores described herein, there is no evidence that the Kullsberg buildups were exposed subaerially (Tobin and Walker, 1996, p. 730). In Waulsortian mounds, Miller (1986) described a widespread type of pores that are up to a few centimeters wide, that originated at least in part by dissolution of calcium carbonate that, according to Miller (1986, p. 327) probably was driven by organic matter oxidation. Some of these pores are associated with dewatering fractures widened locally by dissolution (cf. Miller, 1986, p. 327).

The observation that the Fe/Mn-rich crusts line the inner part of pores and coat dissolution intraclasts indicates that these crusts formed last in the "corrosion succession". Thus, a first phase of carbonate dissolution in suboxic to anoxic pore waters, probably driven mainly by sulfate reduction and iron sulfide precipitation, was followed by suboxic to oxic conditions. If iron and manganese were present, within sulfate-depleted pore waters, these elements were largely oxidized, with resulting corrosion. A similar diagenetic succession was reconstructed by Bourque and Boulvain (1993, p. 616f, Fig. 14) for the diagenetic succession in *Stromatactis* of Late Palaezoic carbonate mounds. After sulfate reduction in a shallow anoxic layer, in a depth layer below, microbial oxidation of iron sulfides took place with suboxic to oxic pore waters. The oxidation of iron sulfide may well be accompanied by dissolution, since it liberates hydrogen ions (cf. e.g. Berner and Westrich, 1985; Boudreau, 1991). Farther below, perhaps under more than 10 m of burial, when the sediment was in a semi-lithified to incipiently brittle state, crack fissures opened (cf. Bourque and Boulvain, 1993, Fig. 14). Thus, vertical shifts of organic matter oxidation layers because of burial and re-excavation are not necessary to shift from cementation to dissolution, but may be related to pore water evolution. Depending on the relative amounts of organic sulfur, manganese and iron, the degree of openness of the diagenetic system, and release or consumption of hydrogen ions as a result of prevalent redox reactions involving sulfate or sulfur (see Machel et al., 1995; Böttcher and Thamdrup, 2001), it seems possible that dissolution pores in one case become lined by ferromanganese crusts, in another, by pyrite fringes.

3.6. Dissolution along hardgrounds

Along a drowning unconformity on top of Middle Ordovician neritic downslope buildups of the Appalachians, a hardground is present that is coated by phosphorite crusts and/or by crusts, up to 10 cm thick, of interlaminated iron sulfide and calcite (Fig. 15(3)) (Read, 1982, p. 205). In addition, phosphorite/iron sulfide hardgrounds are also common in interbuildup and buildup limestones (Read, 1982, pp. 204–205). The formation of both types of hardground was associated with dissolution of the immediately underlying limestone, but the limestones along the drowning unconformity seem to have been subject to more aggressive corrosion (cf. Read, 1982, p. 205). The hardgrounds formed in association with an oxic–anoxic interface within the sea water column; this interface probably was situated in neritic depths (see Read, 1982, p. 208). Carbonate dissolution may have been driven by release of H^+ upon oxidation of H_2S encroaching from deeper waters (phosphorite crusts) and, in anoxic sea water, from H^+ release from reaction of dissolved iron with H_2S diffusing up from the buildups (sulfide crusts) (Read, 1982, p. 205). In addition, in pores of the buildups, fibrous marine cements are present that contain dissolution surfaces that formed before drowning of the buildups (Fig. 15(1) and (3)) (Tobin and Bergstrom, 2002). The intermittent dissolution of the cements probably was related to the same or a similar set of processes to those associated with the anoxic–oxic interface in the sea water, i.e. reoxygenation of pore waters containing hydrogen sulfide (Tobin and Bergstrom, 2002, p. 414f). During platform drowning, (episodic) impingement of dys- to anaerobic waters into shallow depths, perhaps, is relatively common (cf. Mallarino et al., 2002). It should be noted here that in Mesozoic and Cainozoic deep-water limestones, evidence for dissolution is very common along hardgrounds, in particular beneath crusts of ferromanganese minerals and/or of phosphorite.

3.7. Pitted microspar crystals

In tropical–subtropical limestones, a microsparitic matrix previously was thought to represent a product of aggrading neomorphism during micrite recrystallization (see e.g. summary in Bathurst, 1975). Scanning electron microscopy, however, reveals that a portion of many microsparites that originated from aragonite-rich muds, in fact is a finely crystalline cement (Steinen, 1982; Lasemi and Sandberg, 1984). In lithified limestones ranging (with gaps in documentation) in age from Silurian to Pleistocene, "pitted" microspar cement crystals are widespread (Table 1) (Lasemi and Sandberg, 1993; Munnecke et al., 1997). The pits within the microspar crystals are reminiscent of the shape of former aragonite needles. The diameter of the pits of much less than 1 μm, however, is smaller than the average diameter of aragonite needles in Recent platform muds (as discussed by Lasemi and Sandberg, 1993, p. 180, Fig. 13.3; compare also Munnecke et al., 1997, Figs. 3 and 4). In addition, relicts of aragonite needles are engulfed in the microsparites. Both the pits and the aragonite relicts in the microspar crystals are interpreted as a result of aragonite dissolution (Lasemi and Sandberg, 1993; Munnecke et al., 1997). In the microspar crystals, the preservation of pits that probably represent aragonite needle moulds indicates that dissolution occurred after precipitation of microspar cement. For Silurian and Pliocene microsparites, Munnecke et al. (1997, p. 987) suggest that dissolution of aragonite needles proceeded in marine-derived pore fluids, in association with oxidation of organic matter. Because of a disparity, by number, of preserved aragonite relicts and needle moulds in microspar crystals relative to the amount of aragonite needles in Recent aragonite muds, Lasemi and Sandberg (1993, p. 180) state that it is not established whether all of the microsparite represents a cement. If a large part of aragonite dissolution proceeded concomitant with microspar precipitation, around more-or-less widely spaced crystallization centres (cf. Lasemi and Sandberg, 1993), only a "leftover portion" of aragonite needles may have dissolved subsequent to the bulk of microspar precipitation, leaving moulds (cf. Munnecke et al., 1997, Fig. 5).

4. Calcium carbonate saturation in marine pore fluids: overview and concept

4.1. Introductory remarks

In view of substantial uncertainties with respect to near-equilibrium carbonate reaction kinetics in low-temperature, natural environments (see Morse and Arvidson, 2002, for review), the following concept of calcium carbonate dissolution in marine-derived pore fluids, and in more-or-less pure, unlithified carbonate sediments is held at a descriptive level. The concept contains two main elements, (1) oxidation of both organic matter and oxidation of reaction by-products that influence calcium carbonate saturation state, by releasing/consuming chemical compounds that interact with the carbonate system, and (2) the degree of openness of the system. In neritic sediments, depending on local conditions, a wide spectrum of redox reactions during organic carbon remineralization may occur (see e.g. Boudreau, 1991; Canfield et al., 1993; Anschutz et al., 2000). Below an oxic to suboxic surface layer up to a few centimeters thick, shallow-water carbonate sediments are essentially anoxic (cf. Chilingar et al., 1979; Morse et al., 1985; Walter and Burton, 1990). In pure neritic carbonate sediments, concentrations of nitrate, manganese oxide and iron oxyhydroxide are very low (e.g. Morse et al., 1985; Walter and Burton, 1990; Ku et al., 1999), pyrite formation is iron-limited (Berner, 1970, 1984), and organic carbon remineralization takes place mainly by aerobic oxidation and sulfate reduction; denitrification and methanogenesis overall are of subordinate significance (e.g. Berner, 1984; Berner and Westrich, 1985; Crill and Martens, 1987; Henrichs and Reeburgh, 1987, Table 4; Walter and Burton, 1990; Canfield and Raiswell, 1991; Henrichs, 1992; Canfield et al., 1993; Ku et al., 1999). The pH and alkalinity of pore waters are determined largely by both sulfate reduction and oxidation of reaction by-products of organic matter diagenesis, such as oxidation of hydrogen sulfide (see Table 2) (e.g. Berner, 1970, 1984; Morse et al., 1985; Pigott and Land, 1986; Henrichs and Reeburgh, 1987; Sansone et al., 1990; Tribble et al., 1990; Walter and Burton, 1990; Boudreau and Canfield, 1993; Tribble, 1993; Ku et al., 1999).

Carbon dioxide dissociates into solution orders of magnitude more rapidly than it evolves (e.g. Schmalz, 1967; Bathurst, 1975). Once the step of slow gas dissolution is taken, CO_2 dissociates via a chain of mainly rapid reactions. At seawater pH (7.9–8.3), the carbonate system can be represented as (e.g. Milliman, 1974; Bathurst, 1975, pp. 231–233):

$$CO_2(aq) + H_2O = H_2CO_3;$$

$$H_2CO_3 + OH^- = HCO_3^- + H_2O;$$

$$H_2CO_3 = HCO_3^- + H^+;$$

$$HCO_3^- = CO_3^{2-} + H^+$$

At the surface of calcium carbonate, the equilibrium can be written as:

$$CaCO_3 = Ca^{2+} + CO_3^{2-}$$

Net equation (Milliman, 1974):

$$CO_2 + H_2O + CaCO_3 = Ca^{2+} + 2HCO_3^-$$

Table 2
Reactions of organic matter oxidation considered in the present paper

Reaction	Net equation(s)	Reference
Aerobic oxidation of organic matter (CH_2O)	$CH_2O + O_2 \rightarrow H_2O + CO_2$	Demaison and Moore (1980)
Aerobic oxidation of reduced by-products: Oxidation of hydrogen sulfide	$H_2S + 2O_2 \rightarrow SO_4^{2-} + 2H^+$ $HS^- + 2O_2 \rightarrow SO_4^{2-} + H^+$ $NH_4^+ + 2O_2 \rightarrow NO_3^- + H_2O + 2H^+$	Boudreau (1991, 1993) (Walter and Burton, 1990; Canfield et al., 1993)
Sulfate reduction	$2CH_2O + SO_4^{2-} \rightarrow H_2S + 2HCO_3^-$ $2CH_2O + SO_4^{2-} \rightarrow HCO_3^- + HS^- + H_2O + CO_2$	Berner (1971) and Raiswell (1988a) Berner (1971) and Raiswell (1976)
Sulfate reduction (extended)	A1: $4R–CH_3 + 3SO_4^{2-} + 6H^+ \rightarrow 4R–COOH + 4H_2O + 3H_2S$ A2: $R–CH_3 + 2R{=}CH_2 + CH_4 + 3SO_4^{2-} + 5H^+$ $\rightarrow 3R–COOH + HCO_3^- + 3H_2O + 3H_2S$ A3: $2CH_2O + SO_4^{2-} \rightarrow 2HCO_3^- + H_2S$ B1: $2H_2S + O_2 \rightarrow 2S + 2H_2O$ B2: $3H_2S + SO_4^{2-} + 2H^+ \rightarrow 4S + 4H_2O$ B3: $H_2S + SO_4^{2-} + 2H^+ \rightarrow S + 2H_2O + SO_2$ B4: $S^{2-} \rightarrow S$ (bacterial sulfide-sulfur oxidation) C: $4S + 1.33(–CH_2–)$ $+ 2.66H_2O + 1.33OH^- \rightarrow 4H_2S + 1.33HCO_3^-$	All equations: Machel et al. (1995, Fig. 2)
Bacterial disproportionation of elemental sulfur	$4H_2O + 4S \rightarrow 3H_2S + SO_4^{2-} + 2H^+$	Böttcher et al. (2001)
Anaerobic methane oxidation	$CH_4 + SO_4^{2-} \rightarrow HS^- + H_2O + HCO_3^-$ $CH_4 + 2H^+ + SO_4^{2-} \rightarrow H_2S + 2H_2O + CO_2$ $CH_4 + SO_4^{2-} \rightarrow H_2S + CO_3^{2-} + H_2O$	Reeburgh (1980, 1983), Devol and Ahmed (1981) and Raiswell (1988b) Canfield and Raiswell (1991, p. 428) Aharon and Fu (2000)
Methanogenesis	$2CH_2O + 2H_2O \rightarrow 2CO_2 + 4H_2$ Followed by: $4H_2 + CO_2 \rightarrow CH_4 + 2H_2O$	Claypool and Kaplan (1974), Berner (1980) and Raiswell (1988a)

Each chemical equation represents a simplified net reaction. For each reaction, only a few references are given.

In CO_2–water systems, at 25 °C and in a pCO_2 and pH 6–8 range including that of most pore waters (Baas Becking et al., 1960; Berner, 1981), calcium carbonate dissolution proceeds by several reactions (cf. Plummer et al., 1978; Morse, 1983; Boudreau, 1987; Chou et al., 1989; Svensson and Dreybrodt, 1992; Arakaki and Mucci, 1995):

(1) $CaCO_3 = Ca^{2+} + CO_3^{2-}$

(2) $CaCO_3 + H^+ = Ca^{2+} + HCO_3^-$

(3) $CaCO_3 + 2H^+ = Ca^{2+} + H_2CO_3$

(4) $CaCO_3 + H_2CO_3 = Ca^{2+} + 2HCO_3^-$

(5) $CaCO_3 + H_2O = Ca^{2+} + HCO_3^- + OH^-$

Depending on pH, alkalinity and pCO_2, one of these reactions prevails. Reactions involving hydrogen ions tend to be most rapid (e.g. Plummer et al., 1978). From the reactants driving dissolution, the hydrogen ions may be produced by the carbonate system (see above), but more efficiently by oxidation of hydrogen sulfide (Table 2). Both in natural sea water and artificial solutions, and with natural and reagent-grade $CaCO_3$, respectively, the rate of dissolution increases exponentially with degree of undersaturation (Morse, 1978; Keir, 1982; Archer et al., 1989; Chou et al., 1989, Fig. 11(a); Svensson and Dreybrodt, 1992, Fig. 2; but compare Hales and Emerson, 1997 with Eisenlohr et al., 1999).

In sea water, calcium carbonate dissolution is inhibited by adsorbed organic substances (Suess, 1970, 1973; Morse, 1986; Thomas et al., 1993) and by adsorbed metal ions and phosphate (Berner and Morse, 1974; Morse, 1974; Sjöberg, 1976; Plummer et al., 1978; Svensson and Dreybrodt, 1992). For bioclasts, their structure and reactive surface area rather than their mineralogy may influence or even control dissolution (e.g. Walter and Morse, 1984; Henrich and Wefer, 1986). If a solution is undersaturated for one carbonate polymorph but oversaturated for another, mineralogy is the main control on dissolution. By contrast, if a solution is undersaturated for all carbonates present, skeletal structure takes control (Walter and Morse, 1984; Walter, 1985). Although predictions on the reactivity of biogenic carbonates thus are fraught with uncertainty (Morse, 1983; Morse and Arvidson, 2002), it appears safe to state that high-magnesium calcitic and aragonitic bioclasts, in by far the majority of cases, dissolve more readily than calcitic bioclasts (cf. Walter and Burton, 1990; Patterson and Walter, 1994). Within a microstructural-mineralogical class, the rate of dissolution increases overall linearly with decreasing grain size or reactive surface area, respectively (Walter and

Morse, 1984; Walter, 1985). Porous, thin calcitic shells or tests may be of equal or higher solubility than compact aragonitic hard parts (Flessa and Brown, 1983; Sanders, 1999).

Slow precipitation of calcium carbonate is caused, in part, by CO_2 release during the process (e.g. Schmalz, 1967; Bathurst, 1975), by precipitation inhibitors such as magnesium (calcite), sulfate (calcite), orthophosphate (aragonite), adsorbed organics (Suess, 1970, 1973; Berner and Morse, 1974; Morse, 1974; Berner et al., 1978; Zullig and Morse, 1988; Zuddas and Mucci, 1994; Hoch et al., 2000; Zhang and Dawe 1, 2000), and probably because of slow stabilization of newly precipitated $CaCO_3$ (Chou et al., 1989, p. 279). Chemical modelling indicates that a fall of pH because of oxic CO_2 production can be buffered by dissolution of calcium carbonate whereas, as a result of the coupled reactions of the carbonate system, precipitation induces only a moderate lowering of pH (Boudreau and Canfield, 1993). In a solution with mixed carbonate polymorphs, the more unstable polymorph tends to dissolve more rapidly than the less-soluble phase precipitates (Schmalz, 1967; Schmalz and Swanson, 1969).

4.2. Discrete layers of organic matter oxidation

Although "layer" concepts of early diagenesis are a stark simplification of potential chemical and taphonomic pathways (e.g. Powell et al., 2002, p. 29), they provide an easy-to-visualize framework and, overall, are consistent with bulk pore water characteristics with depth (see below). At present, no "non-layer" predictive model on the relation between calcium carbonate saturation, preservation of bioclasts, depositional environment, depth and rate of burial, water depth, bioturbation and sediment type and composition is available (cf. Powell et al., 2002). In a first approach, the oxidation of organic matter is considered to take place according to decreasing energy gain per oxidation reaction that each, in turn, corresponds to a discrete layer within the sediment (Fig. 20(A)) (Froelich et al., 1979; Demaison and Moore, 1980; Reeburgh, 1980). No exchange between layers is allowed for. The topmost layer, i.e. the layer of aerobic oxidation, typically is a few millimeters to a few centimeters thick. In the oxic layer, a pH fall due to aerobic CO_2 production can be buffered by $CaCO_3$ dissolution (cf. Table 2) (e.g. Froelich et al., 1979; Bender and Heggie, 1984; Boudreau and Canfield, 1993). Lowering of the pH by oxic respiration may result in undersaturation for aragonite and, in some cases, also for calcite (e.g. Canfield and Raiswell, 1991).

Below, the zone of bacterial sulfate reduction (Fig. 20(A)) may extend down to 200–300 cm (e.g. Reeburgh, 1980, Fossing et al., 2000). Upon sulfate reduction, release of substantial quantities of CO_2 results in alkalinity rise from bicarbonate production; this may re-establish

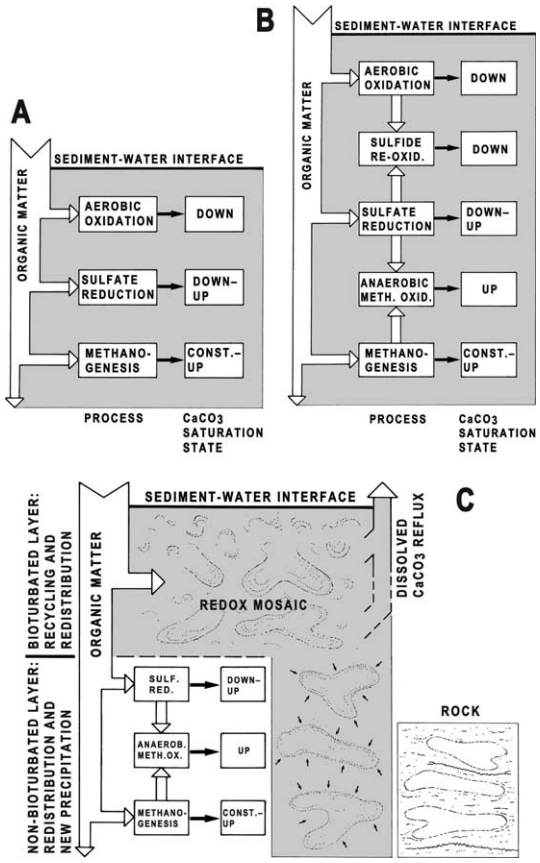

Fig. 20. Concepts for early dissolution of calcium carbonate related to progressive oxidation of organic matter in the sediment. (A) Discrete layer concept, with resulting effect on carbonate saturation state. (B) Layer concept, with chemical exchange between different layers allowed (white arrows). (C) Concept involving a bioturbated layer with a "redox mosaic", underlain by an unbioturbated layer with coupled layers. In the bioturbated layer, burrowing intensifies dissolution and enables reflux of dissolved calcium carbonate into the sea. Below, in the unbioturbated layer, inhomogeneites of the sediment (e.g. burrow-fills) cause gradients for dissolution and precipitation of calcium carbonate, driven by diffusion. See text for further description.

$CaCO_3$ saturation (Table 2) (Boudreau, 1991, p. 154; cf. Berner, 1984, p. 606). During several types of bacterial sulfate reduction, per mole sulfate up to 2 moles of hydrogen ions are consumed (see Machel et al., 1995, Fig. 2), raising pH (Table 2). For each mole of calcite precipitated in association with sulfate reduction, however, one mole of both CO_2 and H^+ are released (e.g. Birnbaum and Wireman, 1984; Canfield and Raiswell, 1991; Visscher et al., 2000); this, in turn, tends to maintain supersaturation (cf. Raiswell, 1988b, p. 574). Production of hydrogen ions by anaerobic, sulfur-disproportionating bacteria may be important in maintaining low pH (Table 2) (cf. Böttcher et al., 2001). In iron-poor closed systems, at modest degrees of sulfate reduction, dissolution of calcium carbonate takes place; at sulfate reduction higher than some threshold (see Walter and Burton, 1990, Fig. 5(B)), however, satura-

tion to oversaturation result from the alkalinity rise and, hence, precipitation may take place (Walter and Burton, 1990, p. 626ff). Both chemical modelling and field observations indicate that sulfate reduction initially leads to undersaturation for calcium carbonate, but in later stages, upon continued bicarbonate addition and resulting alkalinity rise, to oversaturation (Canfield and Raiswell, 1991). In closed, iron-poor systems, accumulation of the weak acid H_2S tends to lower pH (Gardner, 1973), in some cases down to less than 7 (Walter and Burton, 1990; Tribble, 1993), and carbonate undersaturation may persist down to low sulfate concentrations (Canfield and Raiswell, 1991, p. 421f). Calcium carbonate-precipitating, sulfate-reducing bacteria require removal of hydrogen sulfide as a prerequisite for calcium carbonate precipitation (Castanier et al., 1999). In the sulfate reduction zone, pore waters typically are oversaturated for calcium carbonate by up to one order of magnitude (e.g. Raiswell, 1988b). Because of the barriers to the precipitation of calcium carbonate (see above), oversaturation may persist for hundreds of years at least (e.g. Berner et al., 1978).

The lowest layer of organic matter oxidation (in this scheme) is characterized by bacterial methanogenesis (Fig. 20(A)). In marine sediments, the largest part of biogenic methane forms by reduction of carbon dioxide (Table 2) (e.g. Claypool and Kaplan, 1974; Oremland and Taylor, 1978; Whiticar et al., 1986). Although only part of the CO_2 produced during methanogenesis is consumed in the next step of fermentation (Demaison and Moore, 1980), undersaturation may be attained only if pH was sufficiently low before (Canfield and Raiswell, 1991, pp. 429–431). Although the rate of methanogenesis is probably one or two orders of magnitude lower than those of sulfate reduction and aerobic oxidation (Henrichs and Reeburgh, 1987), pore water profiles typically show a low to negative saturation state for calcium carbonate in the layer of methanogenesis (Middelburg et al., 1990, p. 401; Canfield and Raiswell, 1991). Potential effects of acetogenic bacteria together with methanogens (cf. Ehrlich, 1998, p. 54f) on pore water pH are as yet unexplored.

4.3. Coupled layers of organic matter oxidation

In this concept, diffusion of chemical compounds is possible among layers (Fig. 20(B)). Oxidation of by-products of anaerobic organic matter oxidation, such as hydrogen sulfide, induces pH lowering and in many cases dissolution of $CaCO_3$ (e.g. Revelle and Fairbridge, 1957, p. 282; Chilingar et al., 1979, p. 257). In chemical layer models either closed or open to steady-state diffusion, both types of models behave similarly, qualitatively, with respect to pH and carbonate saturation (Boudreau and Canfield, 1993, p. 317). Anoxic pore waters of carbonate sediments contain hydrogen sulfide species and ammonia as by-products of organic matter oxidation (Walter and Burton, 1990). The hydrogen sulfides and ammonia diffuse towards the oxic layer, where they are oxidized (Fig. 20(B), Table 2) (e.g. Crill and Martens, 1987; Henrichs and Reeburgh, 1987; Boudreau, 1991; Boudreau and Canfield, 1993). Oxidation of hydrogen sulfides and ammonia releases hydrogen ions, hence promoting undersaturation for $CaCO_3$ (e.g. Berner, 1970, 1984; Aller, 1982; Boudreau, 1991; Boudreau and Canfield, 1993). In iron-poor systems, the net result either of H^+ release or of oxidation of elemental sulfur to sulfuric acid is pH lowering (cf. Machel, 2001, p. 155). Another effect of reoxidation is both a narrowing of the aerobic layer and an increase in the relative proportion of organic matter oxidized by sulfate reduction (Crill and Martens, 1987; Boudreau, 1991; Boudreau and Canfield, 1993). The main result of reduced by-product oxidation is to keep alkalinity low over a thicker part of the sediment column and, as a consequence, to thicken the zone of undersaturation for calcium carbonate (Boudreau and Canfield, 1993, p. 331f). In the sulfate reduction zone, the same processes as outlined above in Section 4.2 pertain. Removal of hydrogen sulfide by diffusion, however, decreases the concentration of a major barrier to bacterially-induced carbonate precipitation (cf. Castanier et al., 1999, Fig. 3, p. 11).

Upon consumption of sulfate with depth and upward diffusion of methane, a layer up to a few tens of centimeters thick of anaerobic methane oxidation is established (Fig. 20(B), Table 2) (Reeburgh, 1980). Because anaerobic methane oxidation often is stoichiometrically related to sulfate reduction, methanogens probably thrive in consortium with sulfate-reducers (Harder, 1997; see also Canfield and Raiswell, 1991, p. 428). In its net effect, thus, the zone of anaerobic methane oxidation may be considered a downward extension of sulfate reduction. The lower limit of anaerobic methane oxidation is given by exhaustion of sulfate, the upper limit by exhaustion of methane (e.g. Reeburgh, 1980; Devol and Ahmed, 1981; Raiswell, 1988a,b; Canfield and Raiswell, 1991). Because anaerobic methane oxidation produces carbonate species and consumes hydrogen ions, it results in net pH lowering and alkalinity rise (Canfield and Raiswell, 1991). Pore water profiles indicate alkalinity rise and supersaturation for calcium carbonate in anaerobic methane oxidation zones, particularly in the upper, most active part of the layer (e.g. Reeburgh, 1980; Middelburg et al., 1990; Burns, 1998). Below, in the layer of methanogenesis, the effect on saturation state may be similar to the discrete layer model.

4.4. Bioturbated layer and diffusively coupled layers

In pore waters of Recent carbonate sediments undergoing dissolution, hydrogen sulfide oxidation upon

episodic reoxygenation is a major source of hydrogen ions for carbonate dissolution (Ku et al., 1999). Thus, in a last step, a bioturbated layer underlain by an unbioturbated interval may be considered (Fig. 20(C)). The bioturbated layer is a mechanically and chemically open system with a frequently changing "redox mosaic" of aerobic/anaerobic organic matter oxidaton (e.g. Aller, 1982, 1994; Aller and Aller, 1998; Walter and Burton, 1990; Anschutz et al., 2000; Fossing et al., 2000). Burrowing increases both the metabolism and population of sediment-dwelling microbes (e.g. Aller, 1982; Aller and Aller, 1998). This, in turn, promotes removal of dissolution inhibitors adsorbed onto crystals (Thomas et al., 1993; see also Suess, 1970, 1973). Burrowing speeds turnover of chemical components, and replenishes both oxidants and reactive organic matter (e.g. Goldhaber et al., 1977; Berner and Westrich, 1985; Walter and Burton, 1990; Aller and Aller, 1998; Fossing et al., 2000). Because of bioturbation turnover, a 1–2% standing crop of organic matter is sufficient to sustain high rates of sulfate reduction (Walter and Burton, 1990; see also Morse et al., 1985). In bioturbated sediment, only a small portion escapes chemical concentration gradients around burrows (Aller, 1980). In the walls of crustacean burrows and in crustacean-bioturbated sediments, the microbial biomass is dominated by both aerobic and anaerobic bacteria, and microbial activity is elevated within burrow walls (Bird et al., 2000). Deep-tiered crustacean burrows are present in carbonate substrates ranging from lime mud (e.g. Shinn, 1968) to bioclastic sand rich in coarse, large bioclasts (Miller and Curran, 2001; Sanders, 2001). Burrowers such as callianassid crustaceans can completely turn over the upper 1–2 m of sediment within 100–600 years and, over time, irrigate huge amounts of water into the sediment (see Griffis and Suchanek, 1991; Tedesco and Aller, 1997). Bioturbated sediments typically are recycled a few hundreds to thousands of times before ultimate burial (Canfield et al., 1993, p. 3867; Aller and Aller, 1998). By reexposing anoxic sediment with partly degraded organic matter to oxygen, and by introducing labile organic matter, burrowing raises the total rate of remineralization, including the anaerobic pathway (e.g. Henrichs and Reeburgh, 1987; Canfield and Van Cappellen, 1992; Canfield et al., 1993; Aller, 1994; Aller and Aller, 1998; Kristensen and Holmer, 2001). Since CO_2 production by aerobic oxidation is rapid (e.g. Froelich et al., 1979; Bender and Heggie, 1984), also in overall anoxic but bioturbated sediments, repeated undersaturation for $CaCO_3$ by aerobic CO_2 release can be set up during short episodes of oxic respiration (cf. Aller, 1982; Boudreau, 1987, p. 1985; Aller and Aller, 1998). Reoxidation of pore waters along the shoots of sea grass or the rhizomes of benthic algae (Ku et al., 1999) or by bioturbation (Morse et al., 1985; Walter and Burton, 1990) affects pore water chemistry both within burrows and along the grass shoots or the rhizomes, and also the pore water within the adjacent sediment (Aller, 1994; Aller and Aller, 1998; Ku et al., 1999).

In bioturbated sediments, because of consumption of O_2 and NO_3 in discrete sites within and adjacent to burrows, across reaction zones a few millimeters thick, pH may vary by a full unit, and chemical concentrations may strongly deviate from average (Aller, 1982, 1994; Boudreau, 1991, p. 145; Aller and Aller, 1998; Brandes and Devol, 1995). Sulfate reduction can proceed simultaneously, in suboxic or anoxic small-scale environments, with aerobic oxidation (Canfield and Des Marais, 1991). Elemental sulfur is a common product of sulfate reduction by bacteria that mainly are aerobic (Table 2) (Machel et al., 1995, Fig. 2, p. 377). Along anaerobic–aerobic interfaces (Machel et al., 1995, p. 377), or in bioturbated redox mosaics, bacterial disproportionation of elemental sulfur by anaerobic bacteria releases hydrogen ions and hydrogen sulfide (Table 2) (e.g. Böttcher et al., 2001). With respect to carbonate dissolution, oxidation of hydrogen sulfide (Walter and Burton, 1990; Canfield and Raiswell, 1991; Ku et al., 1999) and, perhaps, disproportionation of sulfur (cf. Böttcher et al., 2001) are effective in producing hydrogen ions. A result of the burrow-mediated redox cycling in Recent, bioturbated shallow-water carbonates is that the rate of sulfide oxidation, which is largely balanced by the rate of sulfate reduction, correlates with the amount of calcium carbonate dissolved, according to the net reaction (Ku et al., 1999, p. 2537, Eq. (7)):

$$2CaCO_3 + 2O_2 + 2CH_2O = 2Ca^{2+} + 4HCO_3^-$$

The main effect of bioturbation is that the same volume of sediment is driven many times through a cycle of oxic to anoxic organic matter remineralization and oxidation of reaction by-products, with many reactions resulting in or promoting undersaturation for calcium carbonate. In a bioturbated-bioirrigated system, a part of the supersaturated pore water may be recycled to the water column before substantial carbonate reprecipitation takes place. In the sediment below the bioturbated layer, the anaerobic oxidation of organic matter may show a heterogeneous distribution with respect to processes and/or intensity (Fig. 20(C)). Such inhomogeneities may be inherited from the active layer, such as patches with different texture and/or with different contents in organic matter due to burrowing and buried carcasses, and from buried shells or skeletons. Below the bioturbated layer, diffusion drives comparatively slow material transport. Dissolution of calcium carbonate associated with sulfate reduction and/or with methanogenesis will be followed by diffusion and reprecipitation, since no reoxidation of reaction by-products takes place and sufficient time is available for precipitation (compare e.g. Fürsich, 1973; Raiswell, 1988a,b; El Albani et al., 2001).

The present concept contains elements similar to a concept presented by Melim et al. (2002) for dissolution of aragonite and high-Mg calcite during marine burial diagenesis of platform slope limestones (see also Saller, 1986). In their "open-system style" of diagenesis, carbonate is dissolved in high-permeability intervals and, by inference, is recycled to the sea (p. 40). In the "closed-system style", carbonate is dissolved in muddy, low-permeability intervals, but is largely reprecipitated as a microsparitic cement in the same interval (pp. 40–41). Their concept, however, differs from the present one in that it treats processes deeper within the sediment column, in a burial diagenetic environment (cf. Melim et al., 2002, p. 44). Both concepts, of course, are not mutually exclusive. With respect to early dissolution of calcium carbonate in marine-derived pore fluids, the most important points are (1) that dissolution (or transient undersaturation, at least) is an inherent result of some processes of organic matter oxidation, and (2) that sulfate reduction has a "double face" in early diagenesis, in one case mediating precipitation, in another case dissolution of calcium carbonate, depending on the degree of mechanical and chemical openness of the system.

5. Discussion: potential significance of early dissolution

5.1. Carbonate production and destruction

5.1.1. Carbonate production

With respect to carbonate production rates, the compilation of Enos (1991, Fig. 2), supplemented by additional data, provides a well-readable figure (Fig. 21). Because the figure shows Recent carbonate production rates, besides the decrease of production with depth, it shows that shallow-water carbonate production ranges over at least two orders of magnitude, largely as a function of different settings (shallow reef, deep reef, lagoon, reef zonation) and as a result of different "scales" of observation, ranging from individual corals to entire reefs and mudbanks (see caption to Fig. 21). Carbonate production also varies in time, ranging from diurnal and seasonal variations at a given site (e.g. Broecker and Takahashi, 1966; Traganza, 1967; Kinsey, 1985; Kinsey and Hopley, 1991) to global fluctuations on a scale of thousands of years (e.g. Kinsey, 1985, p. 519; Kennedy and Woodroffe, 2000; Ryan et al., 2001) to millions to tens of millions of years (e.g. Schlager et al., 1998; Schlager, 1999; Kiessling et al., 2000).

Reef calcification rates deduced by community metabolism (0.3–9 mm/a; Kinsey, 1985, p. 519) overlap with aggradation rates of Holocene catch-up and keep-up reefs (0.9–7 mm/a; Camoin et al., 1997). Rates of Holocene reef aggradation of up to 20.6 mm/a (bar labelled "Tahiti" in Fig. 21) probably can be sustained only over up to a few hundreds of years (Montaggioni, 2000) and in part result from substantial microbialite precipitation in the reef framework (Montaggioni and Camoin, 1993; Camoin et al., 1999). Holocene reefs may be classified into (Montaggioni, 2000), (1) fast-growing reefs, with aggradation rates up to 10 mm/a sustained over 3–5 ka, corresponding to a net production of up to 10 kg $CaCO_3/m^2$ a, (2) moderately-fast growing reefs, with aggradation rates of 5–7 mm/a corresponding to a net production of 3–5 kg $CaCO_3/m^2$ a, and (3) slow-growing reefs, with rates of 1–4 mm/a corresponding to 1–2.5 kg $CaCO_3/m^2$ a production. Calcification rates of Holocene reefs are zonal, i.e. they depend largely on the physiography of the carbonate depositional system (shape of reef, and relative shape and relative size of reef versus lagoon), type of reef (Kinsey and Hopley, 1991), the microscale distribution of bottom communities (e.g. Andréfouet and Payri, 2000) and vary strongly with depth (e.g. Bosscher and Schlager, 1992; Vecsei, 2001). Early Holocene rates of reef growth at least at some sites were distinctly higher than during the late Holocene (Kinsey, 1985, p. 519; Kennedy and Woodroffe, 2000; Ryan et al., 2001).

Although doubts persist on the nature of whitings (Shinn et al., 1989; Morse and He, 1993), they may represent precipitates of calcium carbonate in the water column, triggered by picoplankton blooms and cellular components (Robbins and Blackwelder, 1992; Milliman et al., 1993). On Great Bahama Bank (GBB), mud produced by whitings may amount to nearly three times the mud present on the banktop and to more than 40% of the mud along the western slope (Robbins et al., 1997). Recent GBB banktop mud may stem mainly from codiacean algae and whitings (Milliman et al., 1993; Robbins et al., 1997, p. 949). The estimated production of mud by whitings ranges from 300 to 500 g/m^2 a (Broecker and Takahashi, 1966; Milliman et al., 1993; 410 g/m^2 a: Robbins et al., 1997). If a production rate of 300–500 g/m^2 a is calculated for an aragonitic mud with 80% porosity, it shows as an accumulation rate of 35–65 Bubnoff (mm/ka), sufficient to keep up a platform only under very slow sea-level rise (see Fig. 21).

5.1.2. Carbonate destruction

From Chapter 3, it is obvious that syndepositional dissolution of calcium carbonate must be considered in palaeoecological reconstructions, also for tropical–subtropical neritic carbonates (Sanders, 2001). In a large-scale, two-year experiment with mollusc shells deployed on the bank shoulder to upper slope (15–267 m water depth) of the Great Bahama Bank, shell dissolution was a prevalent process of taphonomic alteration (Powell et al., 2002). There is an increasing data set on rates of different types of bioerosion mainly in coral reefs (see Table 3). The bioerosion rates, if converted to a "negative accumulation rate" (Fig. 22) show that destruction

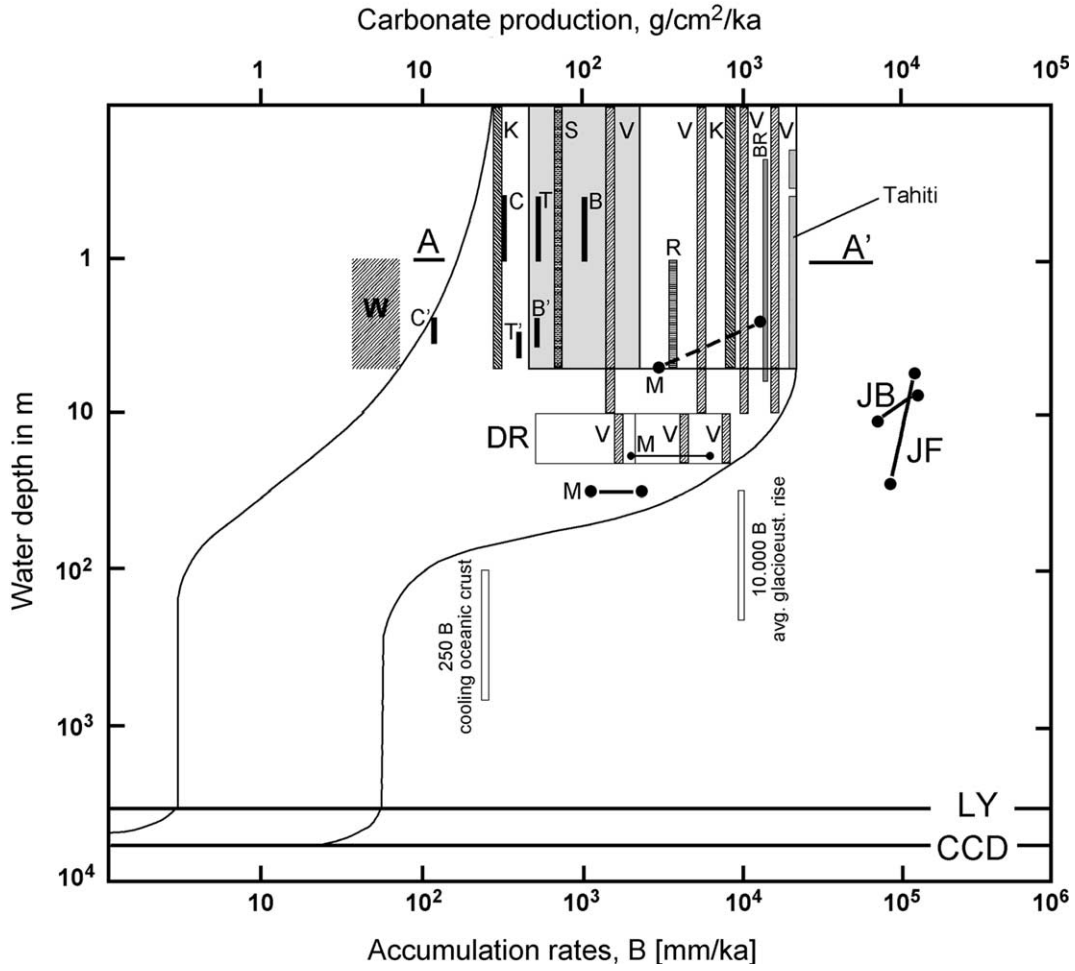

Fig. 21. Carbonate production rates and reef aggradation rates versus depth, modified and extended from Enos (1991, Fig. 2). Black outer envelope curves shows assumed minimum and maximum values of production with depth. With exception of a slight deviation in the depth interval 0–1 m to accomodate a 300 Bubnoff (1 Bubnoff = 1 mm/ka) production rate for 90–95% of total reef systems (cf. Kinsey, 1985, p. 519), the envelope of production has been redrawn from Enos (1991, Fig. 2). Labels: B, C, T: total carbonate production on mudbanks Buchanan Bank, Upper Cross Bank, Tavernier Key (all in South Florida; Bosence, 1989). C′, B′, T′: interbank production adjacent to the mentioned mudbanks. BR: productivity of a sheltered Barbabos reef (Stearn et al., 1977). DR (deep reef): compiled *aggradation* rates of reefs in 10–20 m water depth (from Schlager, 1981). Bars labelled V in field DR: carbonate production in fore reefs, 10–20 m water depth, based on modified census method (Vecsei, 2001); left: minimum production, *biodetrital* reefs, Caribbean; center: minimum production, *framework* reefs, Caribbean; right: maximum production, *framework* reefs, Caribbean. JB, JF: growth rate versus depth for the branched coral *Acropora cervicornis* in a backreef and forereef setting, Jamaica (Tunnicliffe, 1983). LY: calcite lysocline (from Scholle et al., 1983). CCD: calcite compensation depth (Berger and Winterer, 1974). M: maximum and minimum growth rates of *Montastrea annularis* in shallow water down to 5 m, and in waters of 18 and 30 m depth (from Bosscher and Schlager, 1992, Fig. 1). K: carbonate production for 90–95% of total reef area (left), carbonate production for 1–2% of reef area (right) (Kinsey, 1985, p. 519). R: Recent carbonate production rate of "total reef top" of Wistari reef, Great Barrier Reef Province (Ryan et al., 2001). S: mean production of "entire reef systems" (from Smith, 1983, cit. in Kinsey, 1985, p. 511). V: carbonate production in fore reefs, 0–10 m water depth, based on modified census method (Vecsei, 2001); left: minimum production, *biodetrital* reefs, Caribbean; left-center: maximum production, *biodetrital* reefs, Caribbean; right-center: minimum production, *framework* reefs, Caribbean; right: maximum production, *framework* reefs, Caribbean. W (dashed area): estimated carbonate production by whitings on Great Bahama Bank, 300–500 g/m^2 (Broecker and Takahashi, 1966; Milliman et al., 1993; Robbins and Evans, 1997), calculated for aragonite mud with 80% porosity. White area delimited by black line, 0–5 m water depth: compiled *aggradation* rates of reefs at less than 5 m in depth (from Schlager, 1981). Light grey area: range of production rate of "complete reef systems" (cf. Kinsey, 1985, p. 511, 519) (some overlap with white field for shallow reef accretion). "Tahiti": maximum known *aggradation* rate of a Holocene coral reef, 20.600 Bubnoff, recorded for Papeetee barrier reef, Tahiti (Montaggioni, 2000), plots just along the limit of the production envelope of Enos (1991, Fig. 2). Carbonate production rates from literature (given mostly in kg $CaCO_3$/m^2 a) have been transferred to potential accumulation rates according to 10 B = 1 g/cm^2/10^{3}a; this applies to aragonitic sediment of 65% porosity (see Enos, 1991, Fig. 2). The rectangles below the production curve indicate the rate of subsidence caused by cooling of young oceanic crust (250 B; Pitman and Golovchenko, 1983), and a mean rate of Holocene glacio-eustatic sea-level rise of 10 kB (e.g. Schlager, 1981). Note that within 1 m water depth along transect A–A′, carbonate production ranges over 2 orders of magnitude.

of carbonate by biological dissolution (microboring, macroboring), by grazing, and by combined grazing and boring widely overlaps even with relatively high rates of carbonate production (Fig. 21). Even in unstressed reefs,

Table 3
Rates of "biological" carbonate destruction, expressed in Bubnoff (1 Bubnoff = 1 mm/ka) negative sediment accumulation

Location	Rate or percentage of $CaCO_3$ removal (rate in kg/m^2 a)	Negative sediment accmulation in B (mm/ka)	Reference
Bahamas	6–7 kg/m^2 a from carbonate cobbles removed by clionid boring (experiment)	6000–7000 B (probably includes grazing and microboring)	Neumann (1966)
St. Croix, West Indies	Layer 20–30 μm thick removed over 2 years from sand grains by microborers	12.5 B	Perkins and Tsentas (1976)
Davies Reef, Australia	0.35 kg/m^2 a (microborers)	350 B	Tudhope and Risk (1985)
Black Rock, Little Bahama Bank	0.26 kg/m^2 a at 2 m depth (microbial bioerosion)	260 B	Hoskin et al. (1986)
Great Barrier Reef	0.01–0.19 kg/m^2 a (total boring)	10–190 B	Kiene (1988), cit. in Chazottes et al. (1995, p. 194)
Great Barrier Reef	0.01–1.69 kg/m^2 a: bioerosion by grazing	10–1690 B	Kiene (1988), cit. in Chazottes et al. (1995, p. 194)
Panama	−6.3 to −14 kg/m^2 a, total net change on exp. substrata	6300–14,000 B	Eakin (1992)
Réunion, Mascarene Islands, Indian Ocean	Microbial bioerosion. 20–80 g/m^2 a	20–80 B	Chazotte (1994); cit. in Vogel et al. (2000, p. 200)
Lizard Island, Great Barrier Reef	−0.1 to −2.0 kg/m^2 a, total net change on exp. substrata	100–2000 B	Kiene and Hutchings (1994)
Moorea barrier reef, French Polynesia	0.2–0.6 kg/m^2 a (microborers)	200–600 B	Chazottes et al. (1995)
Moorea barrier reef, French Polynesia	0.09 kg/m^2 a (macroborers)	90 B	Chazottes et al. (1995)
Moorea barrier reef, French Polynesia	2.62 kg/m^2 a: bioerosion by grazing	2620 B	Chazottes et al. (1995)
Tiahura, French Polynesia	0.84 kg/m^2 a (total bioerosion, dead Porites)	840 B	Chazottes et al. (1995)
French Polynesia	Microbial bioerosion. 0.57 kg/m^2 a after 2 months (not shown in Fig. 22) 0.20 kg/m^2 a after 24 months	200 B	Peyrot-Clausade et al. (1995)
French Polynesia, several reef sites	+0.5 to −10.5 kg/m^2 a mean −1.6 kg/m^2 a, total net change	+500 to −10.500 B, mean −1.600 B	Peyrot-Clausade et al. (1995)
Galapagos	−4.1 kg/m^2 a	4100 B	Reaka-Kudla et al. (1996)
Panama	10–20 kg/m^2 a, grazing by urchins	10,000–20,000 B	Sammarco (1996, p. 149, and refs. therein)
Galapagos	20–40 kg/m^2 a, grazing by urchins	20,000–40,000 B	Sammarco (1996, p. 149, and refs. therein)
Faaa reef, French Polynesia	6.9 kg/m^2 a, grazing by urchins	6900 B	Pari et al. (1998)
Jamaica	10–20% of coral reef framework typically removed by clionids	Not shown in Fig. 22	Perry (1999)
Jamaica	Avg. 25.3% of sandy substrate on reef foreslope (down to 30 m) removed by macroboring	Not shown in Fig. 22	Perry (1999)
Jamaica	Avg. 16.7% of sediment removed by macroboring from fore reef terraces	Not shown in Fig. 22	Perry (1999)
Jamaica	Avg. of 8.6% of sediment in shallow fore-reef removed by macroboring	Not shown in Fig. 22	Perry (1999)
Jamaica	Avg. of 16% of coral patch reef in open back-reef site removed by macroboring	Not shown in Fig. 22	Perry (1999)
Okinawa, Ryukyu Islands	+0.7 to −0.7 kg/m^2 a, mean +0.2 kg/m^2 a, total net change	+700 to −700 B	Hibino and van Woesik (2000)
Lee Stocking Island, Bahamas	Microbial bioerosion (6 m deep open subtidal site): 2 years avg: >0.35 kg/m^2 a Highest mean: 0.57 kg/m^2 a	570 B	Vogel et al. (2000)
Lee Stocking Island, Bahamas	Microbial bioerosion. *Acropora* reef, 2 m water depth, mean rate: 0.27 kg/m^2 a (after 6 months)	270 B	Vogel et al. (2000)
Lee Stocking Island, Bahamas	Microbial bioerosion. 30 m deep windward reef, 2 years average: <0.20 kg/m^2 a	150 B chosen	Vogel et al. (2000)
Lee Stocking Island, Bahamas	Microbial bioerosion. Strombus shell, mean of 2 years: 0.09 kg/m^2 a	Not shown in Fig. 22	Vogel et al. (2000)
One Tree Island, Great Barrier Reef	Microbial bioerosion. Tridacna shell, mean of 2 years: 0.02–0.03 kg/m^2 a	Not shown in Fig. 22	Vogel et al. (2000)

(*continued on next page*)

Table 3 (*continued*)

Location	Rate or percentage of $CaCO_3$ removal (rate in kg/m^2 a)	Negative sediment accmulation in B (mm/ka)	Reference
Kenya E coast	0.0503 kg/m^2 a, grazing by urchins, unstressed totally protected reef	50.3 B	Carreiro-Silva and McClanahan (2001)
Kenya E coast	0.711 kg/m^2 a, grazing by urchins, reef newly protected from fishing	711 B	Carreiro-Silva and McClanahan (2001)
Kenya E coast	1.18 kg/m^2 a, grazing by urchins, heavily fished reef	1180 B	Carreiro-Silva and McClanahan (2001)
French Polynesia (seven reef sites; 5 years experiment, final results)	0.8 (min) to 18.15 (max) kg/m^2 a (total bioerosion incl. boring and grazing, without reef accretion)	800–18,150 B	Pari et al. (2002, Fig. 4)
French Polynesia (seven reef sites; 5 years experiment)	−1.39 (min) to −3.02 (max) kg/m^2 a (net erosion, including accretion and all types of bioerosion; unstressed to stressed reefs)	1390–3020 B	Pari et al. (2002, Table 1)

Standard deviations of measurements indicated in some of the cited papers were not taken into account, and are not shown in Fig. 22. The conversion of bioerosion rates to negative sediment accumulation rates is based on the same relation than the production rates in Fig. 21, i.e. 1 B = 0.1 g aragonitic sediment with 65% porosity/cm^2 ka. This conversion, although including some error due to different substrata used by different investigators, shall give an impression of the magnitude of bioerosional carbonate destruction.

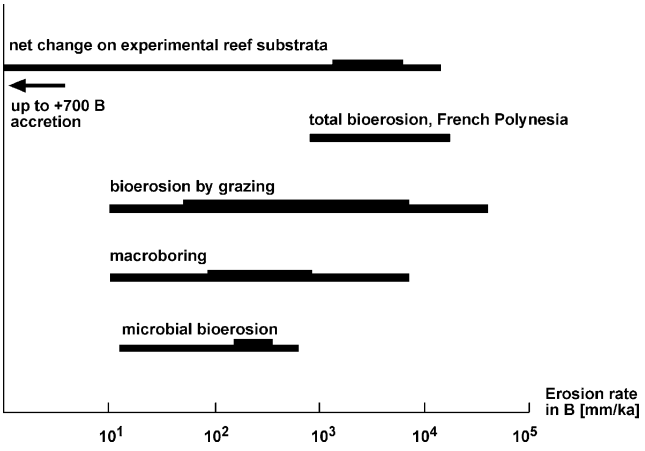

Fig. 22. Ranges of bioerosion rates in reef settings, given in Bubnoff (1 Bubnoff = 1 mm/ka). See Table 3 for sources. The thicker interval on each bar indicates the range wherein most of the data plot. On experimental reef substrates, the net change ranges from moderately swift accretion (up to 700 B) to rapid erosion. Compare with Fig. 21.

rates of net erosion of more than 2 kg $CaCO_3$/m^2 a may occur (cf. Pari et al., 2002). Episodes of ecological disturbance (e.g. by El Niño) of reefs may result in substantial carbonate loss (e.g. Eakin, 1996; Lewis, 2002), including extremely high rates of bioerosion by grazing of 7–40 kg $CaCO_3$/m^2 a over larger tracts of reefs (e.g. Sammarco, 1996, p. 149, and refs. therein; Pari et al., 1998; Hibino and van Woesik, 2000). At least in Tertiary to Recent settings, the intensity of macro- and microboring tends to be lowest in shallow, high-energy reef settings but increases both towards back-reef and fore-reef to upper slope settings (Perry, 1998, 1999; Perry and Bertling, 2000).

Dissolution of up to 50% of the annual carbonate mass introduced to the site was deduced by Walter and Burton (1990) and Ku et al. (1999) for muddy, bioturbated substrates of the South Florida Bay. Dissolution also prevails in the bioturbated, mainly muddy sediments of the Bahamas banktops (Morse et al., 1985). Recent surface sediments of some carbonate lagoons are depleted in or, locally, devoid of silt- and mud-sized high-magnesium calcite and/or aragonite, despite the standing biota produces these polymorphs (e.g. Maxwell et al., 1964; Roberts, 1971; Bathurst, 1975). The depletion to absence of unstable polymorphs is ascribed to dissolution in the soft sediment (Bathurst, 1975, p. 258; cf. Walter and Burton, 1990, p. 632). In Recent sediments, downcore variations of prevalent mineralogy of carbonate muds, from aragonite in the upper part to high-magnesium calcite in the lower, or vice versa, may be related to changing environment over time (Neumann and Land, 1975; Ward et al., 1985, pp. 47–48) or, perhaps, to syndepositional dissolution. In intensely bioturbated sediments, potential downcore variations in mineralogy may be offset by bioturbation, but quantification of bioclast flux to deduce dissolution-induced changes is difficult (Patterson and Walter, 1994).

In Recent reefs, coral cover rarely exceeds 70% and often is distinctly lower. In living corals, Hubbard (1972) observed both cementation and dissolution in diagenetic microenvironments. In *Porites furcata*, for instance, up to 25% of intraskeletal cement is precipitated immediately below the living polyp; in the lower part of the skeleton, up to 20% is dissolved and up to 10% is corroded, giving rise to a highly porous, thinned skeleton in the inner/lower part of the corallite (Hubbard, 1972, Fig. 2). In the reef coral *Pocillopora damicornis*, enhanced zooxanthellar metabolism due to elevated nutrient level slows calcification (Stambler et al., 1991) by substantial redissolution of coral skeleton (Yamashiro, 1992, cit. in Dubinsky and Jokiel, 1994, p. 315). Unfortunately, no other investigations of dissolution in vitro of coral skeletons seem to exist. On coral reefs, intervening areas of substrate, mostly sand,

are distinctly less productive (e.g. Kinsey, 1985). In sand areas, both aerobic respiration and anaerobic oxidation of organic matter at least locally give rise to calculated net dissolution of calcium carbonate (Charpy-Roubaud et al., 1996; Boucher et al., 1998, p. 279, Table 5). On a lateral distance of tens of meters to more than 1000 m, carbonate production may vary by orders of magnitude, from net loss to net production (Andréfouet and Payri, 2000, Fig. 2, p. 261ff; Hibino and van Woesik, 2000). In the same area and on the same substrate type, short-term (a few years) carbonate production may, again, range over orders of magnitude, up from zero (Andréfouet and Payri, 2000, Table 2, p. 264, and refs. therein). Notwithstanding the environmental cause-effect relations of the changes in production rate, these local/temporal variations impede up-scaling.

5.1.3. Compartmentalized carbonate preservation

From the above, it is obvious that both carbonate production and destruction are highly variable in space and time. In a given area, the ratio of carbonate production P to destruction D may range from >1 (net production) to <1 (net loss) (Fig. 23). Although unstressed reefs are sites of effective carbonate production and accumulation (P/D > 1), they, too, contain areas with P/D only slightly above 1, and areas with P/D < 1 (e.g. dead coral rubble subject to grazing) (Fig. 23). As discussed, carbonate destruction by "chemical" syndepositional dissolution appears to be favoured by specific substrates and specific environments, such as muddy lagoonal bottoms with deep-tiered burrowing.

The sediment accumulation rates of buildups and carbonate platforms decrease roughly linearly with increasing time interval of consideration (Schlager, 1981; Sadler, 1981). Although the decrease of long-term accumulation rates may result largely from diastems and hiatuses (cf. Sadler, 1981), because this feature is stable against scaling (Bosscher and Schlager, 1993; Schlager et al., 1998), this implies that carbonate production rate becomes lower with increasing time interval of consideration (Schlager, 1999, 2000). The described compartmentalization, in space, of the P/D ratio thus represents a snapshot, or momentary time-slice, of the phenomenon of decreasing carbonate production rate with increasing time interval of observation.

5.2. $CaCO_3$ redistribution and recycling

For deep-water limestones and nodular neritic limestones, it was assumed that aragonite dissolved within the sediment is used for local cementation (e.g. Jenkyns, 1974; Hallam, 1986; Möller and Kvingan, 1988; Munnecke and Samtleben, 1996). Limestone-marl or limestone-shale alternations were explained by vertical fluctuations of an aragonite solution zone in the unlithified sediment (e.g. Eder, 1982; Hallam, 1986; Munnecke and Samtleben, 1996). In these models, the largest part of the dissolved $CaCO_3$ stays within the sediment, but is redistributed by dissolution and reprecipitation. Redistribution may prevail where the sediment is not subject to intense physical disturbance, hence diffusion has time to work out (see Section 4). By contrast, in more intensely bioturbated sediments, a portion of the dissolved calcium carbonate is recycled into sea water (Fig. 20(C)) (e.g. Alexandersson, 1978; Morse et al., 1985; Davies et al., 1989; Walter and Burton, 1990; Ku et al., 1999), while another portion reprecipitates within the sediment, or within bioclasts, as more stable carbonate phases (Walter et al., 1993; Patterson and Walter, 1994; Reid and Macintyre, 1998). On a global average, a portion of the Ca, Sr and HCO_3^- buried in sediment is recycled to the oceanic water column, at least in part as a result of early dissolution (cf. Morse and Mackenzie, 1990, Tables 9.13., 9.15. and 9.16., Figs. 9.21. and 9.23.). Because the largest mass of aragonite and Mg-calcite accumulates in shallow neritic environments, it can be expected that early dissolution of these minerals constitutes a sizeable portion of the global backflux, but the amount is as yet poorly quantified (cf. Mackenzie and Morse, 1992).

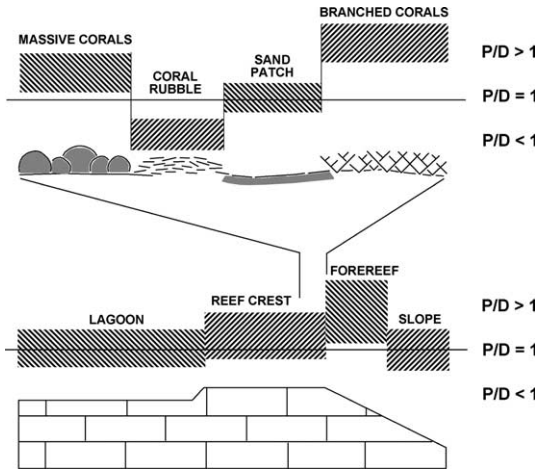

Fig. 23. Cartoon to visualize compartmentalization of carbonate production (P) versus destruction (D; bioerosion and dissolution). No quantitative scale implied; effects of sediment transport neglected. P/D > 1: net accumulation. P/D < 1: net erosion. See text for discussion.

To quantify the potential amount of dissolution recycling to the sea, a fairly reliable standard, or base-line, were needed. In open-ocean, deep-water environments, carbonate flux varies over a single order of magnitude, from local maxima of about 50 g/m^2 a to a global mean of about 8 g/m^2 a (1000 m depth), to less than 5 g/ m^2 a (Milliman et al., 1999, p. 1656). A marked disparity of tens of percent between carbonate flux at a given depth (above the lysocline) and ocean surface alkalinity indicates dissolution within the water column (e.g. Archer, 1997; Milliman et al., 1999). By contrast, meaningful quantification of recycling loss from carbonate budgets

seems difficult at present. Reasons for this include (1) the wide range of rates of carbonate production and "biological" destruction, varying over at least 2 orders of magnitude (Figs. 21 and 22), (2) the heterogeneity of the P/D ratio in space, (Fig. 23), and (3) scarcity of quantitative data on dissolved carbonate reflux out of sediments. The items (1)–(3) impede simple up-scaling in space and time that were necessary to derive a reliable value for quantification of dissolution recycling. Even in careful estimates based on a dense network of data, calculated values of carbonate production range within 2–4.5 times (cf. Boardman and Neumann, 1984, p. 1122). The global, Holocene rates of "carbonate flux" for coral reef complex, banks/bays and entire carbonate shelves include an error factor that ranges from 0.5 for coral reef complex to possibly >1 for entire carbonate shelves (Milliman and Droxler, 1996, Table 1). Thus, syndepositional dissolution recycling may be hidden within the uncertainty range. Considering the geological evidence for substantial dissolution in carbonate rocks (Sanders, 1999, 2001; Cherns and Wright, 2000), however, recycling perhaps sizeably detracts from the long-term sediment budget (see also Walter and Burton, 1990).

5.3. Calcite seas, aragonite seas

At first glance, the concept of aragonite seas and calcite seas (Sandberg, 1983; Wilkinson et al., 1985; Hardie, 1996; Stanley and Hardie, 1998) might be questioned by the observation that loss mainly of aragonitic fossils may take place. The best examples published to date for substantial dissolution of aragonitic shelly fauna are from Ordovician, Silurian and Upper Cretaceous successions (cf. Palmer et al., 1988; Fürsich and Pandey, 1999; Sanders, 1999, 2001; Cherns and Wright, 2000), i.e. for time intervals of "calcite seas" (cf. Sandberg, 1983; Stanley and Hardie, 1998) (see Fig. 24). Calcite seas correspond to greenhouse conditions with elevated atmospheric pCO_2, warm and equal climate, and a low Mg/Ca ratio of sea water. Conversely, times of aragonite seas are characterized by icehouse conditions, low pCO_2 and high Mg/Ca ratio (see e.g. Sandberg, 1983; Fischer, 1984; Wilkinson et al., 1985; Wilkinson and Given, 1986; Hardie, 1996; Stanley and Hardie, 1998; Berner and Kothavala, 2001; Steuber, 2002). At constant temperature, a rise in atmospheric pCO_2 may lower both the pH and carbonate saturation state of oceanic surface water (cf. Wilkinson and Given, 1986, p. 328; Murray and Wilson, 1997; Gattuso et al., 1998; Kleypas et al., 2001; Wallmann, 2001; Zeebe, 2001; but see Ryan et al., 2001). Thus, during greenhouse times, lowered seawater pH may have increased the potential for dissolution within the sediment, perhaps adding a "taphonomic component" to the presence of a calcite sea.

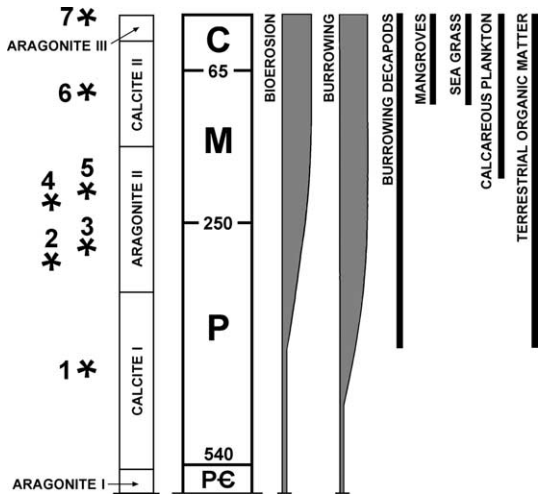

Fig. 24. Phanerozoic time scale (IUGS scale; Remane, 2000), intervals of calcite/aragonite seas (Stanley and Hardie, 1998), and some phenomena that relate to biological and "chemical" carbonate dissolution in neritic carbonate environments. Numbered asterisks mark intervals where syn- to early post-depositional dissolution has been described to date. (1) Ordovician-Silurian; Read (1982), Tobin and Walker (1996), Cherns and Wright (2000) and Tobin and Bergstrom (2002). (2, 3) Late Carboniferous, Early Permian: this paper. (4, 5) Middle Triassic, Late Triassic: this paper. (6) Late Cretaceous: Fürsich and Pandey (1999), Sanders (1999, 2001, and this paper) and El Albani et al. (2001). (7) Holocene shallow-water carbonates: Morse et al. (1985), Walter and Burton (1990) and Ku et al. (1999). See text for discussion.

The thin section data base for the present paper, however, shows that syndepositional dissolution was active also during periods of aragonite seas, from Late Carboniferous to Early Jurassic times (cf. Fig. 24). Also for the Holocene aragonite seas, with their comparatively high alkalinity (Wallmann, 2001), extensive dissolution is documented (Morse et al., 1985; Walter and Burton, 1990; Ku et al., 1999). In the Recent aragonite seas, skeletal magnesian calcite may constitute up to 45% of shallow-water sediment (e.g. Morse et al., 1985; Walter and Burton, 1990). Magnesian calcite with more than 8–12% Mg is more reactive than aragonite (e.g. Plummer and Mackenzie, 1974; Walter and Morse, 1984; Morse and Mackenzie, 1990, Fig. 3.7). This not necessarily implies that bioclasts of calcite with >12% Mg, such as many echinoderm grains (cf. Scholle, 1978, p. xi), suffer marked taphonomic loss. Echinoderm grains stabilize rapidly by intraskeletal calcite precipitation prior to concomitant with incongruent dissolution (e.g. Dickson, 1995), hence most commonly stay well-preserved. Red algal fragments, by contrast, are vulnerable to taphonomic loss by dissolution, leading to a reduction in the volume or to disappearance of grains (Moulin et al., 1985; Walter and Burton, 1990). Notwithstanding the potential amount of the solubility difference between aragonite and magnesian calcite with >12% Mg (see Walter and Morse, 1984), bioclast microstructure and perhaps also the crystal structure of

a biogenic magnesian calcite are important to overriding controls over its dissolution behaviour (Walter, 1985; Morse and Mackenzie, 1990, p. 122f). Walter (1985) established that, in pore water undersaturated for magnesian calcite but saturated to oversaturated for aragonite, magnesian calcite dissolves and calcite or aragonite may precipitate. If the pore water is undersaturated for both aragonite and magnesian calcite, however, then the microstructure of the bioclasts controls dissolution.

As discussed by Stanley and Hardie (1998, p. 5ff), it seems improbable that secular calcite–aragonite oscillations were markedly influenced by atmospheric pCO_2, but were mainly controlled by the Mg/Ca ratio of sea water (see also Steuber, 2002). A high oceanic Mg/Ca ratio would favour precipitation of aragonite and magnesian calcite, giving rise to an aragonite sea (cf. Stanley and Hardie, 1998). Mass-balance modelling of Ca–Mg flux suggests that the Phanerozoic Mg/Ca ratio of sea water ranged, with oscillations, from a Palaeozoic temporary minimum of 0.7 to a present-day maximum of close to 5.2 (Wilkinson and Given, 1986; Wilkinson and Algeo, 1989). The Phanerozoic history of modelled Mg/Ca ratios (Wilkinson and Algeo, 1989, Fig. 16(E) and (F)), however, is in marked discrepancy to the temporal extent of calcite seas and aragonite seas as suggested by the proposed co-variant changes in the mineralogy of ooids, cements, and by the marine biota (cf. Sandberg, 1983; Dickson, 1995; Stanley and Hardie, 1998, Fig. 1). Bates and Brand (1990), however, found no statistically significant correlation between inferred ooid mineralogy and proposed time intervals of calcite–aragonite seas. In any case, a calcite sea floral–faunal record that was exclusively caused by early dissolution of aragonite and magnesian calcite can hardly be reconciled with the contemporaneous prevalence of high-magnesium calcite (HMC) ooids and, in particular, HMC cements. On a global scale and over long intervals of time, taphonomic bias by syndepositional dissolution is not marked nor widespread enough to mask secular calcite–aragonite changes, if they are real. This suggests that, aside some potential background influence of global factors determining calcite/aragonite seas, syndepositional dissolution is mainly controlled by site-specific conditions such as mineralogical composition and skeletal microstructure of the marine biota, sediment texture, sediment accumulation rate, reactivity and input of organic matter, type and intensity of bioturbation, and depth and frequency of reworking. The data base of the present paper, however, is too limited to detect possible secular fluctuations of intensity or amount of syndepositional dissolution over Phanerozoic times. While in aragonite seas, with their high proportion of magnesian calcite, taphonomic loss by syndepositional dissolution was potentially larger than in calcite seas, with the present data available, an influence of the oceanic Mg/Ca ratio over the extent of dissolution cannot be demonstrated quantitatively.

5.4. Syndepositional dissolution in geological time

A consideration of the processes of both biological and chemical dissolution suggests that these increased through Phanerozoic times (Fig. 24). Mesozoic to Cainozoic reefs record a significant increase in presence, density and diversity of macroborings; in Palaeozoic and, in particular, pre-Devonian reefs, macroboring is rare to absent (e.g. Kershaw and Brunton, 1999; Kiessling et al., 2000; Perry and Bertling, 2000). Shell dissolution and dissolution of reef limestones is intense in the acidic pore waters of mangrove swamps (e.g. Revelle and Fairbridge, 1957; Fairbridge, 1967, p. 34), but mangroves have existed only since the Cretaceous. As discussed, oxygenation of the pore water along sea grass shoots and algal rhizomes is important in mediating dissolution (Ku et al., 1999). Sea grass-like marine plants occur since the Early Cretaceous (e.g. Brasier, 1975). Deep-tiered burrowing decapods were absent prior to the Devonian (cf. Schram et al., 1978) but, with exceptions (Tedesco and Wanless, 1995), decapod-type burrows are widespread only in Jurassic to Quaternary rocks (Bromley, 1996). The Phanerozoic acme of reef and carbonate platform development fell into the late Devonian (Kiessling et al., 2000), a time of globally high temperatures, high atmospheric pCO_2, and calcite seas (cf. Stanley and Hardie, 1998). During latest Devonian times, however, because of the rise of the first extensive rain forests and soil development, a rapid increase in atmospheric oxygen content correlates with a drawdown of CO_2, distinct climatic cooling, and a switch to aragonite seas (see summary in Copper, 2002). At the same time, the hitherto unseen input of terrestrial organic matter (TOM) from forests may have increased the potential for post-Famennian platforms to become eutrophied and subject to higher levels of bioerosion (cf. Peterhänsel and Pratt, 2001). Although TOM contains a higher percentage of refractory material which, in turn, seems to increase the relative amount of anaerobic methane oxidation (cf. Devol et al., 1984; Burns, 1998), by supplying the sediment with a new, extra amount of organic matter that (except lignins) is nearly totally remineralized (see de Haas et al., 2002, p. 705), the overall potential for dissolution related to organic matter oxidation may have increased.

Because of the very high rates of bioerosion by echinoid grazing (see Fig. 22, and Table 4), and by the production of a large amount of fine-grained carbonate susceptible to dissolution, echinoids promote carbonate dissolution. Regular echinoids that probably fed by rasping nutrient particles off substrate are present since Ordovician times. At least since the early Devonian, most regular echinoids had a lantern of aristotle similar

to extant forms (e.g. Durham, 1966, p. U269). Both the rate and depth of bioturbation overall increased from Late Ordovician to Recent. From the Early Devonian back to Late Ordovician times, there is evidence for "Phanerozoic-style" softground to firmground burrowing, including three-dimensional burrow networks down to a few decimeters in depth (Droser and Bottjer, 1989; Myrow, 1995). Prior to Late Ordovician times, the intensity of mega- and macrofaunal bioturbation decreases (Droser and Bottjer, 1988, 1989). Middle and Lower Ordovician trace fossils also include infaunal burrows (*Thalassinoides*) with a two-dimensional network, but depth of bioturbation did not exceed about 6 cm (Droser and Bottjer, 1989, p. 851). Cambrian neritic ichnofossil associations include megafaunal softground to firmground burrows, but both depth and degree of bioturbation are markedly lower than in younger Phanerozoic rocks (Droser and Bottjer, 1989; Droser et al., 2001). The quantity of carbonate dissolution by sediment-ingesting fauna is practically unconstrained. Revelle and Fairbridge (1957) indicate that extensive dissolution may occur by sediment-ingesting organisms, but no quantitative data were provided. The pH in the gut of sediment-ingesters such as holothurians may range down to 4.8, and increases to 7 when the gut is filled by calcareous sand, indicating dissolution (see Chilingar et al., 1979, p. 275). Sediment ingestion is a primitive mode of feeding (Bromley, 1996), and ranges back to Neoproterozoic times (Schopf, 1999). At least most of the Neoproterozoic mobile metazoans probably were small macrofaunal to meiofaunal burrowers (Schopf, 1999). The widespread presence and geochemical significance of meiofaunal burrowing is still scarcely explored (e.g. Aller and Aller, 1998; Pike et al., 2001), but implies that biologically mediated carbonate dissolution may not be limited to rocks with obvious, mega- and macrofaunal burrows. From the above, it may appear that the intensity of both, biological and "chemical" dissolution increased over Phanerozoic times.

5.5. Geochemical influence of syn- to early post-depositional carbonate dissolution

Dissolution of aragonite in marine-derived pore fluids may lower the Mg/Ca ratio of pore waters, and start early precipitation of low-magnesium calcite cement, including microspar cement, without meteoric influence (Melim et al., 1995, 2002; Munnecke et al., 1997, p. 987). The described examples for early precipitation of blocky calcite spar while the hosting shell rests in unlithified, bioturbated sediment may also be related to dissolution of (shell) aragonite (see Section 3.4). The overall significance of syn- to early post-depositional dissolution in marine-derived pore fluids for limestone cementation, however, has yet to be explored more completely.

Each of the main processes that drive carbonate dissolution, i.e. aerobic oxidation, sulfate reduction and reoxidation of reaction by-products, leads to a shift of isotope ratios among the chemical constituents involved. In rocks, hints of the processes of early dissolution are recorded in carbonate minerals that precipitated concomitant or subsequent to dissolution. Dissolution even of a small amount of marine carbonate shifts oxygen and carbon isotope ratios of pore waters towards values of "pristine" marine carbonate (cf. Veizer et al., 1999) that may already contain an isotope shift due to very early dissolution-reprecipitation (Patterson and Walter, 1994). The resulting isotope ratio of the authigenic carbonate mineral will represent a mix of sources. If calcium is released by dissolution of calcium sulfate along with sulfate reduction or methanogenesis, a distinct isotope shift caused by these processes may be largely preserved (cf. Machel et al., 1995, p. 381f). Oxygen isotope ratios of carbonates that precipitated as a by-product of sulfate reduction or disproportionation of elemental sulfur may be more negative, relative to marine carbonate, by down to more than 15 per mil (cf. Machel et al., 1995, Fig. 4; Böttcher et al., 2001). Similarly, carbon isotope ratios of carbonates precipitated during sulfate reduction, anaerobic methane oxidation and methanogenesis may be strongly negative relative to marine carbonate (range of −20 to −70 per mil PDB: Machel et al., 1995, Fig. 4; see also Whiticar et al., 1986; Hovland et al., 1987; Burns, 1998). Such marked shifts, however, are likely preserved only if no marine pore water is replenished (Machel et al., 1995, p. 382) and if no carbonate dissolution occurs (cf. Veizer et al., 1999, p. 81f; Tobin and Bergstrom, 2002). Authigenic carbonates with $\delta^{13}C$ values closely similar or identical to marine carbonate may even form if sulfate reduction proceeds mainly by reactions producing no bicarbonate, or if pore waters already supersaturated for calcium carbonate are pushed to precipitation by addition of a small amount of bicarbonate from sulfate reduction (Machel et al., 1995, p. 381).

Melim et al. (1995, 2002, p. 38) took moderately positive oxygen and carbon isotope values in pure, slope limestones as one of several arguments to indicate that documented carbonate dissolution took place in marine-derived pore waters. On the other hand, in carbonate concretions that originated by shell dissolution in unlithified sediment corresponding to marlstones and organic-rich limestones, moderately negative oxygen and carbon isotope ratios were interpreted by El Albani et al. (2001, p. 884) as indicators of dissolution during sulfate reduction or early during methanogenesis. Isotope ratios of rudist limestones that underwent syndepositional dissolution are moderately negative for oxygen and moderately positive for carbon, largely coincident with values reported from both Recent and Cretaceous marine carbonates (Sanders, 2001). The

difference between the isotope values as reported by Melim et al. (1995, 2002), El Albani et al. (2001) and Sanders (2001) may, at least in part, reflect different degrees of openness of the diagenetic system, organic matter content, and different times of dissolution relative to time of deposition. In summary, the oxygen and carbon isotope ratios of authigenic carbonates that precipitated concomitant with or closely subsequent to dissolution driven by organic matter oxidation may vary over a wide range, but may preferentially take moderately negative to near-marine values. For oxygen and carbon, caution is needed in interpretation of absolute values of isotope ratios, also with textural evidence for syndepositional dissolution, because marine climate may have added to the signal (compare e.g. Tobin and Bergstrom, 2002).

6. Conclusions

(1) Syndepositional dissolution of calcium carbonate in tropical–subtropical, neritic carbonate sediments is widespread, and is recorded by compositional, textural and taphonomic features in the resulting rock, including bias towards bioclasts/fossils of primary low-magnesium calcite, ghosts of aragonitic or high-magnesium calcitic bioclasts/fossils, lateral variations in early lithification, corroded early cements (radial-fibrous cement, calcite spar), pores overprinted by dissolution, pitted microspar crystals and aragonite relicts in microspar.

(2) Dissolution is associated with the oxidation of organic matter in the sediment, mainly aerobic oxidation, sulfate reduction and reoxidation of reaction by-products such as hydrogen sulfide (Walter and Burton, 1990; Ku et al., 1999). Depending on the degree of mechanical and chemical openness of the system, the spectrum of reactions of sulfate reduction (and associated reactions involving the reaction by-products) may in one case lead to precipitation, in another to dissolution of calcium carbonate.

(3) Dissolution occurred independent from calcite seas or aragonite seas, and was active at least over large parts of Phanerozoic time. Dissolution seems mainly controlled by site-specific conditions in the sediment, whereas ocean chemistry (Mg/Ca ratio) and atmospheric pCO_2 may have exerted a background influence.

(4) During the Phanerozoic, bioerosion intensified and factors favourable for "chemical" dissolution in the sediment increased, perhaps decreasing the ratio of carbonate production to carbonate "destruction". The limited data available, however, do not allow for recognition of potential secular fluctuations in intensity of syndepositional dissolution.

Acknowledgements

Lynn Walter, Michigan, and Patrick Erikkson, Pretoria, are thanked for constructive reviews. Patrick Eriksson is specifically thanked for the invitation to write this paper. Karl Krainer and Rainer Brandner, University of Innsbruck, provided part of their thin section collections for investigation. Hans-Peter Schönlaub, Geological Survey of Austria, Vienna, is thanked for access to the thin section collection of Palaeozoic carbonates. Susanne Pohler, Vancouver/Vienna, is thanked for expertise on Paleozoic reef builders, and for providing her thin sections from Ordovician and Devonian limestones. Thomas Steuber, Bochum, provided selected thin sections from Cretaceous carbonates. Martin Zuschin, Vienna, and Gudrun Radtke, Wiesbaden, are thanked for help in literature survey on bioerosion.

References

Aharon, P., Fu, B., 2000. Microbial sulfate reduction rates and sulfur and oxygen isotope fractionations at oil and gas seeps in deepwater Gulf of Mexico. Geochim. Cosmochim. Acta 64, 233–246.

Alexandersson, E.T., 1978. Destructive diagenesis of carbonate sediments in the eastern Skagerrak, North Sea. Geology 6, 324–327.

Aller, R.C., 1980. Quantifying solute distributions in the bioturbated zone of marine sediments by defining an average microenvironment. Geochim. Cosmochim. Acta 44, 1955–1965.

Aller, R.C., 1982. Carbonate dissolution in nearshore terrigenous muds: the role of physical and biological reworking. J. Geol. 90, 79–95.

Aller, R.C., 1994. Bioturbation and remineralization of sedimentary organic matter: effects of redox oscillation. Chem. Geol. 114, 331–345.

Aller, R.C., Aller, J.Y., 1998. The effect of biogenic irrigation intensity and solute exchange on diagenetic reaction rates in marine sediments. J. Mar. Res. 56, 905–936.

Amico, S., 1978. Recherches sur la structure du test des Radiolitidae. Trav. Lab. Geol. Hist. Paleont. Marseille 8, 1–131.

Andréfouet, S., Payri, C., 2000. Scaling-up carbon and carbonate metabolism of coral reefs using in-situ data and remote sensing. Coral Reefs 19, 259–269.

Anschutz, P., Sundby, B., Lefrancois, L., Luther III, G.W., Mucci, A., 2000. Interactions between metal oxides and species of nitrogen and iodine in bioturbated marine sediments. Geochim. Cosmochim. Acta 64, 2751–2763.

Arakaki, T., Mucci, A., 1995. A continuous and mechanistic representation of calcite reaction-controlled kinetics in dilute solutions at 25 °C and at 1 atm total pressure. Aquat. Geochem. 1, 105–130.

Archer, D.E., 1997. A data-driven model of the global calcite lysocline. Global Biogeochem. Cycles 10, 511–526.

Archer, D., Emerson, S., Reimers, C., 1989. Dissolution of calcite in deep-sea sediments: pH and O_2 microelectrode results. Geochim. Cosmochim. Acta 53, 2831–2845.

Baas Becking, L.G.M., Kaplan, I.R., Moore, D., 1960. Limits of the natural environment in terms of pH and oxidation–reduction potentials. J. Geol. 68, 243–284.

Baird, G.C., 1976. Coral encrusted concretions: a key to recognition of a "shale on shale" erosion surface. Lethaia 9, 293–302.

Bates, N.R., Brand, U., 1990. Secular variation of calcium carbonate mineralogy; an evaluation of ooid and micrite chemistries. Geol. Rundsch. 79, 27–46.

Bathurst, R.C., 1975. Carbonate Sediments and their Diagenesis. In: Developments in Sedimentology, vol. 12. Elsevier, Amsterdam. 658 pp.

Bender, M.L., Heggie, D.T., 1984. Fate of organic carbon reaching the deep sea floor: a status report. Geochim. Cosmochim. Acta 48, 977–986.

Berger, W.H., Winterer, E.L., 1974. Plate stratigraphy and the fluctuating carbonate line. In: Hsü, K.J., Jenkyns, H.C. (Eds.), Pelagic Sediments: on Land and under the Sea. In: Int. Ass. Sediment. Spec. Publ., vol. 1, pp. 11–48.

Berner, R.A., 1966. Chemical diagenesis of some modern carbonate sediments. Am. J. Sci. 264, 1–136.

Berner, R.A., 1969. Chemical changes affecting dissolved calcium during the bacterial decomposition of fish and clams in seawater. Mar. Geol. 7, 253–262.

Berner, R.A., 1970. Sedimentary pyrite formation. Am. J. Sci. 268, 1–23.

Berner, R.A., 1971. Principles of chemical sedimentology. McGraw-Hill, New York.

Berner, R.A., 1980. Early Diagenesis. A theoretical approach. Princeton University Press, Princeton. 241 pp.

Berner, R.A., 1981. A new geochemical classification of sedimentary environments. J. Sediment. Petrol. 51, 359–365.

Berner, R.A., 1984. Sedimentary pyrite formation: an update. Geochim. Cosmochim. Acta 48, 605–615.

Berner, R.A., Morse, J.W., 1974. Dissolution kinetics of calcium carbonate in sea water. IV. Theory of calcite dissolution. Am. J. Sci. 270, 108–134.

Berner, R.A., Westrich, J.T., Graber, R., Smith, J., Martens, C.S., 1978. Inhibition of aragonite precipitation from supersaturated seawater: a laboratory and field study. Am. J. Sci. 278, 816–837.

Berner, R.A., Westrich, J.T., 1985. Bioturbation and the early diagenesis of carbon and sulphur. Am. J. Sci. 285, 193–206.

Berner, R.A., Kothavala, Z., 2001. Geocarb III: a revised model of atmospheric CO_2 over Phanerozoic time. Am. J. Sci. 301, 182–204.

Bird, F.L., Boon, P.I., Nichols, P.D., 2000. Physicochemical and microbial properties of burrows of the deposit-feeding thalassinidean ghost shrimp *Biffarius arenosus* (Decapoda: Callianassidae). Est. Coast. Shelf Sci. 51, 279–291.

Birnbaum, S.J., Wireman, J.W., 1984. Bacterial sulfate reduction and pH: implications for early diagenesis. Chem. Geol. 43, 143–149.

Boardman, M.R., Neumann, A.C., 1984. Sources of periplatform carbonates: Northwest Providence Channel, Bahamas. J. Sediment. Petrol. 54, 1110–1123.

Böttcher, M.E., Thamdrup, B., 2001. Anaerobic sulfide oxidation and stable isotope fractionation associated with bacterial sulfur disproportionation in the presence of MnO_2. Geochim. Cosmochim. Acta 65, 1573–1581.

Böttcher, M.E., Thamdrup, B., Vennemann, T.W., 2001. Oxygen and sulfur isotope fractionation during anaerobic bacterial disproportionation of elemental sulfur. Geochim. Cosmochim. Acta 65, 1601–1609.

Bottjer, D.J., 1981. Structure of Upper Cretaceous chalk benthic communities, southwestern Arkansas. Palaeogeogr. Palaeoclimatol. Palaeoecol. 34, 225–256.

Bosence, D., 1989. Biogenic carbonate production in Florida Bay. Bull. Mar. Sci. 44, 419–433.

Bosscher, H., Schlager, W., 1992. Computer simulation of reef growth. Sedimentology 39, 503–512.

Bosscher, H., Schlager, W., 1993. Accumulation rates of carbonate platforms. J. Geol. 101, 345–355.

Boucher, G., Clavier, J., Hily, C., Gattuso, J.-P., 1998. Contribution of soft-bottoms to the community metabolism (primary production and calcification) of barrier reef flat (Moorea, French Polynesia). J. Exp. Mar. Biol. Ecol. 225, 269–283.

Boudreau, B.P., 1987. A steady-state diagenetic model for dissolved carbonate species and pH in the porewaters of oxic and suboxic sediments. Geochim. Cosmochim. Acta 51, 1985–1996.

Boudreau, B.P., 1991. Modelling the sulfide-oxygen reaction and associated pH gradients in porewaters. Geochim. Cosmochim. Acta 55, 145–159.

Boudreau, B.P., Canfield, D.E., 1993. A comparison of closed- and open-system models for porewater pH and calcite-saturation state. Geochim. Cosmochim. Acta 57, 317–334.

Bourque, P.-A., Boulvain, F., 1993. A model for the origin and petrogenesis of the red Stromatactis limestone of Paleozoic carbonate mounds. J. Sediment. Petrol. 63, 607–619.

Boyd, D.W., Nice, D.E., Newell, N.D., 1999. Silt injection as a mode of fossilization: a Triassic example. Palaios 14, 545–554.

Brachert, T.C., Dullo, W.-C., 2000. Shallow burial diagenesis of skeletal carbonates: selective loss of aragonite shell material (Miocene to Recent, Queensland Plateau and Queensland trough, NE Australia)—implications for shallow cool-water carbonates. Sediment. Geol. 136, 169–187.

Brandes, J.A., Devol, A.H., 1995. Simultaneous nitrate and oxygen respiration in coastal sediments: evidence for discrete diagenesis. J. Mar. Res. 53, 771–797.

Brasier, M.D., 1975. An outline history of seagrass communities. Paleontology 18, 681–702.

Brett, C.E., Baird, G.C., 1986. Comparative taphonomy: a key to paleoenvironmental interpretation based on fossil preservation. Palaios 1, 207–227.

Broecker, W., Takahashi, T., 1966. Calcium carbonate precipitation on the Bahama Banks. J. Geophys. Res. 71, 1575–1602.

Bromley, R.G., 1996. Spurenfossilien: Biologie, Taphonomie und Anwendungen. Springer, Berlin. 347 pp.

Burns, S.J., 1998. Carbon isotopic evidence for coupled sulfate reduction-methane oxidation in Amazon Fan sediments. Geochim. Cosmochim. Acta 62, 797–804.

Burns, S.J., Swart, P.K., 1992. Diagenetic processes in Holocene carbonate sediments: Florida Bay mudbanks and islands. Sedimentology 39, 285–304.

Camoin, G.F., Colonna, M., Montaggioni, L.F., Casanova, J., Faure, G., Thomassin, B.A., 1997. Holocene sea level changes and reef development in the southwestern Indian Ocean. Coral Reefs 16, 247–259.

Camoin, G.F., Gautret, P., et al., 1999. Nature and environmental significance of microbialites in Quaternary reefs: the Tahiti paradox. Sediment. Geol. 60, 15–49.

Canfield, D.E., Des Marais, D.J., 1991. Aerobic sulfate reduction in microbial mats. Science 251, 1471–1473.

Canfield, D.E., Raiswell, R., 1991. Carbonate precipitation and dissolution. Its relevance to fossil preservation. In: Allison, P.A., Briggs, D.E.G. (Eds.), Taphonomy. Releasing the Data Locked in the Fossil Record. Plenum Press, New York, pp. 411–453.

Canfield, D.E., Van Cappellen, P., 1992. How bioturbation may enhance the degradation rates of refractory sedimentary organics. Geol. Soc. Am., Abstr. Progr., A22.

Canfield, D.E., Jörgensen, B.B., Fossing, H., Glud, R., Gundersen, J., Ramsing, N.B., Thamdrup, B., Hansen, J.W., Nielsen, L.P., Hall, P.O.J., 1993. Pathways of organic carbon oxidation in three continental margin sediments. Mar. Geol. 113, 27–40.

Carreiro-Silva, M., McClanahan, T.R., 2001. Echinoid bioerosion and herbivory on Kenyan coral reefs: the role of protection from fishing. J. Exp. Mar. Biol. Ecol. 262, 133–153.

Castanier, S., Métayer-Levrel, G., Perthuisot, J.-P., 1999. Ca-carbonates precipitation and limestone genesis—the microbiologist point of view. Sediment. Geol. 126, 9–23.

Charpy-Roubaud, C., Charpy, L., Sarazin, G., 1996. Diffusional nutrient fluxes at the sediment–water interface and organic matter mineralization in an atoll lagoon (Tikehau, Tuamotu Archipelago, French Polynesia). Mar. Ecol. Progr. Ser. 132, 181–190.

Chazottes, V., Le Campion-Alsumard, T., Peyrot-Clausade, M., 1995. Bioerosion rates on coral reefs: interactions between macroborers,

microborers and grazers (Moorea, French Polynesia). Palaeogeogr. Palaeoclimatol. Palaeoecol. 113, 189–198.
Cherns, L., Wright, V.P., 2000. Missing molluscs as evidence of large-scale early skeletal aragonite dissolution in a Silurian sea. Geology 28, 791–794.
Chilingar, G.V., Bissell, H.J., Wolf, K.H., 1979. Diagenesis of carbonate sediments and epigenesis (or catagenesis) of limestones. In: Larsen, G., Chilingar, G.V. (Eds.), Diagenesis in Sediments and Sedimentary Rocks. In: Developments in Sedimentology, vol. 25A. Elsevier, Amsterdam, pp. 247–422.
Chou, L., Garrells, R.M., Wollast, R., 1989. Comparative study of the kinetics and mechanisms of dissolution of carbonate minerals. Chem. Geol. 78, 269–282.
Clark II, G.R., 1999. Organic matrix taphonomy in some molluscan shell microstructures. Palaeogeogr. Palaeoclimatol. Palaeoecol. 149, 305–312.
Claypool, G.E., Kaplan, I.R., 1974. The origin and distribution of methane in marine sediments. In: Kaplan, I.R. (Ed.), Natural Gases in Marine Sediments. Plenum Press, New York, pp. 97–139.
Copper, P., 2002. Reef development at the Frasnian/Famennian mass extinction boundary. Palaeogeogr. Palaeoclimatol. Palaeoecol. 181, 27–65.
Crill, P.M., Martens, C.S., 1987. Biogeochemical cycling in an organic-rich coastal marine basin. 6. Temporal and spatial variations in sulfate reduction rates. Geochim. Cosmochim. Acta 51, 1175–1186.
Cummins, H., Powell, E.N., Staff, G., 1986. The rate of taphonomic loss in modern benthic habitats: how much of the potentially preservable community is preserved. Palaeogeogr. Palaeoclimatol. Palaeoecol. 52, 291–320.
Davies, D.J., Powell, E.N., Stanton, R.J., 1989. Relative rates of shell dissolution and net sedimentary accumulation—a commentary: can shell beds form by the gradual accumulation of biogenic debris on the sea floor? Lethaia 22, 207–212.
de Haas, H., van Weering, T.C.E., de Stigter, H., 2002. Organic carbon in shelf seas: sinks or sources, processes and products. Cont. Shelf Res. 22, 691–717.
Demaison, G.J., Moore, G.T., 1980. Anoxic environments and oil source bed genesis. Am. Ass. Petrol. Geol. Bull. 64, 1179–1209.
Devol, A.H., Ahmed, S.I., 1981. Are higher rates of sulphate reduction associated with anaerobic methane oxidation? Nature 291, 407–408.
Devol, A.H., Anderson, J.J., Kuivala, K., Murray, J.W., 1984. A model for coupled sulfate reduction and methane oxidation in the sediments of saanich inlet. Geochim. Cosmochim. Acta 48, 993–1004.
Dickson, J.A.D., 1995. Paleozoic Mg calcite preserved: implications for the Carboniferous ocean. Geology 23, 535–538.
Dix, G.R., Mullins, H.T., 1988. Rapid burial diagenesis of deep-water carbonates: Exuma Sound, Bahamas. Geology 16, 680–683.
Dravis, J., 1979. Rapid and widespread generation of Recent oolitic hardgrounds on a high energy Bahamian platform, Eleuthera Bank, Bahamas. J. Sediment. Petrol. 49, 195–208.
Driscoll, E.G., 1970. Selective bivalve shell destruction in marine environments, a field study. J. Sediment. Petrol. 40, 898–905.
Droser, M.L., Bottjer, D.J., 1988. Trends in depth and extent of bioturbation in Cambrian marine environments, western United States. Geology 16, 233–236.
Droser, M.L., Bottjer, D.J., 1989. Ordovician increase in extent and depth of bioturbation: implications for understanding early Paleozoic ecospace utilization. Geology 17, 850–852.
Droser, M.L., Jensen, S., Gehling, J.G., Myrow, P.M., Narbonne, G.M., 2001. Lowermost Cambrian ichnofabrics from the Chapel Island formation, Newfoundland: implications for Cambrian substrates. Palaios 17, 3–15.
Dubinsky, Z., Jokiel, P.L., 1994. Ratio of energy and nutrient fluxes regulates symbiosis between zooxanthellae and corals. Pacific Sci. 48, 313–324.
Durham, J.W., 1966. Phylogeny and evolution. In: Moore, R.C. (Ed.), Treatise on Invertebrate Paleontology. In: Echinodermata 3, vol. 1, pp. U266–U269.
Eakin, C.M., 1992. Post-El Nino Panamanian reefs: less accretion, more erosion and damselfish protection. In: Proc. 7th Int. Coral Reef Symp., vol. 1, pp. 393–396.
Eakin, C.M., 1996. Where have all the carbonates gone? A model comparison of calcium carbonate budgets before and after the 1982–1983 El Nino at Uva Island in the eastern Pacific. Coral Reefs 15, 109–119.
Eder, W., 1982. Diagenetic redistribution of carbonate, a process in forming limestone-marl alternations (Devonian and Carboniferous), Rheinisches Schiefergebirge, W. Germany. In: Einsele, G., Seilacher, A. (Eds.), Cyclic and Event Stratification. Springer, Berlin, pp. 98–112.
Ehrlich, H.L., 1998. Geomicrobiology: its significance for geology. Earth-Sci. Rev. 45, 45–60.
Eisenlohr, L., Meteva, K., Gabrovsek, F., Dreybrodt, W., 1999. The inhibiting action of intrinsic impurities in natural calcium carbonate minerals to their dissolution kinetics in aqueous H_2O–CO_2 solutions. Geochim. Cosmochim. Acta 63, 989–1001.
El Albani, A., Vachard, D., Kuhnt, W., Thurow, J., 2001. The role of diagenetic carbonate concretions in the preservation of the original sedimentary record. Sedimentology 48, 875–886.
Emery, K.O., 1946. Marine solution basins. J. Geol. 54, 209–228.
Enos, P., 1977. Tamabra Limestone of the Roza Rica Trend, Cretaceous, Mexico. In: Cook, H.E., Enos, P. (Eds.), Deep-Water Carbonate Environments. In: Soc. Econ. Paleontol. Mineral. Spec. Pub., vol. 25, pp. 273–314.
Enos, P., 1991. Sedimentary parameters for computer modeling. In: Franseen, E.K., Watney, W.L., Kendall, C.G.St.C., Ross, W. (Eds.), Sedimentary Modeling: Computer Simulations and Methods for Improved Parameter Definition. Kansas Geol. Survey Bull. 233, 63–99.
Fairbridge, R.W., 1967. Phases of diagenesis and authigenesis. In: Larsen, G., Chilingar, G.V. (Eds.), Diagenesis in Sediments. In: Developments in Sedimentology, vol. 8. Elsevier, Amsterdam, pp. 19–89.
Fischer, A.G., 1984. The two Phanerozoic supercycles. In: Berggren, W., Van Cuvering, J.A. (Eds.), Catastrophes and Earth History. Princeton University Press, Princeton, New Jersey, pp. 129–150.
Fitzgerald, M.G., Parmenter, C.M., Milliman, J.D., 1979. Particulate calcium carbonate in New England shelf waters: results of shell degradation and resuspension. Sedimentology 26, 853–857.
Flessa, K.W., Brown, T.J., 1983. Selective solution of macroinvertebrate calcareous hard parts: a laboratory study. Lethaia 16, 193–205.
Fossing, H., Ferdelman, T.G., Berg, P., 2000. Sulfate reduction and methane oxidation in continental margin sediments influenced by irrigation (South-East Atlantic off Namibia). Geochim. Cosmochim. Acta 64, 897–910.
Freiwald, A., 1995. Bacteria-induced carbonate degradation: a taphonomic case study of *Cibicides lobatulus* from a high-boreal carbonate setting. Palaios 10, 337–346.
Froelich, P.N., Klinkhammer, G.P., Bender, M.L., Luedtke, N.A., Heath, G.R., Cullen, D., Dauphin, P., Hammond, D., Hartman, B., Maynard, V., 1979. Early oxidation of organic matter in pelagic sediments of the eastern equatorial Atlantic: suboxic diagenesis. Geochim. Cosmochim. Acta 43, 1075–1090.
Fürsich, F., 1971. Hartgründe und Kondensation im Dogger von Calvados. N. Jb. Geol. Paläont., Abh. 138, 313–342.
Fürsich, F.T., 1973. *Thalassinoides* and the origin of nodular limestone in the Corallian Beds (Upper Jurassic) of Southern England. N. Jb. Geol. Paläont. Mh. B., 136–156.
Fürsich, F.T., Pandey, D.K., 1999. Genesis and environmental significance of Upper Cretaceous shell concentrations from the

Chauvery Basin, southern India. Palaeogeogr. Palaeoclimatol. Palaeoecol. 145, 119–139.
Fütterer, D.K., 1974. Significance of the boring sponge *Cliona* for the origin of fine grained material of carbonate sediments. J. Sediment. Petrol. 44, 79–84.
Gardner, L.R., 1973. Chemical models for sulfate reduction in closed anaerobic marine environments. Geochim. Cosmochim. Acta 37, 53–68.
Garrison, R.E., Fischer, A.G., 1969. Deep-water limestones and radiolarites of the Alpine Jurassic. In: Friedman, G.M. (Ed.), Depositional Environments in Carbonate Rocks. In: Soc. Econ. Paleontol. Mineral. Spec. Publ., vol. 14, pp. 20–55.
Gattuso, J.-P., Frankignoulle, M., Bourge, I., Romaine, S., Buddemeier, R.W., 1998. Effect of calcium carbonate saturation level of seaweater on coral calcification. Global Planet. Change 18, 37–46.
Ginsburg, R.N., Schroeder, J.H., 1973. Growth and submarine fossilization of algal cup reefs, Bermuda. Sedimentology 20, 575–614.
Glover, C.P., Kidwell, S.M., 1993. Influence of organic matrix on the post-mortem destruction of molluscan shells. J. Geol. 101, 729–747.
Goldhaber, M.B., Aller, R.C., Cochran, J.K., Rosenfeld, J.K., Martens, C.S., Berner, R.A., 1977. Sulfate reduction, diffusion, and bioturbation in Long Island Sound sediments: report of the FOAM group. Am. J. Sci. 277, 193–237.
Grammer, G.M., Ginsburg, R.N., Swart, P.K., Mc Neill, D.F., Jull, A.J.T., Prezbindowski, D.R., 1993. Rapid growth rates of syndepositional marine aragonite cements in steep marginal slope deposits, Bahamas and Belize. J. Sediment. Petrol. 63, 983–989.
Griffis, R.B., Suchanek, T.H., 1991. A model of burrow architecture and trophic modes in thalassinidean shrimp (Decapoda: Thalassinidea). Mar. Ecol. Progr. Ser. 79, 171–183.
Haberstroh, P.R., Sansone, F.J., 1999. Reef framework diagenesis across wave-flushed oxic–subxoxic–anoxic transition zones. Coral Reefs 18, 229–240.
Hales, B., Emerson, S., 1997. Evidence in support of first-order dissolution kinetics of calcite in seawater. Earth Planet. Sci. Lett. 148, 317–327.
Hallam, A., 1986. Origin of minor limestone-shale cycles: climatically induced or diagenetic. Geology 14, 609–612.
Harder, J., 1997. Anaerobic methane oxidation by bacteria employing ^{14}C-methane uncontaminated with ^{14}C-carbon monoxide. Mar. Geol. 137, 13–23.
Hardie, L.A., 1996. Secular variation in seawater chemistry: an explanation for the coupled secular variation in the mineralogies of marine limestones and potash evaporites over the past 600 m.y. Geology 24, 279–283.
Hendry, J.P., Wilkinson, M., Fallick, A.E., Trewin, N.H., 2000. Disseminated jigsaw piece dolomite in Upper Jurassic shelf sandstones, Central North Sea: an example of cement growth during bioturbation. Sedimentology 47, 631–644.
Henrich, R., Wefer, G., 1986. Dissolution of biogenic carbonates: effects of skeletal structure. Mar. Geol. 71, 341–362.
Henrichs, S., 1992. Early diagenesis of organic matter in marine sediments: progress and perplexity. Mar. Chem. 39, 119–149.
Henrichs, S., Reeburgh, W.S., 1987. Anaerobic mineralization of marine sediment organic matter: rate and the role of anaerobic processes in the oceanic carbon economy. Geomicrobiol. J. 5, 191–237.
Hibino, K., van Woesik, R., 2000. Spatial differences and seasonal changes of net carbonate accumulation on some coral reefs of the Ryukyu Islands, Japan. J. Exp. Mar. Biol. Ecol. 252, 1–14.
Hoch, A.R., Reddy, M.M., Aiken, G.R., 2000. Calcite crystal growth inhibition by humic substances with emphasis on hydrophobic acids from the Florida Everglades. Geochim. Cosmochim. Acta 64, 61–72.
Hoskin, C.M., Reed, J.K., Mook, D.H., 1986. Production and off-bank transport of carbonate sediment, Black Rock, South-west Little Bahama Bank. Mar. Geol. 73, 125–144.
Hover, V.C., Walter, L.M., Peacor, D.R., 2001. Early marine diagenesis of biogenic aragonite and Mg-calcite: new constraints from high-resolution STEM and AEM analyses of modern platform carbonates. Chem. Geol. 175, 221–248.
Hovland, M., Talbot, M.R., Qvale, H., Olaussen, S., Aasberg, L., 1987. Methane-related carbonate cements in pockmarks of the North Sea. J. Sediment. Petrol. 57, 881–892.
Hubbard, J.A.E.B., 1972. Cavity formation in living scleractinian reef corals and fossil analogues. Geol. Rundsch. 61, 551–564.
James, N.P., 1997. The cool-water carbonate depositional realm. In: James, N.P., Clarke, J.A.D. (Eds.), Cool-Water Carbonates. In: Soc. Econ. Paleontol. Mineral. Spec. Publ., vol. 56, pp. 1–20.
James, N.P., Ginsburg, R.N., 1979. The seaward margin of Belize barrier and atoll reefs. In: Morphology, Sedimentology, Organism Distribution and Late Quaternary History. In: Int. Ass. Sedimentol. Spec. Publ., vol. 3. Blackwell, Oxford. 191 pp.
Jenkyns, H.C., 1974. Origin of red nodular limestones (Ammonitico Rosso, Knollenkalke) in the Mediterranean Jurassic: a diagenetic model. In: Hsü, K.J., Jenkyns, H.E. (Eds.), Pelagic Sediments on Land and Under the Sea. In: Int. Ass. Sedimentol. Spec. Publ., vol. 1, pp. 249–271.
Johnson, C.C., Sanders, D., Kauffman, E.G., Hay, W.W., 2002. Upper Cretaceous reefal patterns and processes affecting their development and demise. In: Kiessling, W., Flügel, E., Golonka, J. (Eds.), Phanerozoic Reef Patterns. Soc. Econ. Paleontol. Mineral. Spec. Publ., vol. 72, pp. 549–585.
Keir, R.S., 1982. Dissolution of calcite in the deep sea: theoretical prediction for the case of uniform size particles settling into a well-mixed sediment. Am. J. Sci. 282, 193–236.
Kennedy, W.J., Garrison, R.E., 1975. Morphology and genesis of hardgrounds and nodular chalks in the Upper Cretaceous of Southern England. Sedimentology 22, 311–386.
Kennedy, D.M., Woodroffe, 2000. Holocene lagoonal sedimentation at the latitudinal limits of reef growth, Lord Howe Island, Tasman Sea. Mar. Geol. 169, 287–304.
Kershaw, S., Brunton, F.R., 1999. Palaeozoic stromatoporoid taphonomy: ecologic and environmental significance. Palaeogeogr. Palaeoclimatol. Palaeoecol. 149, 313–328.
Kidwell, S.M., 1989. Stratigraphic condensation of marine transgressive records: origin of major shell deposits in the Miocene of Maryland. J. Geol. 97, 1–24.
Kidwell, S.M., 1998. Time-averaging in marine fossil record: overview of strategies and uncertainties. Geobios 30, 977–995.
Kidwell, S.M., Bosence, D., 1991. Taphonomy and time-averaging of marine shelly faunas. In: Allison, P.A., Briggs, D.E.G. (Eds.), Taphonomy, Releasing the data locked in the fossil record. Plenum Press, New York, pp. 115–209.
Kiene, W.E., Hutchings, P.A., 1994. Bioerosion experiments at Lizard Island, Great Barrier Reef. Coral Reefs 13, 91–98.
Kiessling, W., Flügel, E., Golonka, J., 2000. Fluctuations in the carbonate production of Phanerozoic reefs. In: Insalaco, E., Skelton, P.W., Palmer, T.J. (Eds.), Carbonate Platform Systems: Components and Interactions. In: Geol. Soc. London Spec. Publ., vol. 178, pp. 191–215.
Kim, J.C., Lee, Y.I., 1996. Marine diagenesis of Lower Ordovician carbonate sediments (Dumugol Formation), Korea: cementation in a calcite sea. Sediment. Geol. 105, 241–257.
Kinsey, D.W., 1985. Metabolism, calcification and carbon production. I. Systems levels studies. In: Proc. 5th Int. Coral Reef Congr., vol. 4, pp. 505–526.
Kinsey, D.W., Hopley, D., 1991. The significance of coral reefs as global carbon sinks—response to Greenhouse. Palaeogeogr. Palaeoclimatol. Palaeoecol. 89, 363–377.
Kleypas, J.A., Buddemeier, R.W., Gattuso, J.-P., 2001. The future of coral reefs in an age of global change. Int. J. Earth Sci. 90, 426–437.
Koch, C.F., Sohl, N.F., 1983. Preservational effects in paleoecological studies: Cretaceous mollusc examples. Paleobiology 9, 26–34.

Krainer, K., 1992. Fazies, Sedimentationsprozesse und Paläogeographie im Karbon der Ost- und Südalpen. Jb. Geol. B.-A. 135, 99–193.
Krainer, K., 1995. *Anthracoporella* Mounds in the Late Carboniferous of Auernig Group, Carnic Alps (Austria). Facies 32, 195–214.
Kristensen, E., Holmer, M., 2001. Decomposition of plant materials in marine sediment exposed to different electron acceptors (O_2, NO_3^-, and SO_4^{2-}), with emphasis on substrate origin, degradation kinetics, and the role of bioturbation. Geochim. Cosmochim. Acta 65, 419–433.
Ku, T.C.W., Walter, L.M., Coleman, M.L., Blake, R.E., Martini, A.M., 1999. Coupling between sulfur recycling and syndepositional carbonate dissolution: evidence from oxygen and sulfur isotope composition of pore water sulfate, South Florida Platform, USA. Geochim. Cosmochim. Acta 63, 2529–2546.
Lasemi, Z., Sandberg, P.A., 1984. Transformation of aragonite-dominated lime muds to microcrystalline limestones. Geology 12, 420–423.
Lasemi, Z., Sandberg, P., 1993. Microfabric and compositional clues to dominant mud mineralogy of micrite precursors. In: Rezak, R., Lavoie, D.L. (Eds.), Carbonate Microfabrics. Frontiers in Sedimentary Geology. Springer, Berlin, pp. 173–185.
Lees, A., Buller, A.T., 1972. Modern temperate-water and warm-water shelf carbonate sediments contrasted. Mar. Geol. 13, M67–M73.
Lees, A., Miller, J., 1995. Waulsortian banks. In: Monty, C.L.V., Bosence, D.W.J., Bridges, P.H., Pratt, B.R. (Eds.), Carbonate Mud-Mounds. Their Origin and Evolution. In: Int. Ass. Sedimentol. Spec. Publ., vol. 23, pp. 191–271.
Lewis, J.B., 2002. Evidence from aerial photography of structural loss of coral reefs at Barbados, West Indies. Coral Reefs 21, 49–56.
Machel, H.G., 2001. Bacterial and thermochemical sulfate reduction in diagenetic settings—old and new insights. Sediment. Geol. 140, 143–175.
Machel, H.G., Krouse, H.R., Sassen, R., 1995. Products and distinguishing criteria of bacterial and thermochemical sulfate reduction. Appl. Geochem. 10, 373–389.
Mackenzie, F.T., Morse, J.W., 1992. Sedimentary carbonates through Phanerozoic time. Geochim. Cosmochim. Acta 56, 3281–3295.
Mallarino, G., Goldstein, R.H., Di Stefano, P., 2002. New approach for quantifying water depth applied to the enigma of drowning of carbonate platforms. Geology 30, 783–786.
Malone, M.J., Slowey, N.C., Henderson, G.M., 2001. Early diagenesis of shallow-water periplatform carbonate sediments, leeward margin, Great Bahama Bank (Ocean Drilling Program Leg 166). Geol. Soc. Am. Bull. 113, 881–894.
Maxwell, W.G.H., Jell, J.S., McKellar, R.G., 1964. Differentiation of carbonate sediments in the Heron island reef. J. Sediment. Petrol. 34, 294–308.
Melim, L.A., Swart, P.K., Maliva, R.G., 1995. Meteoric-like fabrics forming in marine waters: implications for the use of petrography to identify diagenetic environments. Geology 23, 755–758.
Melim, L.A., Westphal, H., Swart, P.K., Eberli, G.P., Munnecke, A., 2002. Questioning carbonate diagenetic paradigms: evidence from the Neogene of the Bahamas. Mar. Geol. 185, 27–53.
Middelburg, J.J., de Lange, G.J., Kreulen, R., 1990. Dolomite formation in anoxic sediments of Kau Bay, Indonesia. Geology 18, 399–402.
Miller, J., 1986. Facies relationships and diagenesis in Waulsortian mudmounds from the Lower Carboniferous of Ireland and N. England. In: Schroeder, J.H., Purser, B.H. (Eds.), Reef Diagenesis. Springer, Berlin, pp. 311–335.
Miller, M.F., Curran, H.A., 2001. Behavioral plasticity of modern and Cenozoic burrowing thalassinidean shrimp. Palaeogeogr. Palaeoclimatol. Palaeoecol. 166, 219–236.
Milliman, J.D., 1974. Marine Carbonates. Springer, Berlin. 375 pp.
Milliman, J.D., Freile, D., Steinen, R.P., Wilber, R.J., 1993. Great Bahama Bank aragonitic muds: mostly inorganically precipitated, mostly exported. J. Sediment. Petrol. 63, 589–595.
Milliman, J.D., Droxler, A., 1996. Neritic and pelagic carbonate sedimentation in the marine environment: ignorance is not bliss. Geol. Rundsch. 85, 496–504.
Milliman, J.D., Troy, P.J., Balch, W.M., Adams, A.K., Li, Y.H., Mackenzie, F.T., 1999. Biologically mediated dissolution of calcium carbonate above the chemical lysocline? Deep-Sea Res. I 46, 1653–1669.
Möller, N.K., Kvingan, K., 1988. The genesis of nodular limestones in the Ordovician and Silurian of the Oslo Region (Norway). Sedimentology 35, 405–420.
Montaggioni, L., 2000. Postglacial reef growth. C.R. Acad. Sci. Paris, Sci. Terre Planétes 331, 319–330.
Montaggioni, L.F., Camoin, G.F., 1993. Stromatolites associated with coralgal communities in Holocene high-energy reefs. Geology 21, 149–152.
Morse, J.W., 1974. Dissolution kinetics of calcium carbonate in sea water.V. Effects of natural inhibitors and the position of the chemical lysocline. Am. J. Sci. 274, 638–647.
Morse, J.W., 1978. Dissolution kinetics of calcium carbonate in seawater: VI. The near-equilibrium dissolution kinetics of calcium carbonate-rich deep sea sediments. Am. J. Sci. 278, 344–353.
Morse, J.W., 1983. The kinetics of calcium carbonate dissolution and precipitation. In: Reeder, R.J. (Ed.), Carbonates: Mineralogy and Chemistry. In: Reviews in Mineralogy, vol. 11, pp. 227–264.
Morse, J.W., 1986. The surface chemistry of calcium carbonate minerals in natural waters: an overview. Mar. Chem. 20, 91–112.
Morse, J.W., Arvidson, R.S., 2002. The dissolution kinetics of major sedimentary carbonate minerals. Earth-Sci. Rev. 58, 51–84.
Morse, J.W., He, S., 1993. Influences of T, S and P_{CO_2} on the pseudo-homogeneous precipitation of $CaCO_3$ from seawater; implications for whiting formation. Mar. Chem. 41, 291–297.
Morse, J.W., Mackenzie, F.T., 1990. Geochemistry of Sedimentary Carbonates. Developments in Sedimentology, vol. 48. Elsevier, Amsterdam.
Morse, J.W., Zullig, J.J., Bernstein, L.D., Millero, F.J., Milne, P., Mucci, A., Choppin, G.R., 1985. Chemistry of calcium carbonate-rich shallow water sediments in the Bahamas. Am. J. Sci. 285, 147–185.
Moulin, E., Jordens, A., Wollast, R., 1985. Influence of the aerobic bacterial respiration on the early dissolution of carbonates in coastal sediments. Proc. Progr. Belgium Oceanogr. Res. Brussels, 196–208.
Mullins, H.T., Wise Jr., S.W., Gardulski, A.F., Hinchey, E.J., Masters, P.M., Siegel, D.I., 1985. Shallow subsurface diagenesis of Pleistocene periplatform ooze: northern Bahamas. Sedimentology 32, 473–494.
Munnecke, A., Samtleben, C., 1996. The formation of micritic limestones and the development of limestone-marls alternations in the Silurian of Gotland, Sweden. Facies 34, 159–176.
Munnecke, A., Westphal, H., Reijmer, J.J.G., Samtleben, C., 1997. Microspar development during early marine burial diagenesis: a comparison of Pliocene carbonates from the Bahamas with Silurian limestones from Gotland (Sweden). Sedimentology 44, 977–990.
Murray, C.N., Wilson, T.R.S., 1997. Marine carbonate formations: their role in mediating long-term ocean-atmosphere carbon dioxide fluxes. Energy Convers. Manage. 38 (suppl.), S287–S294.
Murray, J.W., Alve, E., 1999. Natural dissolution of modern shallow water benthic foraminifera: taphonomic effects on the palaeoecological record. Palaeogeogr. Palaeoclimatol. Palaeoecol. 146, 195–209.
Myrow, P.M., 1995. *Thalassinoides* and the enigma of Early Paleozoic open-framework burrow systems. Palaios 10, 58–74.
Neumann, A.C., 1966. Observations on coastal erosion in Bermuda and measurements of the boring rate of the sponge, *Cliona lampa*. Limnol. Oceanogr. 11, 92–108.
Neumann, A.C., Land, L.S., 1975. Lime mud deposition and calcareous algae in the Bight of Abaco, Bahamas: a budget. J. Sed. Pet. 45, 763–786.

Oremland, R.S., Taylor, B.F., 1978. Sulfate reduction and methanogenesis in marine sediments. Geochim. Cosmochim. Acta 42, 209–214.

Palmer, T.J., Hudson, J.D., Wilson, M.A., 1988. Palaeoecological evidence for early aragonite dissolution in ancient calcite seas. Nature 335, 809–810.

Pari, N., Peyrot-Clausade, M., Le Campion-Alsumard, T., Hutchings, P., Chazottes, V., Golubic, S., Le Campion, J., Fontaine, M.F., 1998. Bioerosion of experimental substrates on high islands and atoll lagoons (French Polynesia) after two years of exposure. Mar. Ecol. Progr. Ser. 166, 119–130.

Pari, N., Peyrot-Clausade, M., Hutchings, P.A., 2002. Bioerosion of experimental substrates on high islands and atoll lagoons (French Polynesia) during 5 years of exposure. J. Exp. Mar. Biol. Ecol. 276, 109–127.

Patterson, W.P., Walter, L.M., 1994. Syndepositional diagenesis of modern platform carbonates: evidence from isotopic and minor element data. Geology 22, 127–130.

Perkins, R.D., Tsentas, C.I., 1976. Microbial infestation of carbonate substrates planted on the St. Croix shelf, West Indies. Geol. Soc. Am. Bull. 87, 1615–1628.

Perry, C.T., 1998. Grain susceptibility to the effects of microboring: implications for the preservation of skeletal carbonates. Sedimentology 45, 39–51.

Perry, C.T., 1999. Reef framework preservation in four contrasting modern reef environments, Discovery Bay, Jamaica. J. Coastal Res. 15, 796–812.

Perry, C.T., 2000. Factors controlling sediment preservation on a north Jamaican fringing reef: a process-based approach to microfacies analysis. J. Sediment. Res. 70, 633–648.

Perry, C.T., Bertling, M., 2000. Spatial and temporal patterns of macroboring within Mesozoic and Cenozoic coral reef systems. In: Insalaco, E., Skelton, P.W., Palmer, T.J. (Eds.), Carbonate Platform Systems: Components and Interactions. In: Geol. Soc. London Spec. Publ., vol. 178, pp. 33–50.

Peterhänsel, A., Pratt, B.R., 2001. Nutrient-triggered bioerosion on a giant carbonate platform masking the postextinction Famennian benthic community. Geology 29, 1079–1082.

Peyrot-Clausade, M., Le Campion-Alsumard, T., Hutchings, P., Le Campion, J., Payri, C., Fontaine, M.-F., 1995. Initial bioerosion and bioaccretion on experimental substrates in high island and atoll lagoons (French Polynesia). Oceanol. Acta 18, 531–541.

Pigott, J.D., Land, L.S., 1986. Interstitial water chemistry of Jamaican reef sediment: sulfate reduction and submarine cementation. Mar. Chem. 19, 355–378.

Pike, J., Bernhard, J.M., Moreton, S.G., Butler, I.B., 2001. Microbio-irrigation of marine sediments in dysoxic environments: implications for early sediment fabric formation and diagenetic processes. Geology 29, 923–926.

Pitman, W.C., Golovchenko, X., 1983. The effect of sealevel change on the shelfedge and slope of passive margins. In: Stanley, D.J., Moore, G.T. (Eds.), The Shelfbreak: Critical Interface on Continental Margins. In: Soc. Econ. Paleontol. Mineral. Spec. Publ., vol. 33, pp. 41–58.

Plummer, L.N., Mackenzie, F.T., 1974. Predicting mineral solubility from rate data: application to the dissolution of magnesian calcites. Am. J. Sci. 274, 61–83.

Plummer, L.N., Wigley, T.M.L., Parkhurst, D.L., 1978. The kinetics of calcite dissolution in CO_2–water systems at 5 °C to 60 °C and 0.0 to 1.0 ATM CO_2. Am. J. Sci. 278, 179–216.

Powell, E.N., Parsons-Hubbard, K.M., Callender, W.R., Staff, G.M., Rowe, G.T., Brett, C.E., Walker, S.E., Raymond, A., Carlson, D.D., White, S., Heise, E.A., 2002. Taphonomy on the continental shelf and slope: two-year trends—Gulf of Mexico and Bahamas. Palaeogeogr. Palaeoclimatol. Palaeoecol. 184, 1–35.

Pratt, B.R., 2001. Septarian concretions: internal cracking caused by synsedimentary earthquakes. Sedimentology 48, 189–213.

Pytkowicz, R.M., 1971. Sand-seawater interactions in Bermuda beaches. Geochim. Cosmochim. Acta 35, 509–515.

Raiswell, R., 1976. The microbiological formation of carbonate concretions in the Upper Lias of NE England. Chem. Geol. 18, 227–244.

Raiswell, R., 1988a. Chemical model for the origin of minor limestone-shale cycles by anaerobic methane oxidation. Geology 16, 641–644.

Raiswell, R., 1988b. Evidence for surface reaction-controlled growth of carbonate concretions in shales. Sedimentology 35, 571–575.

Rasmussen, H.W., 1971. Echinoid and crustacean burrows and their diagenetic significance in the Maastrichtian-Danian of Stevns Klint, Denmark. Lethaia 4, 191–216.

Read, J.F., 1982. Geometry, facies, and development of Middle Ordovician carbonate buildups, Virginia Appalachians. Am. Ass. Petrol. Geol. Bull. 66, 189–209.

Reaka-Kudla, M.l., Feingold, J.S., Glynn, W., 1996. Experimental studies of rapid bioerosion of coral reefs in the Galapagos Islands. Coral Reefs 15, 101–107.

Reaves, C.M., 1986. Organic matter metabolizability and calcium carbonate dissolution in nearshore marine muds. J. Sediment. Petrol. 56, 486–494.

Reeburgh, W.E., 1980. Anaerobic methane oxidation: rate depth distributions in Skan Bay sediments. Earth Planet. Sci. Lett. 47, 345–353.

Reeburgh, W.E., 1983. Rates of biogeochemical processes in anoxic sediments. Ann. Rev. Earth Planet. Sci. 11, 269–298.

Reid, R.P., Macintyre, I.G., 1998. Carbonate recrystallization in shallow marine environments: a widespread diagenetic process forming micritized grains. J. Sediment. Res. 68, 928–946.

Reitner, J., 1993. Modern cryptic microbialite/metazoan facies from Lizard Island (Grat Barrier Reef, Australia). Formation and concepts. Facies 29, 3–40.

Remane, J., 2000 (compilator). International Stratigraphic Chart. UNESCO-IUGS.

Revelle, R., Emery, K.O., 1957. Chemical erosion of beach rock and exposed reef rock. Bikini and nearby atolls, Marshall Island. US Geol. Surv. Prof. Paper 260-T, pp. 699–709.

Revelle, R., Fairbridge, R., 1957. Carbonates and carbon dioxide. In: Hedgpeth, J.W. (Ed.), Treatise on Marine Ecology and Paleoecology. Geol. Soc. Mem. 67 (1), 239–296.

Robbins, L.L., Blackwelder, P.L., 1992. Biochemical and ultrastructural evidence for the origin of whitings: a biologically induced calcium carbonate precipitation mechanism. Geology 20, 464–468.

Roberts, H.H., 1971. Mineralogical variation in lagoonal carbonates from North Sound, Grand Cayman island (British West Indies). Sediment. Geol. 6, 201–213.

Robbins, L.L., Tao, Y., Evans, C.A., 1997. Temporal and spatial distribution of whitings on Great Bahama Bank and a new lime mud budget. Geology 25, 947–950.

Rude, P.D., Aller, R.C., 1991. Fluorine mobility during early diagenesis of carbonate sediment: an indicator of mineral transformations. Geochim. Cosmochim. Acta 55, 2491–2509.

Ryan, D.A., Opdyke, B.N., Jell, J.S., 2001. Holocene sediments of Wistari Reef: towards a global quantification of coral reef related neritic sedimentation in the Holocene. Palaeogeogr. Palaeoclimatol. Palaeoecol. 175, 173–184.

Sadler, P.M., 1981. Sediment accumulation rates and the completeness of stratigraphic sections. J. Geol. 89, 569–584.

Saller, A.H., 1986. Radiaxial calcite in Lower Miocene strata, subsurface Enewetak atoll. J. Sediment. Petrol. 56, 743–762.

Sammarco, P.W., 1996. Comments on coral reef regeneration, bioerosion, biogeography, and chemical ecology: future directions. J. Exp. Mar. Biol. Ecol. 200, 135–168.

Sandberg, P.A., 1983. An oscillating trend in Phanerozoic non-skeletal carbonate mineralogy. Nature 305, 19–22.

Sanders, D., 1999. Shell disintegration and taphonomic loss in rudist biostromes. Lethaia 32, 101–112.

Sanders, D., 2001. Burrow-mediated carbonate dissolution in rudist biostromes (Aurisina, Italy): implications for taphonomy in tropical, shallow subtidal carbonate environments. Palaeogeogr. Palaeoclimatol. Palaeoecol. 168, 41–76.

Sanders, D., Pons, J.M., 1999. Rudist formations in mixed siliciclastic-carbonate depositional environments, Upper Cretaceous, Austria: stratigraphy, sedimentology, and models of development. Palaeogeogr. Palaeoclimatol. Palaeoecol. 148, 249–284.

Sansone, F.J., Tribble, G.W., Andrews, C.C., Chanton, J.P., 1990. Anaerobic diagenesis within Recent, Pleistocene, and Eocene marine carbonate frameworks. Sedimentology 37, 997–1009.

Schlager, W., 1974. Preservation of cephalopod skeletons and carbonate dissolution on ancient Tethyan sea floors. In: Hsü, K.J., Jenkyns, H.E. (Eds.), Pelagic Sediments on Land and Under the Sea. In: Int. Ass. Sedimentol. Spec. Publ., 1, pp. 49–70.

Schlager, W., 1981. The paradox of drowned reefs and carbonate platforms. Geol. Soc. Am. Bull. 92, 197–211.

Schlager, W., Marsal, D., van der Geest, P.A.G., Sprenger, A., 1998. Sedimentation rates, observation span, and the problem of spurious correlation. Math. Geol. 30, 547–556.

Schlager, W., 1999. Scaling of sedimentation rates and drowning of reefs and carbonate platforms. Geology 27, 183–186.

Schlager, W., 2000. Sedimentation rates and growth potential of tropical, cool-water and mud-mound carbonate systems. In: Insalaco, E., Skelton, P.W., Palmer, T.J. (Eds.), Carbonate Platform Systems: Components and Interactions. In: Geol. Soc. London Spec. Publ., vol. 178, pp. 217–227.

Schlager, W., James, N.P., 1978. Low-magnesian calcite limestones forming at the deep-sea floor, Tongue of the Ocean, Bahamas. Sedimentology 25, 675–702.

Schmalz, R.F., 1967. Kinetics and diagenesis of carbonate sediments. J. Sediment. Petrol. 37, 60–67.

Schmalz, R.F., Swanson, F.J., 1969. Diurnal variations in the carbonate saturation of seawater. J. Sediment. Petrol. 39, 255–267.

Scholle, P.A., 1978. Carbonate rock constituents, textures, cements, and porosities. Am. Ass. Petrol. Geol. Mem. 27, 241 pp.

Scholle, P.A., Arthur, M.A., Ekdale, A.A., 1983. Pelagic environment. In: Scholle, P.A., Bebout, D.G., Moore, C.H. (Eds.), Carbonate Depositional Environments. Am. Ass. Petrol. Geol. Mem. 33, 619–691.

Schopf, J.W., 1999. Cradle of Life. The Discovery of Earth's Earliest Fossils. Princeton University Press, Princeton. 367 pp.

Schram, F.R., Feldmann, R.M., Copeland, M.J., 1978. The Late Devonian Palaeopalaemonidae and the earliest decapod crustaceans. J. Paleont. 52, 1375–1387.

Scoffin, T.P., 1992. Taphonomy of coral reefs: a review. Coral Reefs 11, 57–77.

Seibold, E., 1962. Untersuchungen zur Kalkfällung und Kalklösung am Westrand der Great Bahama Bank. Sedimentology 1, 50–74.

Seilacher, A., 1971. Preservational history of ceratite shells. Paleontology 14, 16–21.

Shinn, E.A., 1968. Burrowing in Recent lime sediments of Florida and the Bahamas. J. Paleont. 42, 879–894.

Shinn, E.A., Steinen, R.P., Lidz, B.H., Swart, P.K., 1989. Perspectives: whitings, a sedimentologic dilemma. J. Sediment. Petrol. 59, 147–161.

Sjöberg, E.L., 1976. A fundamental equation for calcite dissolution kinetics. Geochim. Cosmochim. Acta 40, 441–447.

Smith, S.V., 1971. Budget of calcium carbonate, southern California continental borderland. J. Sediment. Petrol. 41, 798–808.

Stambler, N., Popper, N., Dubinsky, Z., Stimson, J., 1991. Effects of nutrient enrichment and water motion on the coral *Pocillopora damicornis*. Pacific Sci. 45, 299–307.

Stanley, S.M., Hardie, L.A., 1998. Secular oscillations in the carbonate mineralogy of reef-building and sediment-producing organisms driven by tectonically forced shifts in seawater chemistry. Palaeogeogr. Palaeoclimatol. Palaeoecol. 144, 3–19.

Stearn, C.W., Scoffin, T.P., Martindale, W., 1977. Calcium carbonate budget of a fringing reef on the west coast of Barbados-pt.I, zonation and productivity. Bull. Mar. Sci. 27, 479–510.

Steinen, R.P., 1982. SEM observations on the replacement of Bahaman aragonitic mud by calcite. Geology 10, 471–475.

Steuber, T., 2002. Plate tectonic control on the evolution of Cretaceous platform-carbonate production. Geology 30, 259–262.

Suess, E., 1970. Interaction of organic compounds with calcium carbonate—I. Association phenomena and geochemical implications. Geochim. Cosmochim. Acta 34, 157–168.

Suess, E., 1973. Interaction of organic compounds with calcium carbonate—II. Organo-carbonate association in Recent sediments. Geochim. Cosmochim. Acta 37, 2435–2447.

Svensson, U., Dreybrodt, W., 1992. Dissolution kinetics of natural calcite minerals in CO_2–water systems approaching calcite equilibrium. Chem. Geol. 100, 129–145.

Taft, W.H., Harbaugh, J.W., 1964. Modern carbonate sediments of Southern Florida, Bahamas, and Espiritu Santo Island, Baja California. Stanford Univ. Publ. Geol. Sci., vol. 8/2. Stanford, California, 133 pp.

Tedesco, L.P., Wanless, H.R., 1995. Growth and burrow-transformation of carbonate banks: comparison of modern skeletal banks of south Florida and Pennsylvanian phylloid banks of south-eastern Kansas, USA. In: Monty, C.L.V., Bosence, D.W.J., Bridges, P.H., Pratt, B.R. (Eds.), Carbonate Mud-Mounds. In: Int. Ass. Sedimentol. Publ., 23, pp. 495–521.

Tedesco, L.P., Aller, R.C., 1997. ^{210}Pb chronology of sequences affected by burrow excavation and infilling: Examples from shallow marine carbonate sediment sequences, Holocene South Florida and Caicos platform, British West Indies. J. Sediment. Res. 67, 36–46.

Thomas, M.M., Clouse, J.A., Longo, J.M., 1993. Adsorption of organic compounds on carbonate minerals. 3. Influence on dissolution rates. Chem. Geol. 109, 227–237.

Tobin, K.J., Walker, K.R., 1996. Ordovician low- to intermediate-Mg calcite marine cements from Sweden: marine alteration and implications for oxygen isotopes in Ordovician seawater. Sedimentology 43, 719–735.

Tobin, K.J., Bergstrom, S.M., 2002. Implications of Ordovician (c. 460 Myr) marine cement for constraining seawater temperature and atmospheric pCO_2. Palaeogeogr. Palaeoclimatol. Palaeoecol. 181, 399–417.

Traganza, E.D., 1967. Dynamics of the carbon dioxide system on the Great Bahama Bank. Bull. Mar. Sci. 17, 348–366.

Tribble, G.W., 1993. Organic matter oxidation and aragonite diagenesis in a coral reef. J. Sediment. Petrol. 63, 523–527.

Tribble, G.W., Sansone, F.J., Smith, S.V., 1990. Stoichiometric modeling of carbon diagenesis within a coral reef framework. Geochim. Cosmochim. Acta 54, 2439–2449.

Tucker, M.E., 1974. Sedimentology of Paleozoic pelagic limestones: the Devonian Griotte (Southern France) and Cephalopodenkalk (Germany). In: Hsü, K.J., Jenkyns, H.E. (Eds.), Pelagic Sediments on Land and Under the Sea. In: Int. Ass. Sediment. Spec. Publ., vol. 1, pp. 71–92.

Tudhope, A.W., Scoffin, T.P., 1984. The effects of *Callianassa* bioturbation on the preservation potential of carbonate grains in Davies Reef Lagoon, Great Barrier Reef, Australia. J. Sediment. Petrol. 54, 1091–1096.

Tudhope, A.W., Risk, M.J., 1985. Rate of dissolution of carbonate sediments by microboring organisms, Davies Reef, Australia. J. Sediment. Petrol. 55, 440–447.

Tunnicliffe, V., 1983. Caribbean staghorn coral populations—pre-Hurricane Allen conditions in Discovery Bay, Jamaica. Bull. Mar. Sci. 33, 132–151.

Vecsei, A., 2001. Fore-reef carbonate production: development of a regional census-based method and first estimates. Palaeogeogr. Palaeoclimatol. Palaeoecol. 175, 185–200.

Veizer, J., Ala, D., Azmy, K., Bruckschen, P., Buhl, D., Bruhn, F., Carden, G.A.F., Diener, A., Ebneth, S., Godderis, Y., Jasper, T., Korte, C., Pawellek, F., Podlaha, O.G., Strauss, H., 1999. $^{87}Sr/^{86}Sr$, $\delta^{13}C$ and $\delta^{18}O$ evolution of Phanerozoic seawater. Chem. Geol. 161, 59–88.

Visscher, P.T., Reid, R.P., Bebout, B.M., 2000. Microscale observations of sulfate reduction: correlation of microbial activity with lithified micritic laminae in modern marine stromatolites. Geology 28, 919–922.

Vogel, K., Gektidis, M., Golubic, S., Kiene, W.E., Radtke, G., 2000. Experimental studies on microbial bioerosion at Lee Stocking Island, Bahamas and One Tree Island, Great Barrier Reef, Australia: implications for paleoecological reconstructions. Lethaia 33, 190–204.

Walkden, G.M., De Matos, J., 2000. "Tuning" high-frequency cyclic carbonate platform successions using omission surfaces: lower Jurassic of the U.A.E. and Oman. In: Alsharhan, A.S., Scott, R.W. (Eds.), Middle East Models of Jurassic/Cretaceous Carbonate Systems. In: Soc. Econ. Paleontol. Mineral. Spec. Publ., vol. 69, pp. 37–52.

Wallmann, K., 2001. The geological water cycle and the evolution of marine $d^{18}O$ values. Geochim. Cosmochim. Acta 65, 2469–2485.

Walter, L.M., 1985. Relative reactivity of skeletal carbonates during dissolution: implications for diagenesis. In: Schneidermann, N., Harris, P.M. (Eds.), Carbonate Cements. In: Soc. Econ. Paleontol. Mineral. Spec. Publ., vol. 36, pp. 3–16.

Walter, L.M., Morse, J.W., 1984. Reactive surface area of skeletal carbonates during dissolution: effect of grain size. J. Sediment. Petrol. 54, 1081–1090.

Walter, L.M., Burton, E.A., 1990. Dissolution of Recent platform carbonate sediments in marine pore fluids. Am. J. Sci. 290, 601–643.

Walter, L.M., Bischof, S.A., Patterson, W.P., Lyons, T.L., 1993. Dissolution and crystallization in modern shelf carbonates: evidence from pore water and solid phase chemistry. R. Soc. London Philosoph. Trans., Ser. A 344, 27–36.

Ward, W.C., Weidie, A.E., Back, W., 1985. Geology and hydrogeology of the Yucatán and Quaternary geology of northeastern Yucatán Peninsula. New Orleans Geol. Soc, New Orleans, LA. 160 pp.

Whiticar, M.J., Faber, E., Schoell, M., 1986. Biogenic methane formation in marine and freshwater environments: CO_2 reduction vs. acetate fermentation—isotope evidence. Geochim. Cosmochim. Acta 50, 693–709.

Wilkinson, B.H., Algeo, T.J., 1989. Sedimentary carbonate record of calcium-magnesium cycling. Am. J. Sci. 289, 1158–1194.

Wilkinson, B.H., Given, R.K., 1986. Secular variation in abiotic marine carbonates: constraints on Phanerozoic atmospheric carbon dioxide contents and oceanic Mg/Ca ratios. J. Geol. 94, 321–333.

Wilkinson, B.H., Owen, R.M., Carroll, A.R., 1985. Submarine hydrothermal weathering, global eustasy, and carbonate polymorphism in Phanerozoic marine oolites. J. Sediment. Petrol. 55, 171–183.

Wilson, M.A., Palmer, T.J., Guensburg, T.E., Finton, C.D., Kaufman, L.E., 1992. The development of an Early Ordovician hardground community in response to rapid sea-floor calcite precipitation. Lethaia 25, 19–34.

Zeebe, R.E., 2001. Seawater pH and isotopic palaeotemperatures of Cretaceous oceans. Palaeogeogr. Palaeoclimatol. Palaeoecol. 170, 49–57.

Zhang, Y., Dawe 1, R.A., 2000. Influence of Mg^{2+} on the kinetics of calcite precipitation and calcite crystal morphology. Chem. Geol. 163, 129–138.

Zuddas, P., Mucci, A., 1994. Kinetics of calcite precipitation from seawater: I. A classical chemical kinetics description for strong electrolyte solutions. Geochim. Cosmochim. Acta 58, 4353–4362.

Zullig, J.J., Morse, J.W., 1988. Interaction of organic acids with carbonate mineral surfaces in seawater and related solutions: I. Fatty acid adsorption. Geochim. Cosmochim. Acta 52, 1667–1678.